CERN-SPSC-2018-008 / SPSC-P-330-ADD-10
10/04/2018

EUROPEAN LABORATORY FOR PARTICLE PHYSICS

Addendum to the NA61/SHINE Proposal SPSC-P-330

Study of Hadron-Nucleus and Nucleus-Nucleus Collisions at the CERN SPS Early Post-LS2 Measurements and Future Plans

By the NA61/SHINE Collaboration and the CERN team
http://na61.web.cern.ch/

Abstract

NA61/SHINE proposes to continue measurements of hadron and nuclear fragment production properties in reactions induced by hadron and ion beams. The new measurements requested will provide unique data on (i) charm hadron production in Pb+Pb collisions for heavy ion physics, (ii) nuclear fragmentation cross sections for cosmic ray physics and (iii) hadron production in hadron-induced reactions for neutrino physics. The measurements require upgrades of the NA61/SHINE detector that shall increase the data taking rate to about 1 kHz. NA61/SHINE is the only experiment which can conduct the measurements in the near future.

In this document the beam request for the early post-LS2 measurements in 2022 is presented. Plans for a continuation of measurements are also discussed.

April 10, 2018

Contents

The NA61/SHINE Collaboration:

A. Aduszkiewicz[18], E.V. Andronov[24], T. Antićić[3], N. Antoniou[8], B. Baatar[22], M. Baszczyk[16], S. Bhosale[13], A. Blondel[26], M. Bogomilov[2], A. Brandin[23], A. Bravar[26], W. Bryliński[20], J. Brzychczyk[15], S.A. Bunyatov[22], O. Busygina[21], A. Bzdak[16], S. Cao[10], H. Cherif[7], P. Christakoglou[8], M. Ćirković[25], T. Czopowicz[20], A. Damyanova[26], A. Datta[29], N. Davis[13], M. Deveaux[7], F. Diakonos[8], P. von Doetinchem[29], W. Dominik[18], P. Dorosz[16], J. Dumarchez[4], R. Engel[5], G.A. Feofilov[24], L. Fields[27], Z. Fodor[9,19], M. Friend[10], A. Garibov[1], M. Gaździcki[7,12], M. Golubeva[21], K. Grebieszkow[20], F. Guber[21], A. Haesler[26], T. Hasegawa[10], A.E. Hervé[5], S.N. Igolkin[24], A. Ivashkin[21], S.R. Johnson[28], K. Kadija[3], A. Kapoyannis[8], E. Kaptur[17], M. Kiełbowicz[13], V.A. Kireyeu[22], V. Klochkov[7], T. Kobayashi[10], V.I. Kolesnikov[22], D. Kolev[2], A. Korzenev[26], V.N. Kovalenko[24], K. Kowalik[14], S. Kowalski[17], M. Koziel[7], A. Krasnoperov[22], W. Kucewicz[16], M. Kuich[18], A. Kurepin[21], D. Larsen[15], A. László[9], T.V. Lazareva[24], M. Lewicki[19], K. Łojek[15], B. Łysakowski[17], V.V. Lyubushkin[22], M. Maćkowiak-Pawłowska[20], Z. Majka[15], B. Maksiak[20], A.I. Malakhov[22], D. Manić[25], A. Marchionni[27], A. Marcinek[13], A.D. Marino[28], K. Marton[9], H.-J. Mathes[5], T. Matulewicz[18], V. Matveev[22], G.L. Melkumov[22], A.O. Merzlaya[15], B. Messerly[30], Ł. Mik[16], S. Morozov[21,23], S. Mrówczyński[12], Y. Nagai[28], T. Nakadaira[10], M. Naskręt[19], V. Ozvenchuk[13], A.D. Panagiotou[8], V. Paolone[30], M. Pavin[4,3], O. Petukhov[21,23], R. Płaneta[15], P. Podlaski[18], B.A. Popov[22,4], M. Posiadała[18], D.S. Prokhorova[24], S. Puławski[17], J. Puzović[25], W. Rauch[6], M. Ravonel[26], R. Renfordt[7], E. Richter-Wąs[15], D. Röhrich[11], E. Rondio[14], M. Roth[5], B.T. Rumberger[28], A. Rustamov[1,7], M. Rybczynski[12], A. Rybicki[13], A. Sadovsky[21], K. Sakashita[10], K. Schmidt[17], T. Sekiguchi[10], I. Selyuzhenkov[23], A.Yu. Seryakov[24], P. Seyboth[12], A. Shukla[29], M. Słodkowski[20], A. Snoch[7], P. Staszel[15], G. Stefanek[12], J. Stepaniak[14], M. Strikhanov[23], H. Ströbele[7], T. Šuša[3], M. Tada[10], A. Taranenko[23], A. Tefelska[20], D. Tefelski[20], V. Tereshchenko[22], A. Toia[7], R. Tsenov[2], L. Turko[19], R. Ulrich[5], M. Unger[5], F.F. Valiev[24], M. Vassiliou[8], D. Veberič[5], V.V. Vechernin[24], M. Walewski[18], A. Wickremasinghe[30], Z. Włodarczyk[12], A. Wojtaszek-Szwarc[12], O. Wyszyński[15], L. Zambelli[4,10], E.D. Zimmerman[28], and R. Zwaska[27]

The CERN Team:

N. Benekos (EP-NU), S. Bordoni (EP-NU), N. Charitonidis (EN-EA)[1], R. Fernandez (BE-OP), U. Kose (EP-NU), P. Martinengo (EP-DT), A. de Roeck (EP-NU), D. Sgalaberna (EP-NU), A. Weber (EP-NU), L. Whitehead (EP-NU)

[1]The member of CERN personnel having contributed to the study, does not take position nor responsibility towards the required approval processes, as established by the organization.

[1] National Nuclear Research Center, Baku, Azerbaijan
[2] Faculty of Physics, University of Sofia, Sofia, Bulgaria
[3] Ruđer Bošković Institute, Zagreb, Croatia
[4] LPNHE, University of Paris VI and VII, Paris, France
[5] Karlsruhe Institute of Technology, Karlsruhe, Germany
[6] Fachhochschule Frankfurt, Frankfurt, Germany
[7] University of Frankfurt, Frankfurt, Germany
[8] University of Athens, Athens, Greece
[9] Wigner Research Centre for Physics of the Hungarian Academy of Sciences, Budapest, Hungary
[10] Institute for Particle and Nuclear Studies, Tsukuba, Japan
[11] University of Bergen, Bergen, Norway
[12] Jan Kochanowski University in Kielce, Poland
[13] H. Niewodniczański Institute of Nuclear Physics of the Polish Academy of Sciences, Kraków, Poland
[14] National Centre for Nuclear Research, Warsaw, Poland
[15] Jagiellonian University, Cracow, Poland
[16] AGH - University of Science and Technology, Cracow, Poland
[17] University of Silesia, Katowice, Poland
[18] University of Warsaw, Warsaw, Poland
[19] University of Wrocław, Wrocław, Poland
[20] Warsaw University of Technology, Warsaw, Poland
[21] Institute for Nuclear Research, Moscow, Russia
[22] Joint Institute for Nuclear Research, Dubna, Russia
[23] National Research Nuclear University (Moscow Engineering Physics Institute), Moscow, Russia
[24] St. Petersburg State University, St. Petersburg, Russia
[25] University of Belgrade, Belgrade, Serbia
[26] University of Geneva, Geneva, Switzerland
[27] Fermilab, Batavia, USA
[28] University of Colorado, Boulder, USA
[29] University of Hawaii at Manoa, USA
[30] University of Pittsburgh, Pittsburgh, USA

1 Executive Summary

We propose to continue the NA61/SHINE measurements of hadron and nuclear fragment production properties in reactions induced by hadron and ion beams after the Long Shutdown 2. The measurements are requested by heavy ion, cosmic ray and neutrino communities and they will include:

(i) measurements of charm hadron production in Pb+Pb collisions for heavy ion physics,

(ii) measurements of nuclear fragmentation cross section for cosmic ray physics,

(iii) measurements of hadron production induced by proton and kaon beams for neutrino physics.

NA61/SHINE is the only experiment which will conduct such measurements in the near future.

The objective of **charm hadron production measurements** in Pb+Pb collisions is to obtain the first data on mean number of $c\bar{c}$ pairs produced in the full phase space in heavy ion collisions. Moreover, first results on the collision energy and system size dependence will be provided. This, in particular, should significantly help to answer the questions:

(i) What is the mechanism of open charm production?

(ii) How does the onset of deconfinement impact open charm production?

(iii) How does the formation of quark-gluon plasma impact J/ψ production?

The objective of **nuclear fragmentation cross section measurements** is to provide high-precision data needed for the interpretation of results from current-generation cosmic ray experiments. The proposed measurements are of paramount importance to extract the characteristics of the diffuse propagation of cosmic rays in the Galaxy. A better understanding of the cosmic-ray propagation is needed to

(i) study the origin of Galactic cosmic rays and

(ii) evaluate the cosmic-ray background for signatures of astrophysical dark matter.

The objectives of **new hadron production measurements for neutrino physics** are

(i) to improve further the precision of hadron production measurements for the currently used T2K replica target, paying special attention to the extrapolation of produced particles to the target surface;

(ii) to perform measurements for a new target material (super-sialon), both in thin target and replica target configurations, for T2K-II and Hyper-Kamiokande;

(iii) to study the possibility of measurements at low incoming beam momenta (below 12 GeV/c) relevant for improved predictions of both atmospheric and accelerator neutrino fluxes;

(iv) to ultimately perform hadron production measurements with prototypes of Hyper-Kamiokande and DUNE targets.

The new measurements require upgrades of the NA61/SHINE detector that shall increase the data taking rate to about 1 kHz. These are:

(i) Construction of a new Vertex Detector.

(ii) Replacement of the TPC read-out electronics.

(iii) Construction of a new trigger and data acquisition system.

(iv) Upgrade of the Projectile Spectator Detector.

Furthermore, the construction of new Time-of-Flight detectors would be highly desirable for potential future measurements of hadron production in C+C and Mg+Mg collisions which are expected to be needed to understand the onset of fireball phenomenon.

In view of the Memorandum of the CERN DRC (see Appendix B), we ask for beam time for physics data taking only in 2022. Namely, we request:

(i) 42 days of primary Pb beam at 150A GeV/c for data taking on charm hadron production in Pb+Pb collisions (heavy ion physics).

(ii) 24 days of secondary light ion beam at 13A GeV/c for data taking on nuclear fragmentation cross section (cosmic ray physics).

(iii) 35 days of proton beam at 31 GeV/c for data taking on hadron production from the T2K replica target and the Super-Sialon thin target (neutrino physics).

(iv) 28 days of K^+ beam at 60 GeV/c for data taking on hadron production induced by K^+ mesons (neutrino physics)

In addition we plan commissioning and calibration of the upgraded detector in 2021 with hadron beams. Two weeks of beam time will be needed for this purpose. Finally we request a feasibility study of very low energy (1-5 GeV/c) hadron beams needed for neutrino physics.

We plan to continue the measurements of open charm production in 2023 and 2024 as follows:

(i) In 2023 with 28 days of primary Pb beam at 150A GeV/c.

(ii) In 2024 with 28 days of primary Pb beam at 40A GeV/c.

Measurements for cosmic-ray and neutrino physics are also envisaged. The beam requests for years 2023 and 2024 will be the subject of future NA61/SHINE documents.

Recommendation and approval of the NA61/SHINE physics programs presented in this document is mandatory for acquiring resources and additional manpower needed for detector upgrades, data taking, calibration and analysis.

2 Introduction

NA61/SHINE [1] is a multi-purpose experiment to study hadron-proton, hadron-nucleus and nucleus-nucleus collisions at the CERN Super Proton Synchrotron (SPS). The experiment was approved by the CERN Research Board in 2007 based on the request of heavy ion, neutrino and cosmic ray communities. They argued that opportunities offered by the broad momentum range of beam particles, from pions to lead nuclei, together with the large acceptance and high resolution of the NA61/SHINE detector provide the unique opportunity to perform urgently needed measurements. The first physics data with hadron beams were recorded in 2009 and with ion beams (secondary ^{7}Be beams) in 2011. The approved program will be completed in 2018 by data taking on Pb+Pb collisions and hadron-nucleus interactions. Data have been recorded to

(i) study the properties of the onset of deconfinement and search for the critical point of strongly interacting matter,

(ii) provide precise results on hadron production for improving calculations of the initial neutrino beam flux in long-baseline neutrino oscillation experiments as well as well as for more reliable simulations of cosmic-ray air showers.

Among the most important physics results are:

(i) observation of a rapid change of system size dependence of hadron production properties - the onset of fireball,

(ii) reduction of systematic uncertainties of the T2K final results by a factor of about 2,

(iii) precise investigation of mechanisms for muon production in ultra-high energy cosmic-ray air showers.

Based on the success of the currently running program and motivated by new physics needs NA61/SHINE proposes to continue measurements with hadron and ion beams during the period 2022-2024. The measurements are requested by heavy ion, cosmic ray and neutrino communities and include:

(i) measurements of charm hadron production in Pb+Pb collisions for heavy ion physics,

(ii) measurements of nuclear fragmentation cross sections for cosmic ray physics,

(iii) measurements of hadron production in hadron-induced reactions for neutrino physics.

It is important to stress that the beam momentum range provided to NA61/SHINE by the SPS and the H2 beam line is highly important for the heavy ion, neutrino and cosmic ray communities. Namely, it covers:

(i) energies at which the transition from a matter in which quarks and gluons are confined in hadrons to quark gluon plasma takes place in heavy ion collisions - the onset of deconfinement [2],

(ii) proton beams of momenta used to produce neutrino beams at J-PARC, Japan and Fermilab, US [3],

(iii) light nuclei at $> 10A$ GeV/c important for the understanding of the propagation of cosmic rays in the Galaxy.

There is a world-wide effort to construct facilities providing ion and hadron beams in the CERN SPS beam momentum range. These are the fixed-target facilities at FAIR, Germany and J-PARC, Japan as well as the collider facility NICA, Russia. They will start operation after the here requested measurements are completed. The second phase of the beam energy scan at RHIC, US is planned to run in 2019 and 2020. Data will be taken in collider and fixed target modes. The fixed target facilities will operate only at energies below the onset of deconfinement. Data from collider facilities are typically complementary to the corresponding fixed target results. In particular, charm hadron measurements in a wide region of phase space are only possible at the fixed target facilities provided the collision energy and data taking rate are high enough.

In conclusion, NA61/SHINE is the only experiment which can conduct the requested measurements in the near future. Moreover, the NA61/SHINE operation beyond the LS2 leaves open the possibility to perform new measurements which are likely to be requested in the future. In particular, measurements of hadron emission from the DUNE and HyperK replica targets are expected to be requested only after the LS3 once their design will be completed. Moreover, new measurements related to the recent observation of the onset of fireball are likely to be requested soon following the growing experimental evidence.

The document is organized as follows. The status of the NA61/SHINE detector is summarized in Sec. 3. Section 4 presents the physics motivation and the needed detector upgrades for open charm measurements in Pb+Pb collisions which are requested by the heavy ion community. New high-statistics measurements of spectator-induced effects in Pb+Pb collisions are described in Sec. 6. Section 5 presents considerations on future measurements with light primary ion beams motivated by indications of the onset of fireball. Measurements of nuclear fragmentation cross sections and anti-proton production for cosmic-ray research are described in Sec. 7. Future hadron production measurements for neutrino physics are presented in Sec. 8. The parameters of requested data taking are summarized in Sec. 9. Section 10 gives the NA61/SHINE beam request for 2022, the early phase of the post-LS2 physics data taking. Supporting letters and the *Memorandum on Operation of Fixed Target Experiments immediately after LS2* in Appendices A and B close the document.

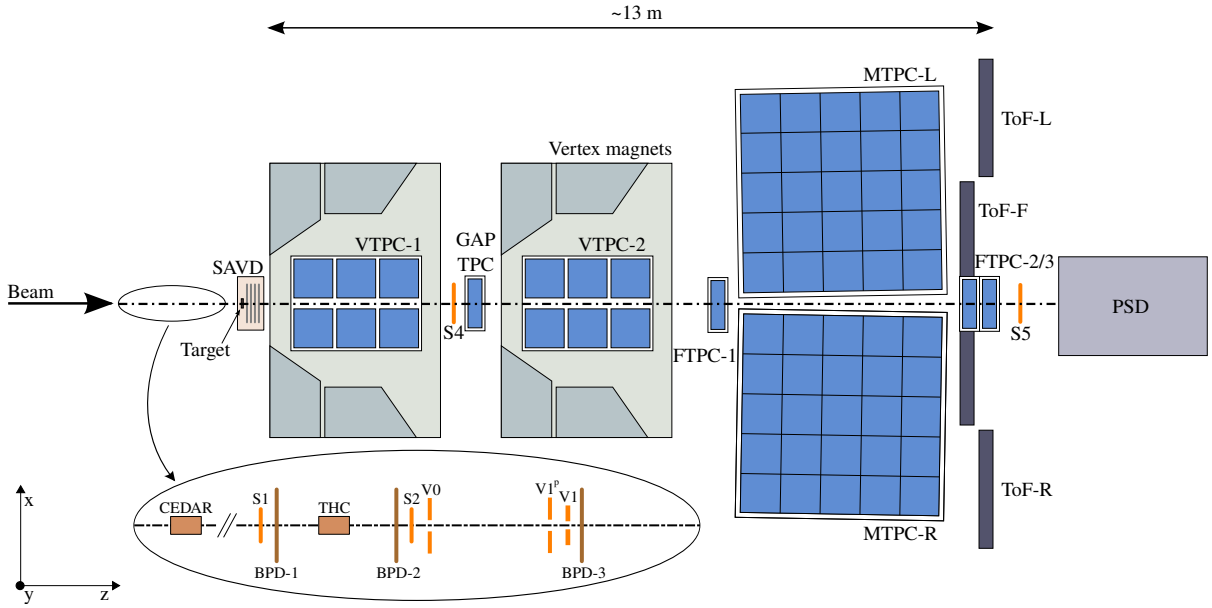

Figure 1: Schematic layout of the NA61/SHINE experiment at the CERN SPS as of 2018 (horizontal cut in the beam plane, not to scale). The beam and trigger counter configuration used for data taking with hadron beams is shown in the inset. The chosen right-handed coordinate system is indicated in the figure. The incoming beam direction is along the z axis. The magnetic field bends charged particle trajectories in the x–z (horizontal) plane. The drift direction in the TPCs is along the y (vertical) axis.

3 NA61/SHINE Detector

NA61/SHINE is a fixed-target experiment located in the H2 line in the North Area of the CERN Super Proton Synchrotron (SPS) [1]. The multi-purpose detector is optimized to study hadron production in hadron-proton, hadron-nucleus and nucleus-nucleus collisions. Figure 1 presents a schematic drawing of the detector as of 2018. It consists of a large acceptance hadron spectrometer with excellent capabilities in charged particle momentum measurements and identification by a set of eight Time Projection Chambers (TPC) as well as Time-of-Flight (ToF) detectors. The Vertex Detector (SAVD) is placed 5 cm centimetres downstream from the target. It consists of four layers of silicon pixel sensors allowing to reconstruct vertices of short-lived charm particles like D^0 mesons. The high resolution forward calorimeter, the Projectile Spectator Detector (PSD), measures energy flow around the beam direction, which in nucleus-nucleus reactions is primarily a measure of the number of spectator (non-interacting) nucleons. An array of beam detectors identifies beam particles, secondary hadrons and ions as well as primary ions, and measures precisely their trajectories.

4 Measurements of charm production in Pb+Pb collisions

The NA61/SHINE Collaboration studies, in particular, properties of hadron production in nucleus-nucleus collisions. The primary aim is to uncover features of the phase transition between confined matter and quark gluon plasma (QGP). Within the current program, data on p+p, Be+Be, Ar+Sc, Xe+La, and Pb+Pb collisions at beam momenta in the range 13A-150A GeV/c have been recorded. Single particle spectra, correlations and fluctuations of light and medium mass hadrons, mostly pions and kaons, have been measured.

Here we present the NA61/SHINE program to measure charm hadron, mostly D mesons, production in central Pb+Pb collisions with the upgraded NA61/SHINE detector at the CERN SPS. This will be the first direct measurements of charm production in heavy ion collision in the CERN SPS energy domain. The charm measurements are possible thanks to the advent of detector technologies that allowed the cost and manpower efficient construction of silicon pixel Vertex Detectors, e.g. the VD of NA61/SHINE. With this detector one can reconstruct decays of D mesons as close as ≈ 1 mm to the primary interaction point.

In the past there were two attempts to measure charm production in Pb+Pb collisions at the CERN SPS. First, the NA49 collaboration in 2002 [4] estimated an upper limit for the D meson multiplicity via analysis of its decay topology into a pair of charged kaon and pion. Later, an indirect estimate of the D meson yield was obtained by the NA60 collaboration by measurements of muons which possibly originate from semi-leptonic charm meson decays [5].

Section 4.1 briefly summarizes the history, status and plans of heavy ion experiments related to the search for and study of the phase transition from confined hadron matter to the quark-gluon plasma. The role of NA61/SHINE and its predecessor NA49 at the CERN SPS is underlined. The motivation of the charm program is discussed in Sec. 4.2. The current status of the program including preliminary results of the first data taking campaigns performed in 2016 and 2017 is presented in Sec. 4.3. The NA61/SHINE plans for systematic charm production measurements in the years $2022-2024$ are discussed in Sec. 4.4. The section also presents the expected physics performance and the uniqueness of the future NA61/SHINE results.

4.1 Heavy Ion Collisions and NA61/SHINE

This section briefly summarizes the history, status and plans of heavy ion experiments related to the search for and study of the phase transition from confined hadron matter to the quark-gluon plasma.

4.1.1 Brief History of Ideas and Measurements

The quark model of hadron classification proposed by Gell-Mann and Zweig in 1964 starts a 15 years-long period in which sub-hadronic particles, quarks and gluons, were discovered and a theory of their interactions, quantum chromodynamics (QCD) was established. In parallel, conjectures were formulated concerning the existence and properties of matter consisting of sub-hadronic particles, soon called the QGP and studied in detail within QCD [6].

Ivanenko, Kurdgelaidze [7], Itoh [8] and Collins, Perry [9] suggested that quasi-free quarks may exist in the centre of neutron stars. Many physicists started to speculate that the QGP can be formed in nucleus–nucleus collisions at high energies and thus it may be discovered in laboratory experiments. Questions concerning QGP properties and properties of its transition to matter consisting of hadrons were considered since the late 1970s.

Cabibbo, Parisi [10] pointed out that the exponentially increasing mass spectrum proposed by Hagedorn [11] may be connected to the existence of the phase in which quarks are not confined. Then Hagedorn and Rafelski [12], Gorenstein, Petrov, and Zinovjev [13] suggested that the Hagedorn massive states are not point-like objects but the quark-gluon bags. These picture leads to the interpretation of the upper limit of the hadron gas temperature, the Hagedorn temperature, as the transition temperature from the hadron gas to a quark gluon plasma. Namely, at $T > 150$ MeV/c the temperature refers to the interior of the quark-gluon bag, i.e., to the QGP. Similar estimates of the (pseudo-)transition temperature result from QCD lattice calculations at vanishing baryochemical potential [14]. Results suggest that the transition is likely to be a continuous cross-over, rather than a phase transition of the first order. On the other hand the transition at high baryochemical potential is believed to be of the first order and happen along a line which ends with decreasing potential in a critical point (of the second order) and then turns into a crossover region [15, 16].

In the mid 1990s numerous results on collisions of light nuclei at the BNL AGS (beams of Si at 14.6A GeV) and the CERN SPS (beams of O and S at 200A GeV) were obtained. Soon after experiments with heavy nuclei were conducted at the top AGS and SPS energies (AGS: Au+Au at 11.6A GeV, SPS: Pb+Pb at 158A GeV). In 2000 the CERN heavy ion community concluded [17]: *a common assessment of the collected data leads us to conclude that we now have compelling evidence that a new state of matter has indeed been created, at energy densities which had never been reached over appreciable volumes in laboratory experiments before and which exceed by more than a factor 20 that of normal nuclear matter. The new state of matter found in heavy ion collisions at the SPS features many of the characteristics of the theoretically predicted quark-gluon plasma*. In particular, the observed suppression of the charmonium states was considered as the key evidence for the formation of a transient quark-gluon phase without colour confinement. A verification of the J/ψ suppression as signal of QGP formation is one of the goals of the NA61/SHINE charm program.

Unambiguous evidence of the QGP state was however missing. The rich and precise

results from RHIC and LHC heavy ion progarms did not change the conclusion. This may be attributed to the difficulty of obtaining unique and quantitative predictions of the expected QGP signals from QCD.

In the mid 1990s the first look at the energy dependence of hadron production in nucleus–nucleus (A+A) collisions at high energies became possible. Compilations, on pion production [18] and on strangeness production [19] resulted in a clear conclusion: the energy dependence of hadron multiplicities measured in A+A collisions and p+p interactions are very different. Furthermore the data on A+A collisions suggested that there is a significant change in the energy dependence of pion and strangeness yields which is located between the top AGS and SPS energies. Based on the statistical approach to strong interactions [20,21] it was conjectured [18,19,22] that the change is related to the onset of deconfinement during the early stage of the A+A collisions. Soon after, following this hypothesis, a quantitative model was developed, the Statistical Model of the Early Stage (SMES) [23]. The model predicts a rapid change of the collision energy dependence of hadron production properties that are sensitive to the QGP, as a signal of a transition to QGP (the onset of deconfinement) in nucleus–nucleus collisions. The onset energy was estimated to be located in the CERN SPS energy range.

The predicted phase transition of strongly interacting matter to the QGP was discovered within the energy scan program of the NA49 Collaboration at the CERN SPS [24, 25]. The scan was conducted between 1999 and 2002. The discovery was based on the observation that several basic hadron production properties measured in heavy ion collisions rapidly change their dependence on collisions energy in a common energy domain [2], see Fig. 2. The NA49 results were confirmed by the data from the RHIC Beam Energy Scan [26]. A smooth evolution of hadron production properties is observed between the top SPS energies and the top RHIC and LHC energies [27]. This supports the interpretation of the rapid changes of the energy dependence at the CERN SPS as due to the transition to a quark-gluon plasma. Clearly, the observation of the qualitative signals of the transition to the QGP serves also as evidence of QGP creation in heavy ion collisions at high enough collision energies.

4.1.2 NA61/SHINE Physics Program

The NA61/SHINE experiment at the CERN SPS was primarily motivated [29] by the results of NA49. Two major questions were asked by the collaboration [30]:

(i) What is the nature of the transition from the anomalous energy dependence measured in central Pb+Pb collisions at SPS energies to the smooth dependence measured in p+p interactions?

(ii) Does the critical point of strongly interacting matter exist and, if it does, where is it located?

Production properties of light and medium mass hadrons, in particular pions and kaons, have been measured. The most important results are briefly summarized below.

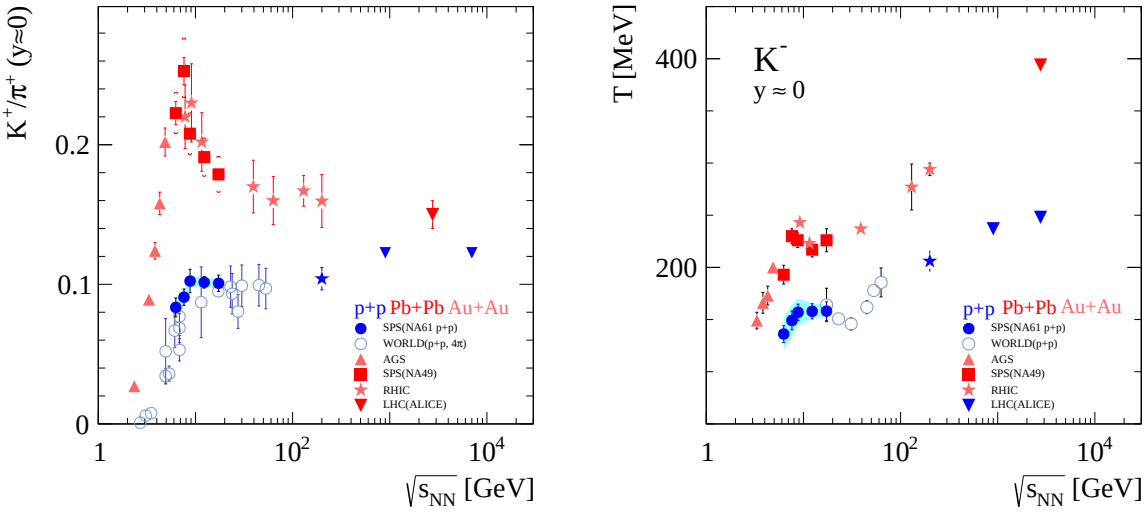

Figure 2: Recent results on the observation of the phase transition in central Pb+Pb (Au+Au) collisions [28]. The horn (*left*) and step (*right*) structures in the energy dependence of the K^+/π^+ ratio and the inverse slope parameter of m_T spectra of K^- signal the onset of deconfinement located at the low CERN SPS energies.

Figure 3 shows example plots on the system size dependence of the ratio of K^+ and π^+ yields at mid-rapidity and of the scaled variance of multiplicity distributions [31]. The Be+Be results are close to p+p independently of collision energy. Moreover, the data show a jump between light (p+p, Be+Be) and intermediate, heavy (Ar+Sc, Pb+Pb) systems.

Here one recalls the following:

(i) The K^+/pip ratio in p+p interactions is below the predictions of statistical models. However, the ratio in central Pb+Pb collisions is close to statistical model predictions for large volume systems. For detail see e.g. Ref. [32]

(ii) In p+p interactions, and thus also in Be+Be collisions, multiplicity fluctuations are larger than predicted by statistical models. However, they are close to statistical model predictions for large volume systems in central Ar+Sc and Pb+Pb collisions, for detail see Ref. [33].

Thus the observed rapid change of hadron production properties that start when moving from Be+Be to Ar+Sc collisions can be interpreted as the beginning of creation of large clusters of strongly interacting matter - the onset of fireball [31]. One notes that non-equilibrium clusters produced in p+p and Be+Be collisions seem to have similar properties at all beam momenta studied here.

Consequently the two-dimensional scan conducted by NA61/SHINE by varying collision energy and nuclear mass number of colliding nuclei indicates four domains

of hadron production separated by two thresholds: the onset of deconfinement and the onset of fireball. The sketch presented in Fig. 4 illustrates this conclusion.

The results on the onset of fireball can be considered within two theoretical approaches:

(i) The percolation approach [34–38] assumes that with increasing nuclear mass number the density of clusters (partons, strings, ...) in the transverse plane increases. Thus the probability to form large clusters by overlapping many elementary clusters may rapidly increase with A, the behaviour typical for percolation models. However, this approach does not explain the equilibrium properties of large clusters.

(ii) Within the AdS/CFT correspondence [39] creation of strongly interacting matter (system of strongly interacting particles in equilibrium) is dual to the formation of a (black hole) horizon and trapping some amount of information from the distant observer [40]. It was found that the formation of the trapping surface takes place when critical values of model parameters are reached [41]. This may serve as a possible explanation of the onset of the fireball phenomenon - only starting from a sufficiently large nuclear mass number the formation of the trapping surface in A+A collisions is possible. This is then observed as the onset of fireball.

A characteristic feature of a second order phase transition (the critical point or line) is the divergence of the correlation length. The system becomes scale invariant. This leads to large fluctuations in particle multiplicity. Moreover these fluctuations have specific characteristics [42,43]. Also other properties of the system should be sensitive to the vicinity of the critical point [44]. Thus when scanning the phase diagram a region of increased fluctuations may signal the critical point or the critical line.

Example results of NA61/SHINE from the search for the critical point using the $\Delta[P_T, N]$ and $\Sigma[P_T, N]$ fluctuation measures [45] are presented in Fig. 5. No indication for the critical point is observed so far.

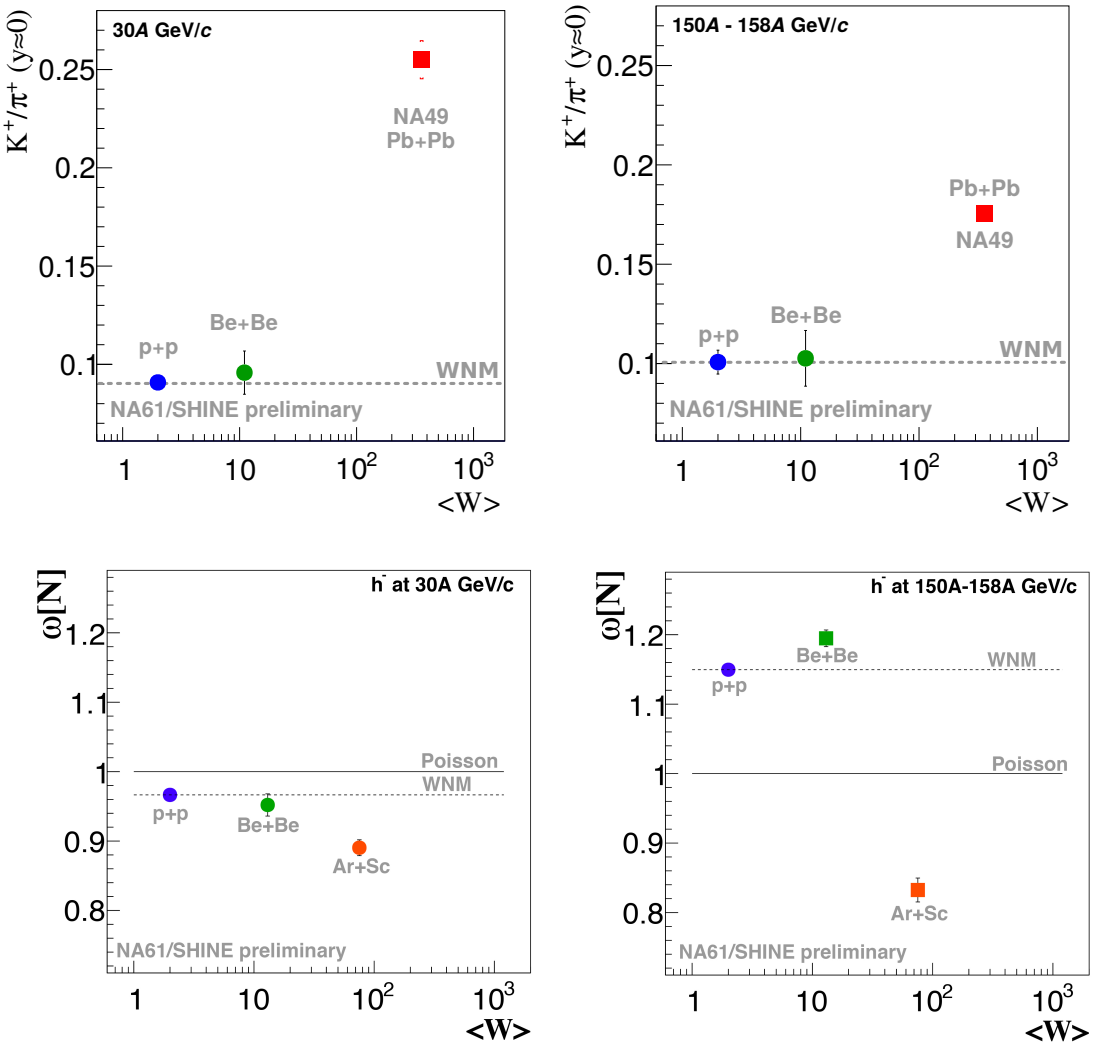

Figure 3: *Top left* and *top right*: System size dependence of the K^+/pip ratio at mid-rapidity at 30A GeV/c and 150A GeV/c. *Bottom left* and *bottom right*: System size dependence of the scaled variance of the multiplicity distribution of negatively charged hadrons at 30A GeV/c and 150A GeV/c.

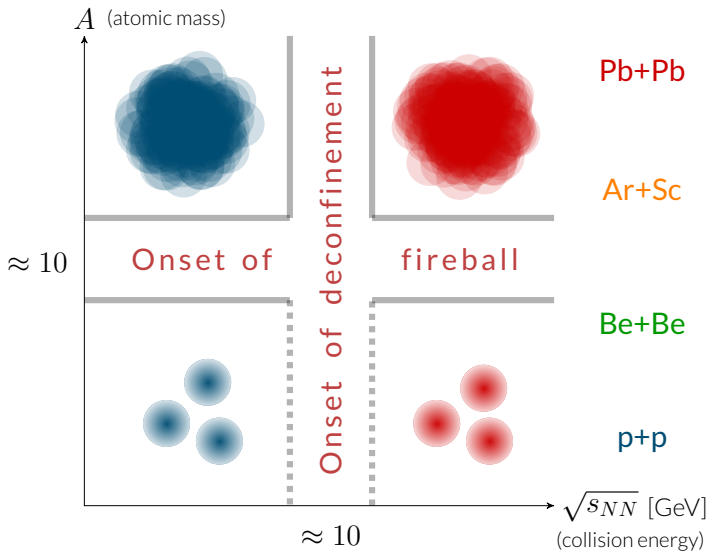

Figure 4: Two-dimensional scan conducted by NA61/SHINE varying collision energy and nuclear mass number of colliding nuclei indicates four domains of hadron production separated by two thresholds: the onset of deconfinement and the onset of fireball. The onset of deconfinement is well established in central Pb+Pb(Au+Au) collisions, its presence in collisions of low mass nuclei, in particular, inelastic p+p interactions is questionable.

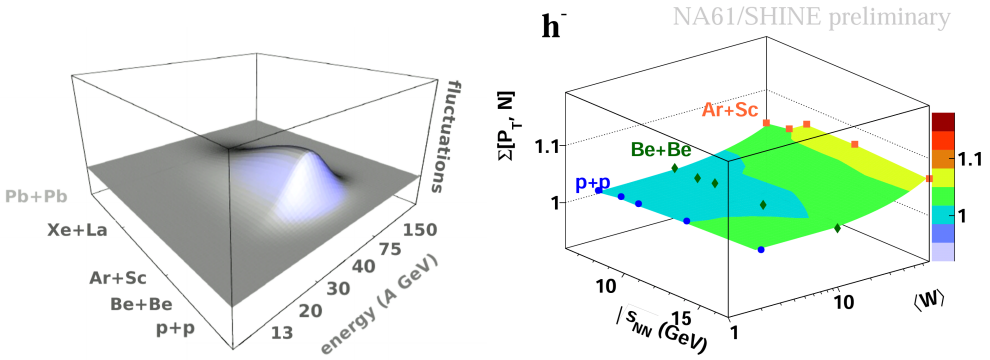

Figure 5: *Left*: Sketch of the hill of fluctuations which may be observed in the (beam momentum) - (system size) scan of NA61/SHINE provided the freeze-out parameters are close to the critical point. *Right*: $\Sigma[P_T, N]$ measured by NA61/SHINE in inelastic p+p interactions and violent Be+Be and Ar+Sc collisions at the CERN SPS energies. Results refer to negatively charged hadrons at forward rapidity ($0 < y_\pi < y_{beam}$) and $p_T < 1.5$ GeV/c.

4.2 Physics Motivation for Charm Measurements

The NA61/SHINE charm program is a natural extension of the previous studies of the phase transition to the quark-gluon plasma. It addresses the question of the validity and the limits of statistical and dynamical models of high energy collisions in the new domain of quark mass, $m_c \approx 1300$ MeV$>> T_C \approx 150$ MeV. Among many questions which might be answered by the new NA61/SHINE program, there are three that primarily motivate it [46], namely:

(i) What is the mechanism of charm production?

(ii) How does the onset of deconfinement impact charm production?

(iii) How does the formation of quark gluon plasma impact J/ψ production?

To answer these questions, knowledge is needed on the mean number of charm–anti-charm quark pairs $\langle c\bar{c}\rangle$ produced in the full phase space of heavy ion collisions. Such data do not exist yet and NA61/SHINE aims to provide them within the coming years.

4.2.1 Mechanism of charm production

Figure 6 presents a compilation of predictions by dynamical and statistical models on $\langle c\bar{c}\rangle$ produced in central Pb+Pb collisions at 158A GeV/c. These predictions are obtained from:

(i) The Hadron String Dynamics (HSD) model [49, 50] - a pQCD-inspired extrapolation of p+p data.

(ii) A pQCD-inspired model [47, 48] - calculation based on model assumptions and nucleon parton density functions only.

(iii) The Hadron Resonance Gas model (HRG) [51] - a calculation of equilibrium yields of charm hadrons assuming parameters of a hadron resonance gas fitted to mean multiplicities of light hadrons.

(iv) The Statistical Quark Coalescence model [51] - a statistical distribution of c and $\bar{c}$ quarks between hadrons. The mean number $\langle c\bar{c}\rangle$ of charm pairs is calculated using the measured $\langle J/\psi\rangle$ multiplicity [52] and the probability of a single $c\bar{c}$ pair hadronizing into a J/ψ calculated within the model.

(v) The Dynamical Quark Coalescence model [53] - quark coalescence as a microscopic hadronization mechanism of deconfined matter. The mean number $\langle c\bar{c}\rangle$ of charm pairs is calculated using the measured $\langle J/\psi\rangle$ multiplicity [52] and the probability of a single $c\bar{c}$ pair hadronizing into a J/ψ calculated within the model.

(vi) The Statistical Model of the Early Stage (SMES) [23] - the mean number of charm quarks is calculated assuming an equilibrium QGP at the early stage of the collision.

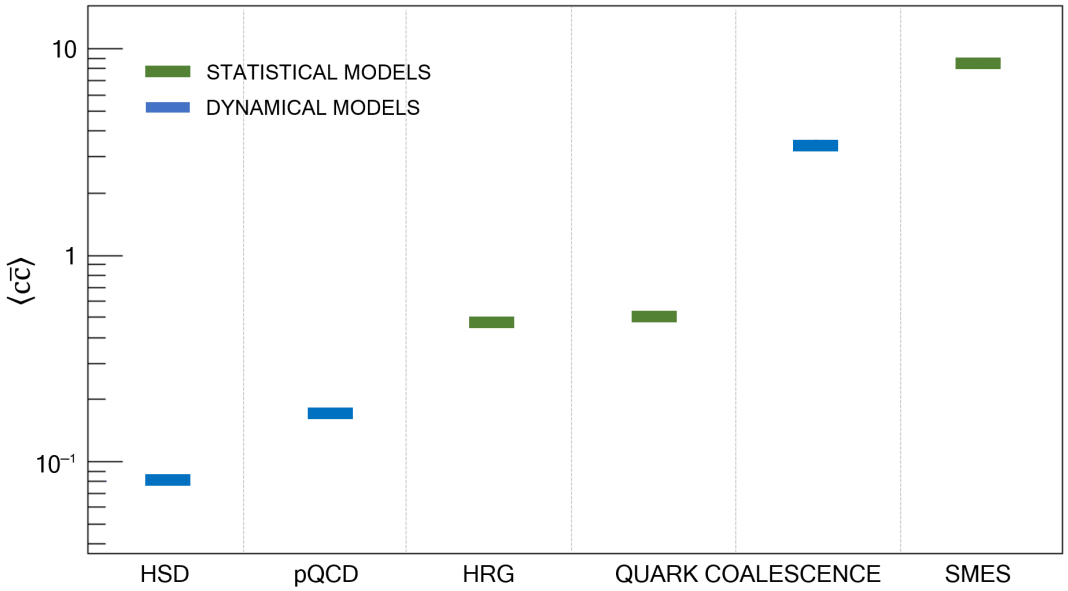

Figure 6: Mean multiplicity of charm quark pairs produced in the full phase space in central Pb+Pb collisions at 158*A* GeV/*c* calculated with dynamical models (blue bars): HSD [49,50], pQCD–inspired [47,48], and Dynamical Quark Coalescence [53], as well as statistical models (green bars): HRG [51], Statistical Quark Coalescence [51], and SMES [23].

The predictions of the models on $\langle c\bar{c}\rangle$ differ by about two orders of magnitude. Therefore, obtaining precise data on $\langle c\bar{c}\rangle$ is expected to allow to narrow the spectrum of viable theoretical models and thus learn about the charm quark and hadron production mechanisms.

4.2.2 Charm production as a signal of onset of deconfinement

The production of charm is expected to be different in confined and deconfined matter. This is caused by differences of the charm carriers in these phases. In confined matter the lightest charm carriers are D mesons, whereas in deconfined matter the carriers are charm quarks. Production of a $D\bar{D}$ pair ($2m_D = 3.7$ GeV) requires an energy about 1 GeV higher than production of a $c\bar{c}$ pair ($2m_c = 2.6$ GeV). The effective number of degrees of freedom of charm hadrons and charm quarks is similar [54]. Thus, more

abundant charm production is expected in deconfined than in confined matter. Consequently, in analogy to strangeness [23, 55], a change of collision energy dependence of $\langle c\bar{c}\rangle$ may be a signal of onset of deconfinement.

Figures 7 and 8 present the collision energy dependence of charm production in central Pb+Pb collisions at 150A GeV/c predicted by two very different models: the Statistical Model of the Early Stage [54] and a pQCD-inspired model [56], respectively.

Figure 7 shows the energy dependence of $\langle c\bar{c}\rangle$ predicted by the Statistical Model of the Early Stage. According to this model, when crossing the phase transition energy range ($\sqrt{s_{\rm NN}} = 7 - 11$ GeV), an enhancement of $\langle c\bar{c}\rangle$ production should be observed. At 150A GeV/c ($\sqrt{s_{\rm NN}} = 16.7$ GeV) an enhancement by a factor of about 4 is expected.

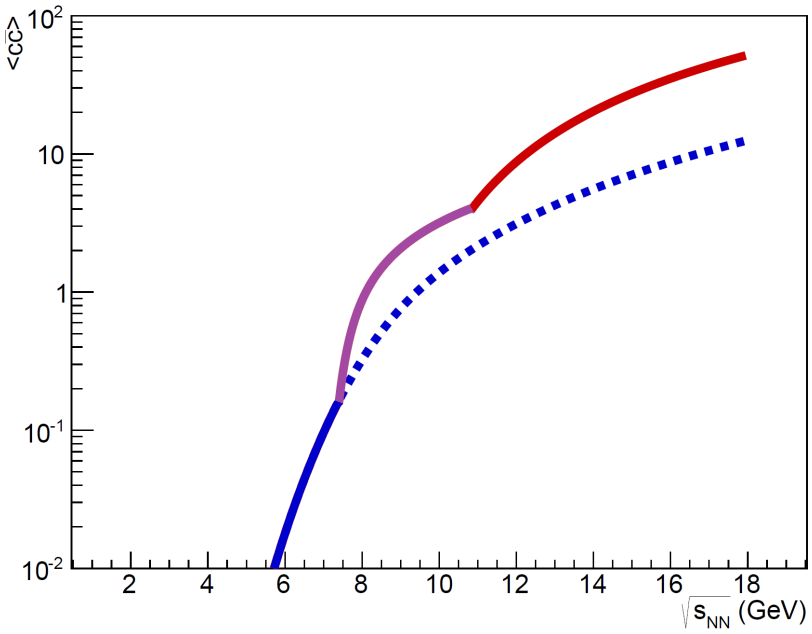

Figure 7: Energy dependence of $\langle c\bar{c}\rangle$ in central Pb+Pb collisions calculated within the SMES model [54, 57]. The blue line corresponds to confined, the purple line to mixed phase, and the red line to deconfined matter. The dashed line presents the prediction without a phase transition.

Figure 8 shows the ratio of mean multiplicity of $c\bar{c}$ pairs in deconfined and confined matter calculated with the pQCD-inspired model of Ref. [56]. Both numerator and denominator were evaluated at the same collision energy. At 150A GeV/c ($\sqrt{s_{\rm NN}} =$ 16.7 GeV) an enhancement by a factor of about 3 is predicted.

Accurate experimental results will allow to test these predictions.

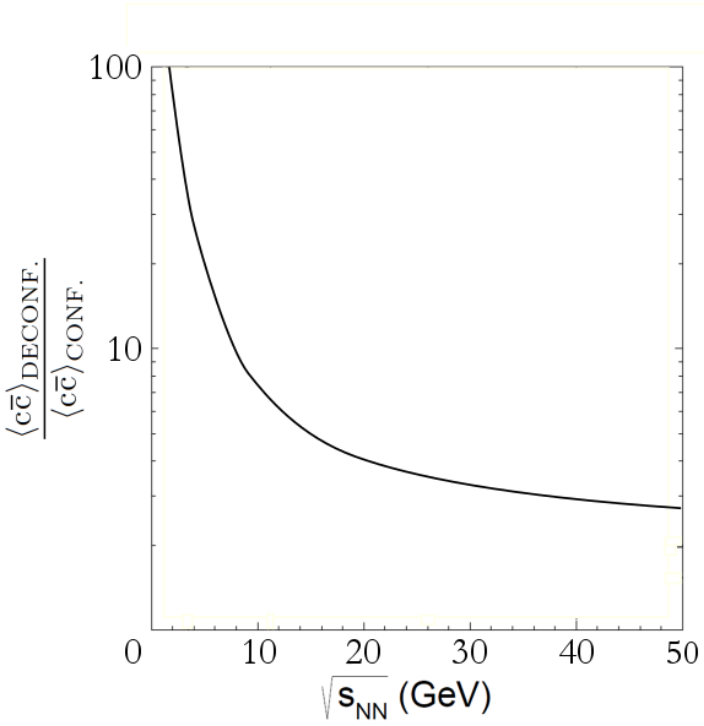

Figure 8: Energy dependence of the ratio of $\langle c\bar{c}\rangle$ in deconfined and confined matter in central Pb+Pb collisions calculated within the pQCD-inspired model of Ref. [56].

4.2.3 J/ψ production as a signal of deconfinement

Suppression of the production of J/ψ mesons in central Pb+Pb collisions at 158A GeV/c was an important argument for the CERN announcement of the discovery of a new state of matter [17]. Within the Matsui-Satz model [58] the suppression is attributed to the formation of the QGP.

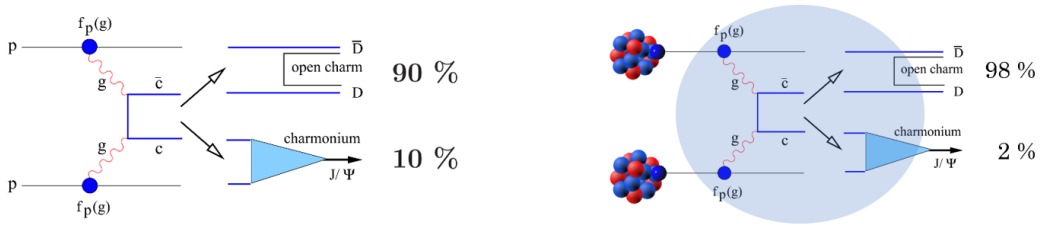

Figure 9: Sketch of the charmonium production mechanism and its relation to $c\bar{c}$ production in p+p interactions (*left*) and central heavy ion collisions (*right*) [59].

Figure 9 presents two scenarios of charmonium production. In the first case (Fig. 9 (*left*)), a produced $c\bar{c}$ pair hadronizes in vacuum - this corresponds to a p+p interaction.

Open charm and charmonia are produced in vacuum with a certain probability, at high collision energies typically 10% of $c\bar{c}$ pairs form charmonia and 90% appear in open charm hadrons.

The second scenario is illustrated in Fig. 9 (*right*). Here the $c\bar{c}$ pair forms a pre-charmonium state in the quark gluon plasma. Due to the color screening, which may lead to disintegration of this state, the probability of charmonium production is suppressed in favor of open charm production.

The probability of a $c\bar{c}$ pair hadronizing to J/ψ is defined as:

$$P\left(c\bar{c} \to J/\psi\right) \equiv \frac{\langle J/\psi \rangle}{\langle c\bar{c} \rangle} \equiv \frac{\sigma_{J/\psi}}{\sigma_{c\bar{c}}}. \tag{1}$$

To be able to calculate this probability, one needs data on both J/ψ and $c\bar{c}$ yields in full phase space. At the CERN SPS precise $\langle J/\psi \rangle$ data was provided by the NA38 [60], NA50 [52], and NA60 [61] experiments, while $\langle c\bar{c} \rangle$ data is not available at the CERN SPS energies.

The problem of the lack of $\langle c\bar{c} \rangle$ data was worked around [52, 58] by assuming that the mean multiplicity of $c\bar{c}$ pairs is proportional to the mean multiplicity of Drell-Yan pairs: $\langle c\bar{c} \rangle \sim \langle DY \rangle$.

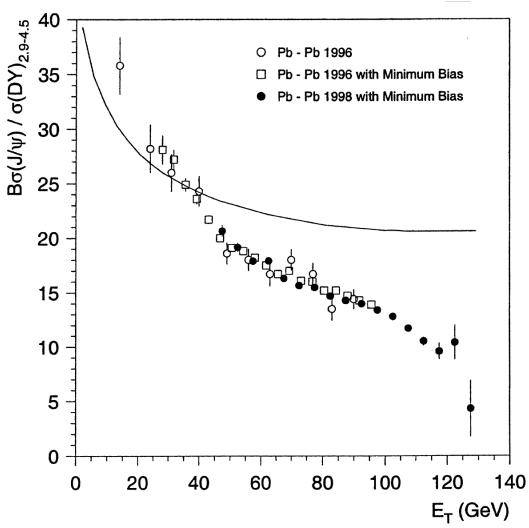

Figure 10: The ratio of $\sigma_{J/\psi}/\sigma_{DY}$ as a function of transverse energy (a measure of collision violence or centrality) in Pb+Pb collisions at 158A GeV measured by NA50. The curve represents the J/ψ suppression due to ordinary nuclear absorption [52].

Figure 10 shows the result from the NA50 experiment [52] that was interpreted as evidence for QGP creation in central Pb+Pb collisions at 158A GeV based on this assumption. However, the assumption $\langle c\bar{c} \rangle \sim \langle DY \rangle$ may be incorrect due to many effects, such as shadowing or parton energy loss [62].

This clearly shows the need for precise data on $\langle c\bar{c} \rangle$ in centrality selected Pb+Pb collisions at 150A GeV/c.

4.3 Preparatory Work

Precise measurements of charm hadron production by NA61/SHINE are expected to be performed in 2022–2024. The related preparations have started already. In 2015 and 2016, a Small Acceptance Vertex Detector was constructed and first measurements of open charm production started in 2016.

4.3.1 Small Acceptance Vertex Detector

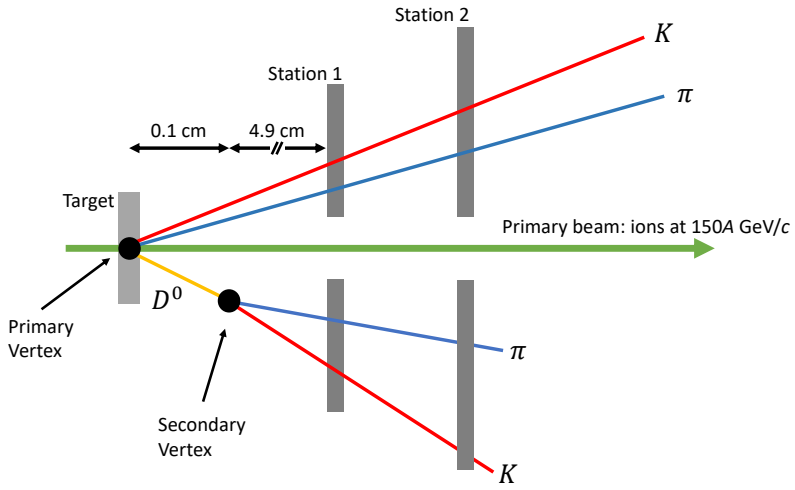

Figure 11: Schematics of reconstruction of a $D^0 \rightarrow \pi^+ + K^-$ decay with help of a vertex detector.

Starting the open charm program required construction of a new high-resolution vertex detector. Its role in measurements of charm hadrons is schematically shown in Fig. 11.

This measurement is challenging due to the short mean lifetime of charm hadrons and the relatively low branching ratios into reconstructable decay channels. Table 1 presents properties of the more frequently produced charm hadrons which are relevant for their measurement.

A big upside of NA61/SHINE is the fact, that it is a fixed-target experiment. Due to the Lorenz boost ($\beta\gamma \approx 10$ at midrapidity and $p_T \approx 0$), the average separation between the primary and the decay vertices of D^0 mesons is about 1 mm. This makes the measurement significantly easier than in the case of collider experiments. In addition, due to the fact that the magnetic field is perpendicular to the beam direction (unlike in a typical collider experiment, where it is parallel to the beam direction), the acceptance extends down to $p_T = 0$.

Table 1: The most frequently produced charm hadrons: their mass, mean life time, and the decay channels best suited for measurements are shown.

Hadron	Decay channel	$c\bar{\tau}$ [μm]	BR
D^0	$\pi^+ + K^-$	123	3.89%
D^+	$\pi^+ + \pi^+ + K^-$	312	9.22%
D_S^+	$\pi^+ + K^- + K^+$	150	5.50%
Λ_c	$p + \pi^+ + K^-$	60	5.00%

For the measurement of D^0 mesons the Small Acceptance Vertex Detector (SAVD) was added to the NA61/SHINE detector in October 2016 and positioned about 80 cm upstream of VTPC-1 (see Fig. 12).

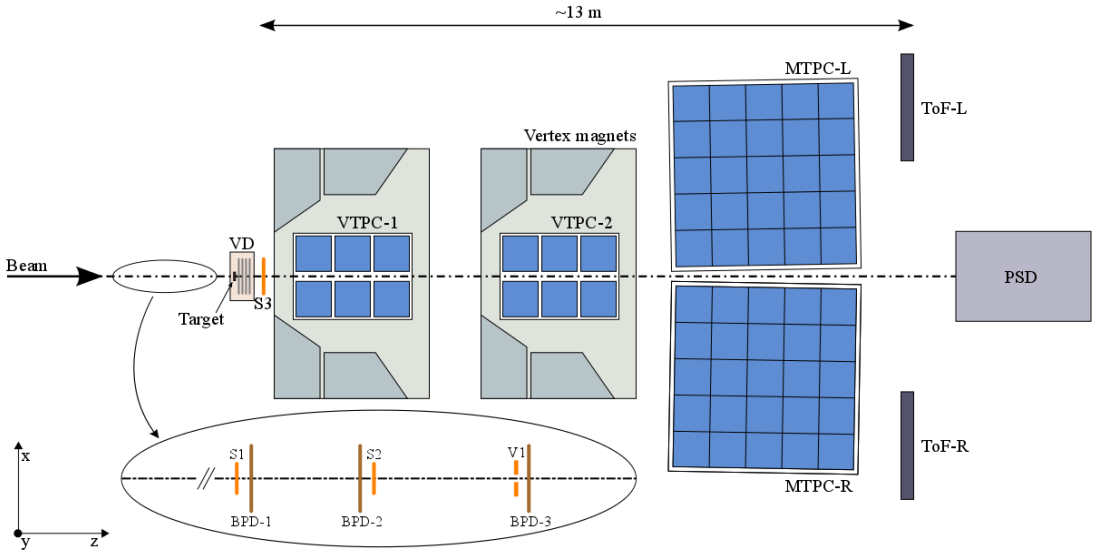

Figure 12: Schematic layout of the NA61/SHINE experiment at the CERN SPS (horizontal cut in the beam plane, not to scale). The beam and trigger counter configuration used for data taking of Pb+Pb collisions in 2016 is presented. The chosen right-handed coordinate system is shown on the plot. The incoming beam direction is along the z axis. The Small Acceptance Vertex Detector together with the integrated target station is located upstream of VTPC-1. The magnetic field bends charged particle trajectories in the x-z (horizontal) plane. The drift direction in the TPCs is along the y (vertical) axis.

The SAVD was built using sixteen CMOS MIMOSA-26 sensors [63]. The basic sensor

properties are:

(i) 18.4×18.4 μm^2 pixels,

(ii) 115 μs time resolution,

(iii) $10\times$ 20 mm^2 surface, 0.66 MPixel,

(iv) 50 μm thick.

The estimated material budget per layer, including the mechanical support, is 0.3% of a radiation length.

The sensors were glued to eight ALICE ITS ladders [64], which were mounted on two horizontally movable arms and spaced by 5 cm along the z (beam) direction. The detector box was filled with He (to reduce beam-gas interactions) and contained an integrated target holder to avoid unwanted material and multiple Coulomb scattering between target and detector.

Simulations of the performance of the SAVD performance using the AMPT model [65] as input has shown that about 5% [66] of all $D^0 \rightarrow \pi^+ + K^-$ decays will be reconstructed and accepted by the analysis cuts. Figure 13 shows the phase space coverage provided by the SAVD.

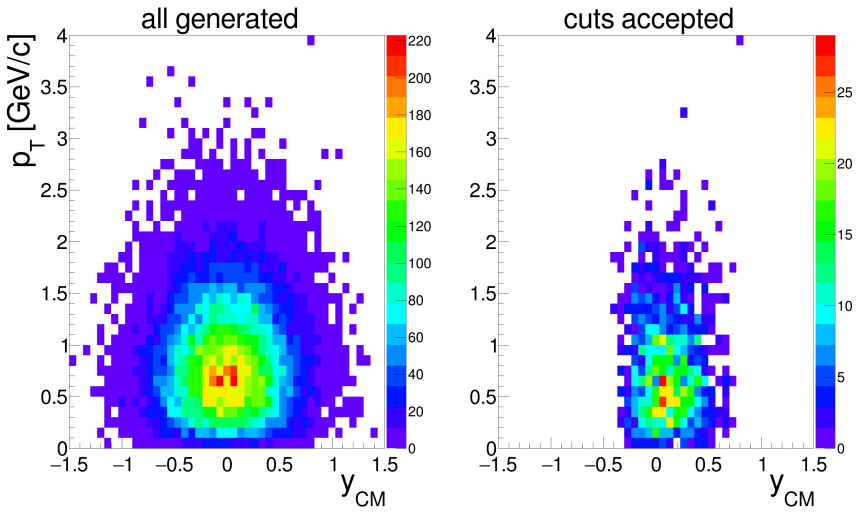

Figure 13: Transverse momentum and rapidity distributions of D^0 + $\overline{D^0}$ mesons produced in central Pb+Pb collisions at 150A GeV/c simulated within the AMPT model and corresponding to $3 \cdot 10^6$ events. *Left*: Results for all produced D^0 + $\overline{D^0}$ mesons. *Right*: results for D^0 + $\overline{D^0}$ mesons fulfilling the following criteria: decay $D^0 \rightarrow \pi^+ + K^-$, both decay products registered by the SAVD, passing background suppression and quality cuts [66].

4.3.2 Test data taking in 2016: Pb+Pb central collisions at 150A GeV/c

The SAVD was used in December 2016 during a Pb+Pb test run. Data on central Pb+Pb collisions at 150A GeV/c were collected. Using these data, the following was demonstrated:

(i) tracking in a large track multiplicity environment,

(ii) precise primary vertex reconstruction,

(iii) TPC and SAVD track matching,

(iv) feasibility to search for the D^0 and $\overline{D^0}$ signals.

Based on these data, the spatial resolution of the SAVD was determined. Cluster position resolution is $\sigma_{x,y}(\mathrm{Cl}) \approx 5$ μm and primary vertex resolution in the transverse plane is $\sigma_x(\mathrm{PV}) \approx 5$ μm, $\sigma_y(\mathrm{PV}) \approx 1.8$ μm[2], and along the beam direction is $\sigma_z(\mathrm{PV}) \approx 30\mu$m for a typical multiplicity of events recorded in 2016. Primary vertex resolution of 30 μm is sufficient to perform the search for the D^0 and $\overline{D^0}$ signals. Figure 14 shows the first indication of a D^0 and $\overline{D^0}$ peak obtained using the data collected during the Pb+Pb run in 2016.

4.3.3 Data taking in 2017 and 2018

Successful performance of the SAVD in 2016 led to the decision to also use it during the Xe+La data taking in 2017. About $5 \cdot 10^6$ events of central Xe+La collisions at 150A GeV/c were collected in October and November 2017. Data were recorded with both minimum bias and 0-20% centrality on-line trigger selection. During these measurements the thresholds of the MIMOSA-26 sensors were tuned to obtain high hit detection efficiency (which was not the case for the Pb+Pb test in 2016). This led to significant improvement in the primary vertex reconstruction precision, namely the spatial resolution of the primary vertices obtained for Xe+La data is on the level of 2.5 μm, 1 μm and 15 μm in x, y, and z coordinates, respectively. The distribution of the longitudinal coordinate (z_{prim}) of the primary vertex is shown in Figure 15 and the distributions of differences between x, y and z coordinates of the primary vertices reconstructed using different sub-events of SAVD tracks (see [31] for details) are shown in Figure 16. Note, that by construction the indicated sigma values (widths of distributions) should to be divided by 2 to obtain the spatial resolution of the full SAVD device.

The Xe+La data are currently under analysis and are expected to lead to physics results in the coming months. To get a first estimate of the number of D^0 and $\overline{D^0}$ decays that can be reconstructed in this data set, simulations for Pb+Pb collisions and p-QCD

[2] $\sigma_x(\mathrm{PV}) > \sigma_y(\mathrm{PV})$ because $B_y \gg B_x$

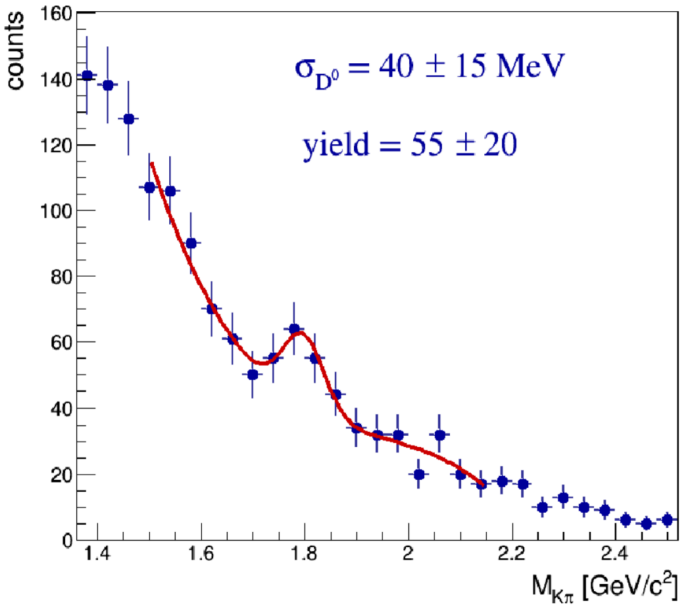

Figure 14: The invariant mass distribution of D^0 and $\overline{D^0}$ candidates in central Pb+Pb collisions at 150A GeV/c after the background suppression cuts. The particle identification capability of NA61/SHINE was not used at this stage of the analysis [66].

inspired system size dependence were combined. Based on these simulations, one expects to reconstruct several hundred of D^0 and $\overline{D^0}$ decays. These statistics could by itself lead to an important physics result.

Moreover, one could combine this measurement with published results on J/ψ production. The NA60 experiment [61] measured J/ψ production in In+In collisions (Fig. 17), which is a system of similar size as Xe+La. This combination of the NA60 data on J/ψ and the NA61/SHINE results on open charm could already challenge theoretical models.

The SAVD is also planned to be used during three weeks of Pb+Pb data taking in 2018 (recommended by the CERN SPS Committee in October 2017). About $1 \cdot 10^7$ central collisions should be recorded and 2500 D^0 and $\overline{D^0}$ decays can be expected to be reconstructed in this data set. The expected signal to background ratio is about 2.6 when using realistic particle identification information.

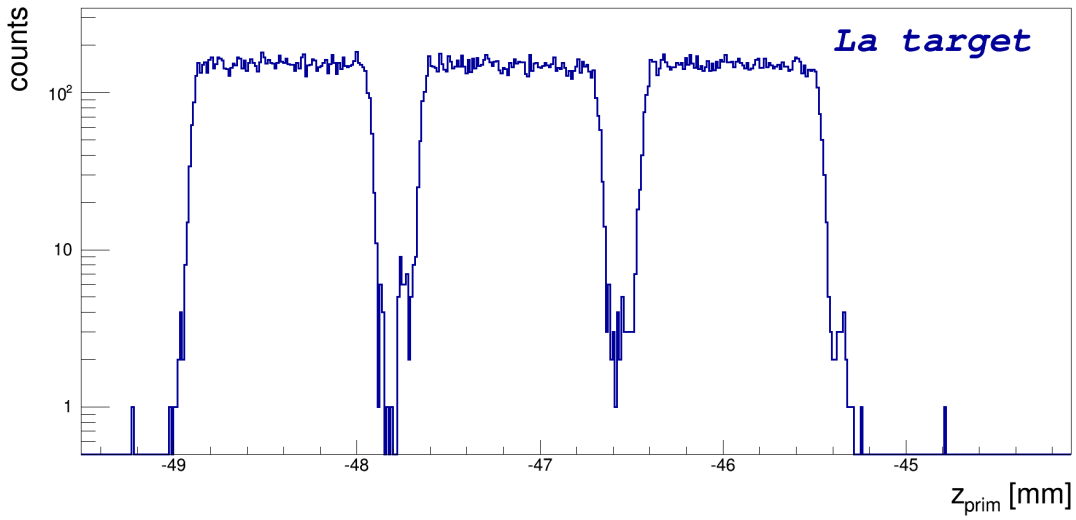

Figure 15: Distribution of longitudinal coordinate of the primary vertex z_{prim} for interactions in the La target, which was composed of three 1 mm plates.

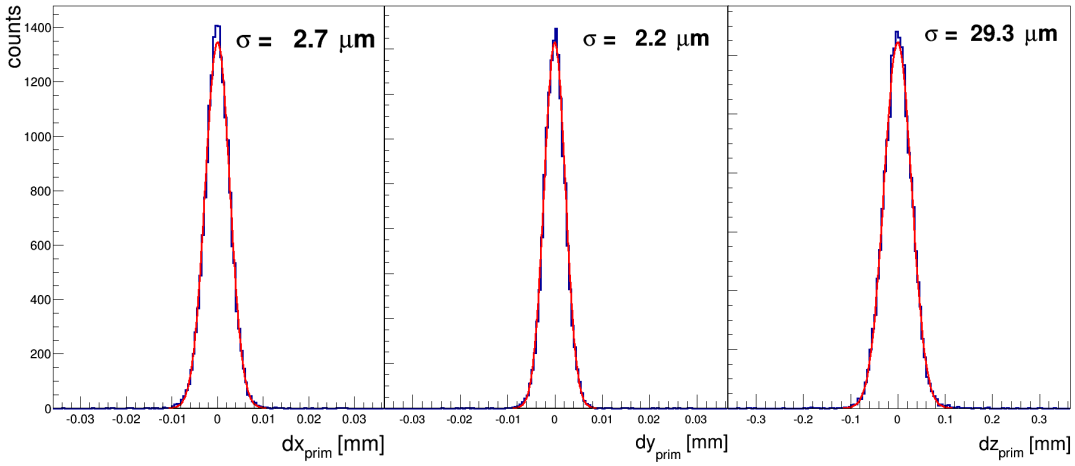

Figure 16: Distributions of differences between x, y and z coordinates of the primary vertices reconstructed using two different sub-events of SAVD tracks.

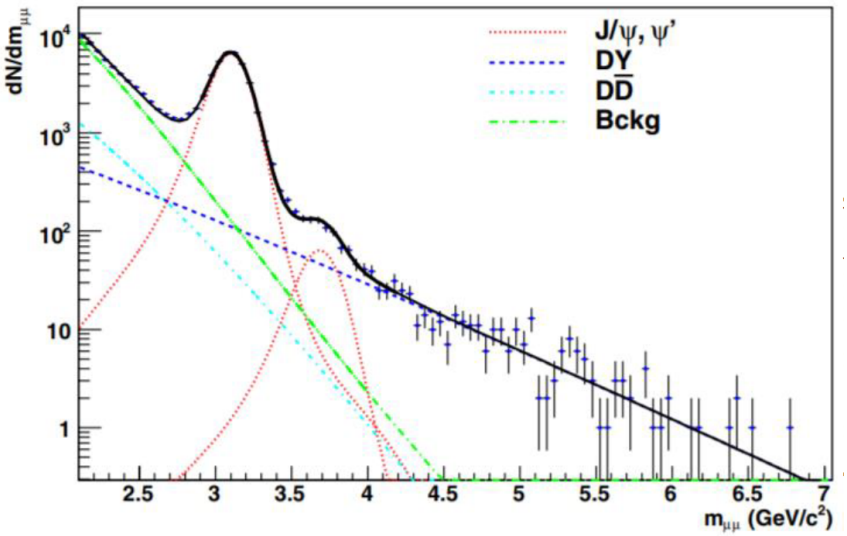

Figure 17: The invariant mass distribution of $\mu^+\mu^-$ pairs produced in In+In collisions at 158A GeV/c showing showing the J/ψ peak [61].

4.4 Future Measurements, Performance and Uniqueness

Data taking on Pb+Pb collisions and reconstruction of decays of various open charm mesons (see Table 1) are planned by NA61/SHINE for the years 2022–2024. In this section required detector upgrades, anticipated results and their uniqueness are presented.

4.4.1 Planned Detector Upgrades

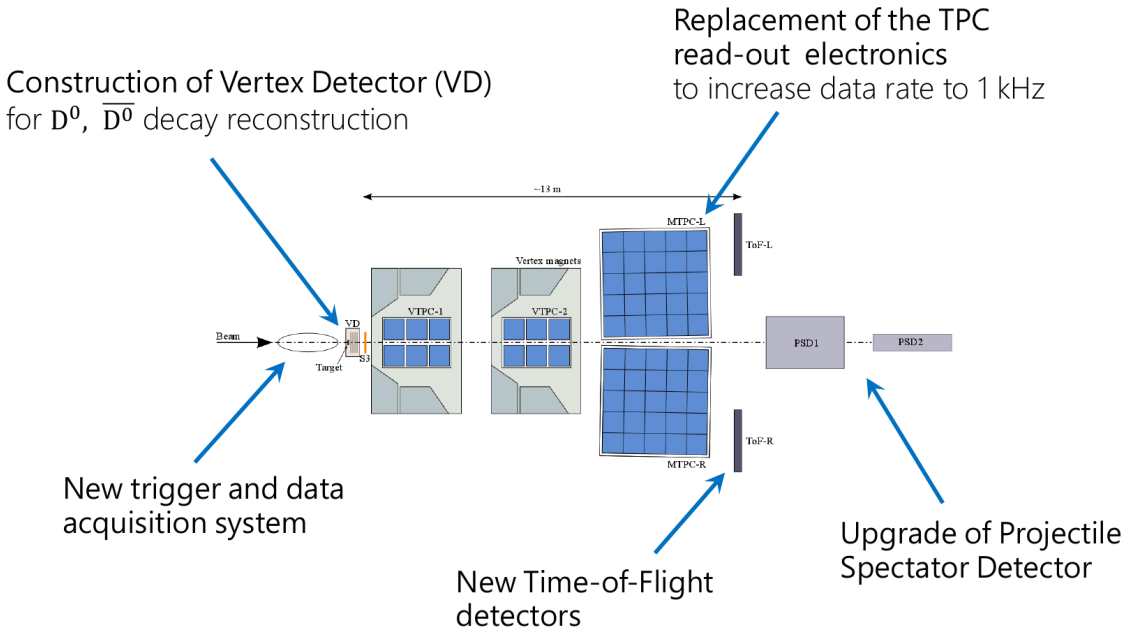

Figure 18: Upgrades of NA61/SHINE planned to be completed during the LS2 period.

During the Long Shutdown 2 at CERN (2019-2020), a significant modification of the NA61/SHINE spectrometer is planned. The upgrade is primarily motivated by the charm program which requires a tenfold increase of the data taking rate to about 1 kHz and an increase of the phase-space coverage of the Vertex Detector by a factor of about 2. This, in particular, requires the following:

(i) construction of the Vertex Detector (VD),

(ii) replacement of the TPC read-out electronics,

(iii) implementation of new trigger and data acquisition systems,

(iv) upgrade of the Projectile Spectator Detector.

Finally, new ToF detectors are planned to be constructed for particle identification at mid-rapidity. This is mainly motivated by possible future measurements related to the

onset of fireball, see Sec. 5 for detail. The detector upgrades are graphically summarized in Fig. 18 and discussed in detail in Sec. 4.5. With the upgraded NA61/SHINE spectrometer, one expects that during one day of data taking $6 \cdot 10^6$ Pb+Pb collisions at 150A GeV/c will be collected, see Sec. 9.1 for detail.

The data taking plan related to the open charm measurements in 2022-2024 is shown in Table 2. All inelastic Pb+Pb collisions at 150A GeV/c will be recorded in 2022 and 2023. This data will provide the mean number of $c\bar{c}$ pairs in central Pb+Pb collisions needed to investigate the mechanism of charm production in this reaction, see Sec. 4.2.1 for detail. Moreover, the data will allow to establish the centrality dependence of $\langle c\bar{c} \rangle$ in Pb+Pb collisions at 150A GeV/c and thus address the question of how the formation of QGP impacts J/ψ production, see Sec. 4.2.3 for detail. Table 3 lists the expected number of charm mesons in centrality selected Pb+Pb collisions at 150A GeV/c assuming statistics of minimum bias collisions as given in Table 2. The estimate is performed assuming that mean multiplicity of charm hadrons is proportional to the number of collisions and using yields calculated for central Pb+Pb collisions within the HSD model [49,50]. Central (0-30%) Pb+Pb collisions at 40A GeV/c are planned to be recorded in 2024. This data together with the result for central Pb+Pb collisions at 150A GeV/c will start a long-term effort to establish the collision energy dependence of $\langle c\bar{c} \rangle$ and address the question of how the onset of deconfinement impacts charm production, see Sec. 4.2.2 for detail.

Table 2: The NA61/SHINE data taking plan related to the charm program: year, beam, number of data taking days, number of recorded Pb+Pb collisions as well as numbers of reconstructed decays of $D^0 + \overline{D^0}$ and $D^+ + D^-$ mesons passing the background suppression cuts are given from left to right. Minimum bias Pb+Pb collisions at 150A GeV/c will be recorded in 2022 and 2023. 30% of the most violent Pb+Pb collisions at 40A GeV/c will be recorded in 2024. This document requests data taking in 2022 only.

Year	Beam	#days	#events	#($D^0 + \overline{D^0}$)	#($D^+ + D^-$)
2022	Pb at 150A GeV/c	42	250M	38k	23k
2023	Pb at 150A GeV/c	42	250M	38k	23k
2024	Pb at 40A GeV/c	42	250M	3.6k	2.1k

Statistics of charm mesons given in Table 2 is based on Monte Carlo simulations that utilize particles transport through the NA61/SHINE upgraded set-up. The momentum distribution of charm mesons was calculated within the AMPT model [67] and mean multiplicities are taken as predicated by the HSD model [50,68] (see Sec. 5.2 in Ref. [66] for detail). This simulation input was selected as the HSD predictions are considered

Table 3: Expected number of charm mesons in centrality selected Pb+Pb collisions at 150A GeV/c assuming 500M minimum bias events recorded in 2022 and 2023, see text for detail. The mean number of wounded nucleons $\langle W \rangle$ calculated within the Wounded Nucleon Model is also given.

	0–10%	10–20%	20–30%	30–60%	60–90%	0–90%
$\#(D^0 + \overline{D^0})$	31k	20k	11k	13k	1.3k	76k
$\#(D^+ + D^-)$	19k	12k	7k	8k	0.8k	46k
$\langle W \rangle$	327	226	156	70	11	105

the most realistic but the HSD momentum distribution was not available. The expected high statistics of reconstructed D^0 and $\overline{D^0}$ decays is due to the high event rate and the relatively large efficiencies of open charm detection in the VD. The efficiency will be about 13% (3 times better than for the SAVD) for the $D^0 \to \pi^+ + K^-$ decay channel and about 9% [3] for D^+ decaying into $\pi^+ + \pi^+ + K^-$.

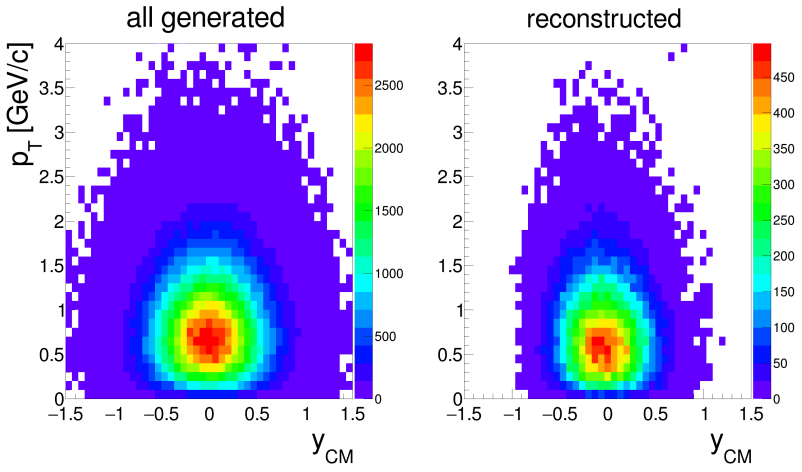

Figure 19: Transverse momentum and rapidity distribution of $D^0 + \overline{D^0}$ mesons produced in about 500M inelastic Pb+Pb collisions at 150A GeV/c for all produced $D^0 + \overline{D^0}$ mesons (*left*) and $D^0 + \overline{D^0}$ mesons fulfilling the following criteria: decay $D^0 \to \pi^+ + K^-$, decay products registered by the VD, passing background suppression cuts *(right)*.

[3] The quoted efficiencies include the geometrical acceptance for $D^0 \to \pi^+ + K^-$ ($D^+ \to \pi^+ + \pi^+ + K^-$) decays and the efficiency of the analysis quality cuts used to reduced the combinatorial background.

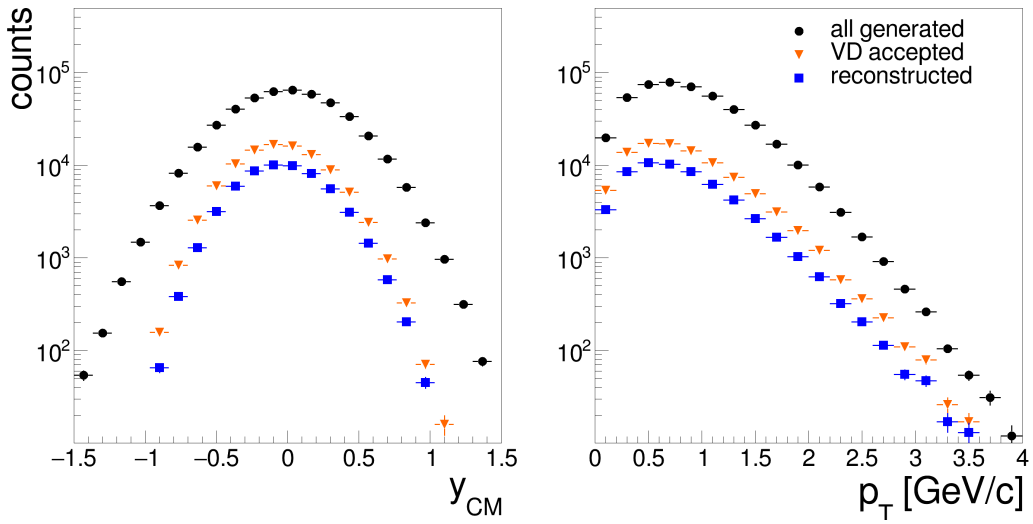

Figure 20: Rapidity (*left*) and transverse momentum (*right*) distributions of $D^0 + \overline{D^0}$ mesons produced in about 500M inelastic Pb+Pb collisions at 150A GeV/c. Dots indicate all generated mesons, triangles mesons within the VD acceptance and squares mesons within the VD acceptance and passing background suppression cuts.

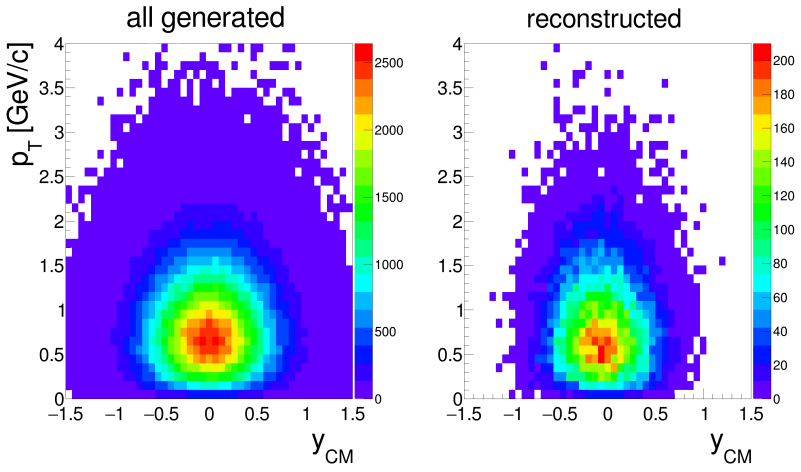

Figure 21: Transverse momentum and rapidity distribution of $D^+ + D^-$ mesons produced in about 500M inelastic central Pb+Pb collisions at 150A GeV/c for all produced $D^+ + D^-$ mesons (*left*) and $D^+ + D^-$ fulfilling the following criteria: decay $D^0 \rightarrow \pi^+ + K^-$, decay products registered by the VD, passing background suppression cuts *(right)*.

Figure 19 (21) shows distribution of $D^0 + \overline{D^0}$ ($D^+ + D^-$) mesons in rapidity and transverse momentum for all generated particles (*left*) and for particles passed the acceptance and background reduction cuts (*right*). The presented plots refer to about 500M inelastic Pb+Pb collisions at 150A GeV/c as indicated in Table 2. To provide more quantitative

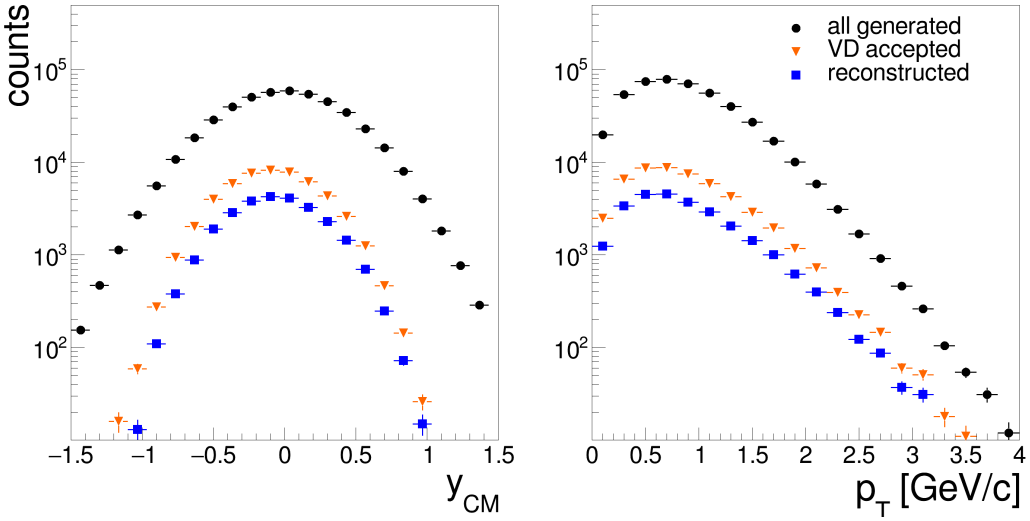

Figure 22: Rapidity (*left*) and transverse momentum (*right*) distributions of $D^+ + D^-$ mesons produced in about 500M inelastic Pb+Pb collisions at 150A GeV/c. Dots indicate all generated $D^+ + D^-$ mesons, triangles mesons for which both decay products are registered by the VD and squares mesons within the VD acceptance and passing background suppression cuts.

view we show also projected rapidity (*left*) and transverse momentum (*right*) distributions for $D^0 + \overline{D^0}$ (Fig. 20) and $D^+ + D^-$ (Fig. 22).

Based on the presented simulations one estimates, that fully corrected results will correspond to more than 90% of the D^0 and $\overline{D^0}$ yield (see Figs. 19 and 20). Total uncertainty of $\langle D^0 \rangle$ and $\langle \overline{D^0} \rangle$ is expected to be about 10% and is dominated by systematic uncertainty.

4.4.2 Anticipated results

Figure 23 shows the foreseen accuracy of the NA61/SHINE data on mean charm multiplicity compared to predictions of charm production models (see Sec. 4.2 for detail). The red band indicates the expected accuracy of the NA61/SHINE result on the charm yield assuming the yield prediction of the HSD model [49]. With that accuracy it should be possible to exclude most of the current models.

Figure 24 shows the expected accuracy of the NA61/SHINE data on $\langle c\bar{c} \rangle$ compared to SMES model predictions (see Sec. 4.2 for details). Red bars indicate the foreseen accuracy of the NA61/SHINE result on charm multiplicity for energies proposed for the NA61/SHINE charm production studies: 40A GeV/c ($\sqrt{s_{NN}} = 8.6$ GeV) and 150A GeV/c ($\sqrt{s_{NN}} = 16.7$ GeV). These results would be a start of confronting data with model predictions on collision energy dependence. Clearly measurements at more energies are necessary. In the future, these can be performed at J-PARC-HI and FAIR SIS-300.

Figure 25 shows the expected accuracy of the future NA61/SHINE results on the

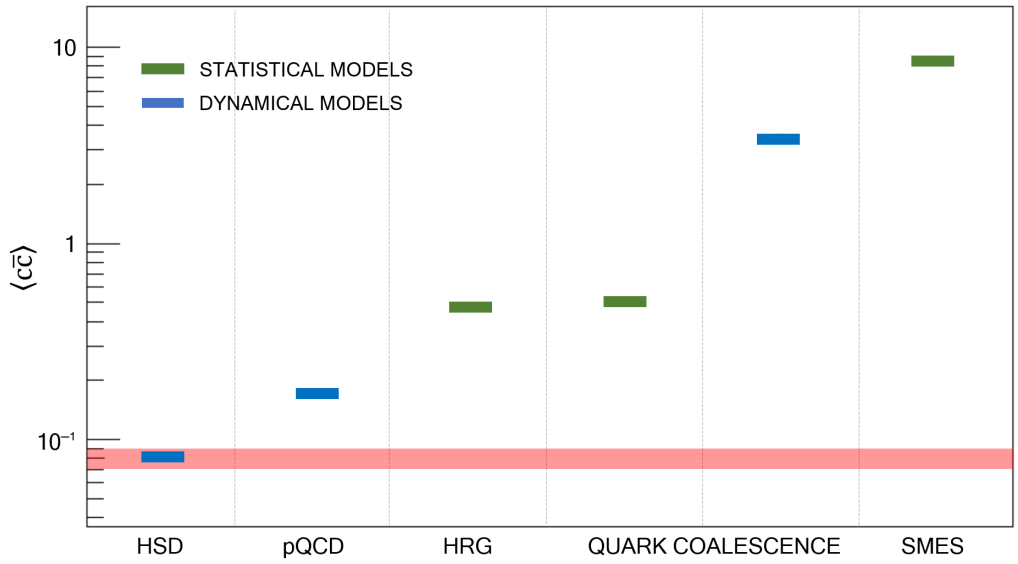

Figure 23: Mean multiplicity of charm quark pairs produced in central Pb+Pb collisions at 158A GeV/c calculated within dynamical models (blue bars) and statistical models (green bars). The width of the red band, at the location assuming HSD predictions, shows the foreseen the accuracy of the NA61/SHINE 2020+ result.

charm yield compared to J/ψ suppression data (see Sec. 4.2 for details). The red bars indicate the foreseen accuracy of the $\sigma_{J/\psi}/\sigma_{c\bar{c}}$ result that was made assuming $\sigma_{c\bar{c}} \propto \sigma_{\pi}$. One will be able to distinguish between two extreme scenarios: $\langle c\bar{c} \rangle \propto \langle DY \rangle$ or $\langle c\bar{c} \rangle \propto \langle \pi \rangle$.

4.4.3 Uniqueness of NA61/SHINE Results

Figure 26 presents a compilation of present and future facilities and their region of coverage in the phase diagram of strongly interacting matter. Their capability to measure charm hadrons in Pb+Pb (Au+Au) collisions is summarized below:

(i) LHC and RHIC at high energies ($\sqrt{s_{NN}} \gtrsim 200$ GeV): measurements of open charm are performed in a significantly limited acceptance; this limitation is due to the collider kinematics and related to the detector geometry [70–73].

(ii) RHIC BES collider ($\sqrt{s_{NN}} = 7.7 - 39$ GeV): measurement not considered in the current program, this may likely be due to difficulties related to collider geometry and kinematics as well as the low charm production cross-section [74,75].

(iii) RHIC BES fixed-target ($\sqrt{s_{NN}} = 3 - 7.7$ GeV): not considered in the current program [76].

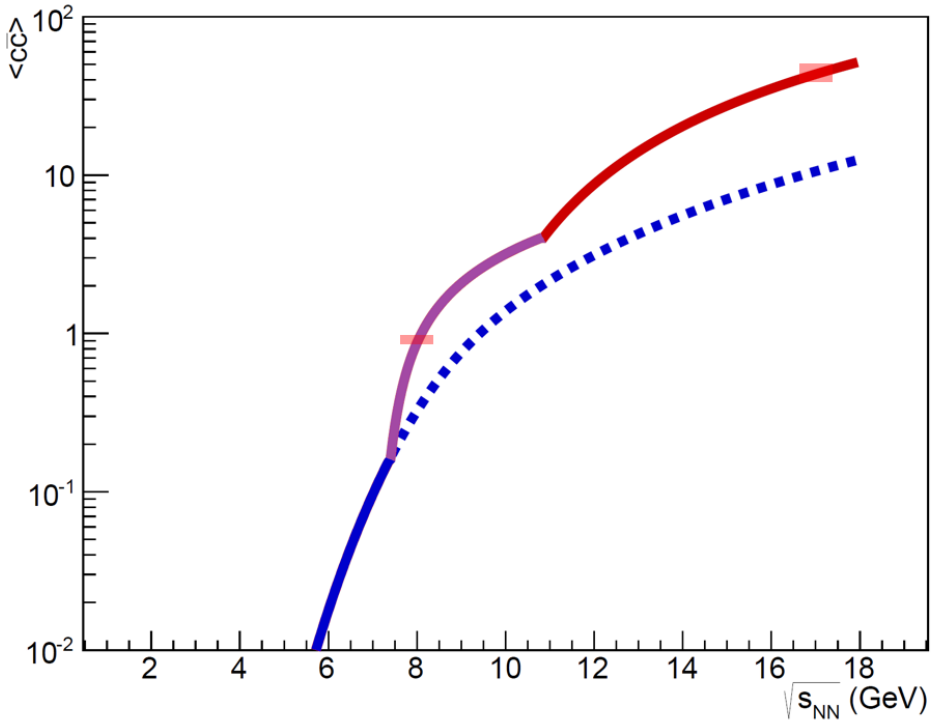

Figure 24: Energy dependence of $\langle c\bar{c} \rangle$ in central Pb+Pb collisions calculated within the SMES model. The red bars show the foreseen accuracy of the NA61/SHINE results for two energies: 40A GeV/c ($\sqrt{s_{\mathrm{NN}}} = 8.6$ GeV) and 150A GeV/c ($\sqrt{s_{\mathrm{NN}}} = 16.7$ GeV), assuming the SMES model yields [23].

(iv) NICA ($\sqrt{s_{\mathrm{NN}}} < 11$ GeV): measurements during stage 2 (after 2023) are under consideration [77,78].

(v) J-PARC-HI ($\sqrt{s_{\mathrm{NN}}} \lesssim 6$ GeV): under consideration, may be possible after 2025 [79,80].

(vi) FAIR SIS-100 ($\sqrt{s_{\mathrm{NN}}} \lesssim 5$ GeV): not possible due to the very low cross-section at SIS-100, systematic charm measurements are planned with SIS-300 ($\sqrt{s_{\mathrm{NN}}} \lesssim 7$ GeV) which is part of the FAIR project, but not of the start version (timeline is unclear) [81,82].

The conclusion is that only NA61/SHINE is able to measure open charm production in heavy ion collisions in full phase space in the near future. The corresponding potential measurements at higher (LHC, RHIC) and lower (FAIR, J-PARC) energies are necessary to complement the NA61/SHINE results and establish collision energy dependence of charm production. Potential measurements at NICA and RHIC BES fixed-target will allow to cross-check the NA61/SHINE data.

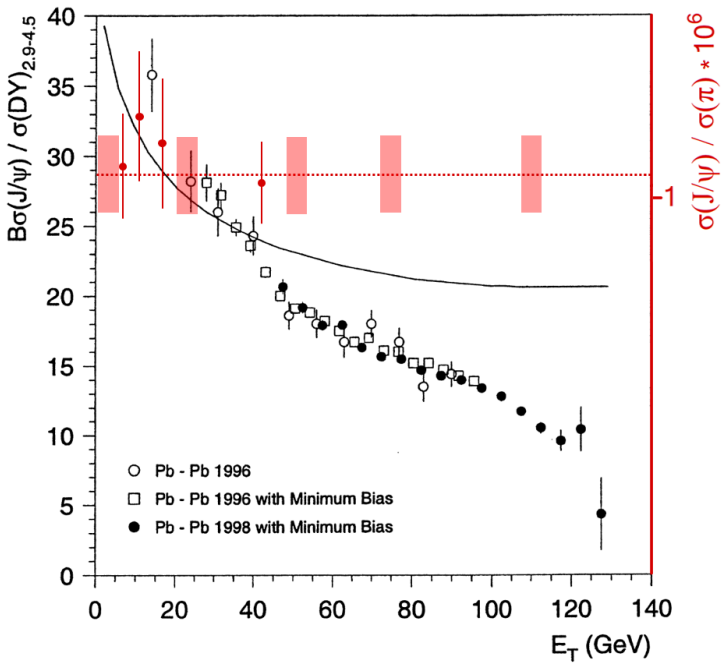

Figure 25: The ratio of $\sigma_{J/\psi}/\sigma_{DY}$ (*left*) and $\sigma_{J/\psi}/\sigma_{\pi}$ (*right*) as a function of transverse energy in Pb+Pb collisions at 158A GeV. The $\sigma_{J/\psi}/\sigma_{DY}$ ratio was measured by NA50 [52] and was used to calculate the $\sigma_{J/\psi}/\sigma_{\pi}$ ratio in Ref. [69]. Red bars mark the expected accuracy of the $\sigma_{J/\psi}/\sigma_{c\bar{c}}$ result of NA61/SHINE 2020+ assuming $\sigma_{c\bar{c}} \propto \sigma_{\pi}$ and scaled to the $\sigma_{J/\psi}/\sigma_{DY}$ ratio in peripheral collisions.

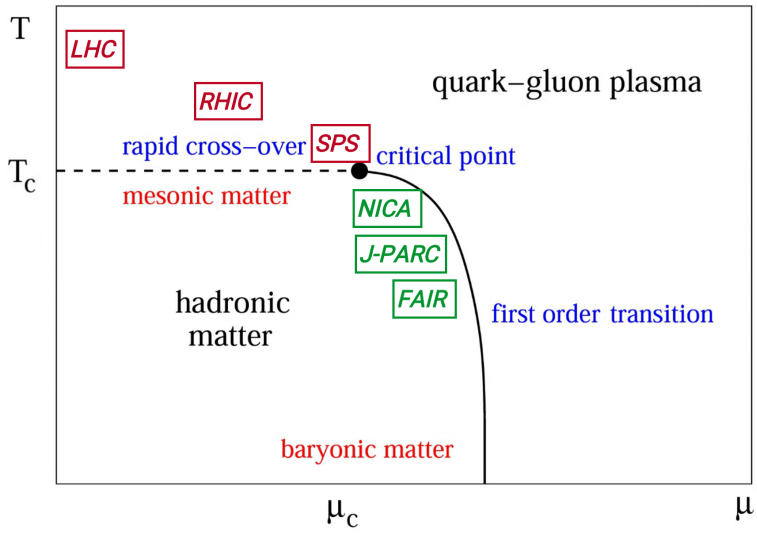

Figure 26: Present (red) and future (green) heavy ion facilities in the phase diagram of strongly interacting matter.

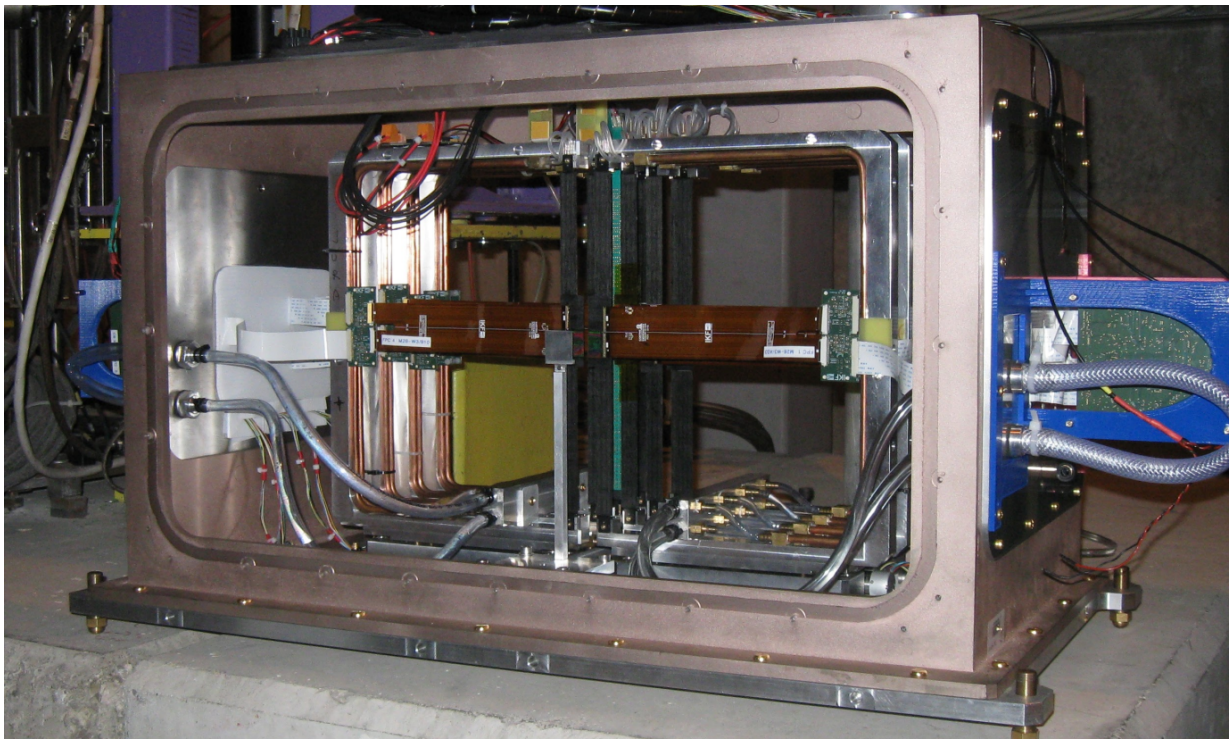

Figure 27: The SAVD used by NA61/SHINE during the data taking in 2016 and 2017

4.5 Detector Upgrades

This section presents the NA61/SHINE detector upgrades primarily required by the charm program. We plan commissioning and calibration of the upgraded detector in 2021 with hadron beams. Two weeks of the beam time will be needed for this purpose.

4.5.1 Upgrade of the NA61/SHINE Vertex Detector

The upgrade of the existing SAVD detector aims to adapt this detector to the requirements of data taking with a 1 kHz trigger rate, and to increase its geometrical acceptance. Both measures will yield significant ($\sim$30$\times$) increase of statistics of the reconstructed decays of charm hadrons.

To fulfil its task, the novel Vertex Detector (VD) will have to provide a rate capability, which exceeds the one of the SAVD by one order of magnitude. The related data rate is found to exceed the possibilities of the successful MIMOSA-26AHR sensors used so far in the SAVD. Moreover, the related increase of the radiation doses has to be considered. The requirements on the sensors can be estimated by scaling the related numbers derived for the SAVD [83] to the novel running scenario. This is done assuming that the VD will operate at a true collision rate of 5 kHz, and at a duty cycle of 0.15. The results for the most exposed point of the VD and an operation time of 40 days are shown in Table 4. No safety margin was considered. One finds the radiation load dominated by

Radiation source	Ionizing	Non-ionizing
	[krad]	[10^{12} n_{eq}/cm^2]
Direct particles	35	1.3
Delta electrons	40	Negligible
Beam halo (scaled)	1200	2.0
Beam halo (measured)	200	0.3
Sum requirements	275-1275	3.3
ALPIDE	> 500	17.0

Table 4: Radiation doses for the most exposed point of the VD and a run of 40 days with 150A GeV/c Pb+Pb. For the radiation dose generated by the beam halo, numbers scaled from Ref. [83] (scaled) and numbers relying on measurements of the beam halo performed during the 2017 Xe+La run at 150A GeV/c (measured) are shown. The beam halo of the Xe–beam was reduced by means of dedicated beam tuning. The related numbers are considered as most representative for future experiments.

the damage caused by direct beam ions from the beam halo, which varies substantially depending on the quality of the beam tuning. The table provides two numbers based on the scaling of our initial assumptions as described in the reference and based on a measurement of the beam halo carried out during the 2017 Xe+La at 150A GeV/c run. One observes that optimizing the beam for a low beam halo yielded into a significant improvement in terms of low radiation load. Despite remaining moderate, the ionizing radiation doses exceed once more the radiation tolerance of the previously used MIMOSA-26AHR sensors.

The novel detector will reuse the mechanics and infrastructure of the SAVD. A photograph of the SAVD just before its installation on the beam for the test measurement in 2016 is shown in Fig. 27. One can see vertically oriented carbon fibre ladders with MIMOSA-26 sensors installed in their centres as well as the Pb target of 1 mm thickness located about 50 mm upstream from the first SAVD station. The carbon fiber ladders are exactly the same as these used in the Inner Barrel of the new ALICE Inner Tracking System (ITS); the group of the St. Petersburg State University involved in their development and construction is also member of NA61/SHINE. More details on the construction and performance of the SAVD are provided in Sec. 4.3.

Table 5: Comparison of basic parameters of MIMOSA and ALPIDE sensors.

	MIMOSA-26AHR	ALPIDE
Sensor thickness (μm)	50	50
Spatial resolution (μm)	3.5	5
Dimensions (mm^2)	10.6×21.2	13.8×30
Power density (mW/cm^2)	250	40
Time resolution (μs)	115.2	10
Detection efficiency (%)	>99	>99
Dark hit occupancy	$\lesssim 10^{-4}$	$\lesssim 10^{-6}$

In spite of the good experience with the MIMOSA-26AHR sensors in the construction and operation of the SAVD, the VD cannot be built using these sensors: in order to cope with the 10-fold increase in beam intensity and interaction rate better (a factor of 10) time resolution is required. We consider the ALPIDE sensor and the detector concept developed for the new ALICE ITS the best candidate for the VD in 2022. In December 2016 one ITS Inner Barrel stave with 9 ALPIDE chips, the green vertical structure in Fig. 27, was already successfully operated in NA61/SHINE during 5 days of the test with Pb+Pb collisions at 150A GeV/c. Discussions concerning further collaboration and technology transfer already started.

In the spirit of the above considerations the upgraded Vertex Detector (VD) will rely on the carbon fibre support structures developed for the ALICE ITS. Instead of the elder MIMOSA-26AHR, they will host the modern ALPIDE CMOS Pixel Sensors [84]. A comparison of the features of both sensors is given in Table 5.

The novel sensors come with a time resolution of 10 μs, which is by more than one order of magnitude faster than the average time between two collisions, and a powerful $\sim$ 1 Gbps data interface. This fact and the capability of ALPIDE to use external trigger information for data reduction assures the rate capability required for the VD. As shown in Table 4, the sensor does as well match the requirements in terms of radiation dose. To estimate its tolerance to direct ion hits in terms of SEE, the sensor was operated for several days in a direct Xe-beam at the SPS in 2017 and no crucial incident was observed. This suggests that the chip is not particularly vulnerable and that no dedicated detector safety system for the case of beam displacement is required. Note that the tolerance of

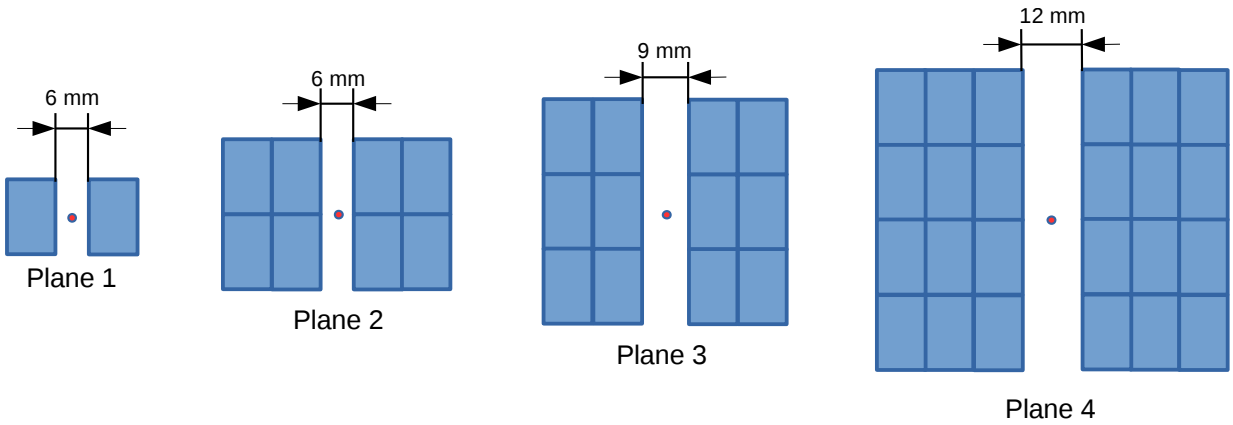

Figure 28: Schematic view of the VD layers based on ALPIDE sensors. From left to right: the first layer with two sensors, the second layer with 8 sensors, the third layer with 12 sensors and the fourth layer with 24 sensors. The total active area of the VD sensors is 190 cm^2.

ALPIDE to ionizing radiation does likely exceed the 500 krad guaranteed so far. This is a subject of ongoing research.

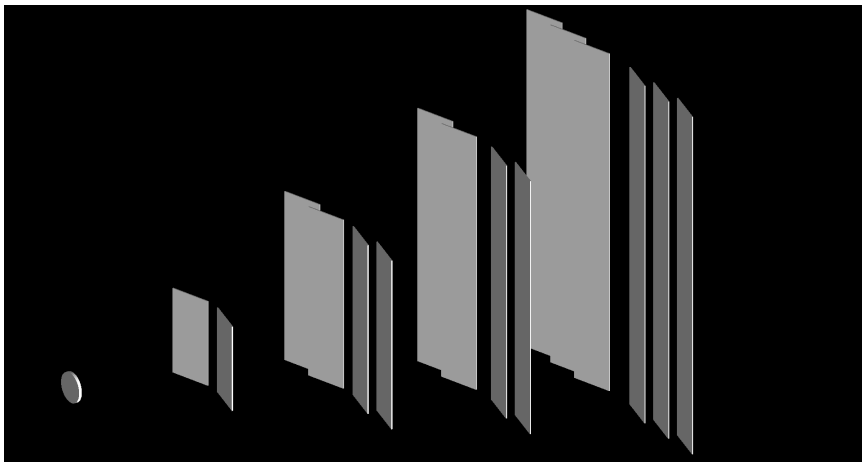

Figure 29: The GEANT4 visualisation of the VD detector geometry described in Fig. 28.

As the fibre supports were initially designed for ALPIDE, the carbon fibre plates required for adapting them mechanically to MIMOSA-26AHR become obsolete, which reduces the material budget by slightly below 0.1% X_0. Moreover, accounting for the very low power consumption of ALPIDE, it is considered not to use the active cooling foreseen in the support structures. The absence of coolant in the structures would once more reduce the material budget of the VD as compared to the SAVD. The obsolete front-end cards and readout electronics of the SAVD will be replaced as well.

The ambitioned extension of the of the VD aims to increase its geometrical acceptance from 33% to 70% of the tracks also detected in the TPCs of NA61/SHINE. This number holds for a Pb+Pb collision system at 158A GeV/c. To reach this goal, it is planned to extend the detector from initially 10 to 16 ladders, which will hold 46 ALPIDE sensors with a total active surface of 190 cm^2. The novel sensor configuration is displayed in Fig. 28 and the related GEANT4 model used for the performance simulations may be found in Fig. 29. Note that the upgrade will require only minor modifications in the mechanical design, as the SAVD was already designed for a compatibility with ALPIDE and the related ladders.

4.5.2 TPC readout upgrade

The increase of the readout speed of the TPCs is an essential and integral part of the upgrade of NA61/SHINE for the charm physics program. The goal is to reach a readout rate of 1 kHz. To achieve this NA61/SHINE can profit from the fact that the ALICE experiment at the LHC is replacing their wire chamber readout of the TPC by a readout scheme based on Gas Electron Multipliers (GEMs). This implies also the exchange of the complete readout electronics chain since the polarity of GEM output signals is reversed compared to wire chambers. NA61 has signed a memorandum of understanding that defines the transfer of part of the ALICE TPC readout electronics to NA61/SHINE.

In the following the two readout schemes are briefly compared and then the steps necessary for the implementation of the ALICE readout chain into NA61/SHINE including services is described in a sequence of work packages.

The design of the NA61/SHINE TPC is very similar to the design of the ALICE TPC. Therefore it is not surprising that the readout electronics shows strong similarities in its key parameters listed in Table 6.

The most relevant difference is the higher digitisation rate which at the end allows a readout rate up to a factor 10 higher than presently possible in NA61/SHINE. In addition the dynamic range is considerably higher due to the 10 bit ADCs. Also the higher sensitivity, the lower noise level and the doubling of the number of time bins should be mentioned here.

For the transport of the data from the front-end-electronics to the DAQ system ALICE has developed a second generation Read-out-Control Unit (RCU) called RCU2. Due to its segmentation into four 40 bit wide readout buses where each readout bus can connect up to 8 front-end-cards (FECs) and a 300 MByte/s optical link sufficient bandwidth is provided.

In the following a detailed work plan organised in work packages of the various steps necessary to replace the existing NA61/SHINE readout by the ALICE components is presented.

Work packages for the upgrade of the TPC readout

(i) **Development of a 3-D model of the NA61/SHINE readout chambers:**

Table 6: Comparison between key parameters of the NA61/SHINE and the ALICE front-end electronics.

		NA61/SHINE	ALICE
signal polarity		positive	positive
signal width (FWHM)	ns	180	190
dynamic range		120:1	900:1
MIP S:N ratio		14:1	14/20/18:1
noise	e	1100	$<$1000
ADC number of bits		8	10
number of time slices		512	1000
power consumption	mW/ch	51	35
sampling rate	MHz	5, 10	5, 10
readout frequency	MHz	0.1	5, 10
integrated non-linearity	%	$<$2	0.2

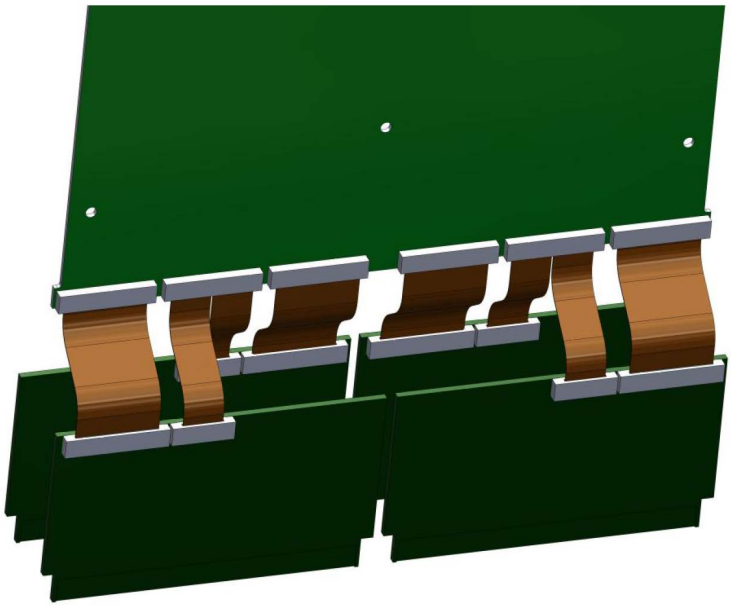

Figure 30: Simulation showing an ALICE FEC with adapter cards and flexible Kapton cables.

The NA61/SHINE TPCs were designed at a time when 3-D design software was not readily available. Therefore it was necessary to incorporate the existing 2-D information, complemented by on-site measurements, into a proper 3-D model. This was then used to design the cable adapters described in the next section. This work is to a large part finished and needs only minor additional effort. The fixation and the cooling of the FECs also has to be considered and is described later.

(ii) **Development, construction and tests of prototype input adapter cables:**

Due to the big differences in readout connector topology and the large difference in the number of channels per front-end card (32 vs 128), a careful study of the design of adapter cables connecting the existing 32 channel NA61/SHINE connectors to the six 22/21 channel input cables of the ALICE FECs was performed. A possible scenario for the connection of the FECs to the NA61/SHINE wire chambers is shown in Fig. 30.

Furthermore, the operation of ALICE has shown a weakness in the input protection circuit (incorporated into the design of the pre-amplifier/shaper CMOS chip) of the ALICE FECs. Therefore an additional protection circuit based on SMD components will be incorporated into the adapter cables.

Based on the 3-D model, prototype adapter boards are being developed and built in Frankfurt, see Fig. 31. The very first test of the effect of the protection network and the increased length of the adapter cables on the noise performance of the

Figure 31: Details of the design of a Kapton adapter cable including the protection circuit.

FECs will be tested in an existing test stand at IKF. Further tests are then foreseen on-detector in NA61/SHINE with a single FEC connected to the upstream corner of a MTPC chamber, using a special adapter/test set-up from ALICE.

(iii) **Design of the mechanical support of the FECs:** The mounting of the FECs requires a dedicated effort. For the MTPCs no major problems are expected as sufficient space is available. However, the confined space in the vertex TPCs requires a special arrangement of the FECs (mounting under an angle). This is presently studied together with the design of the adapter cards on the output side of the FECs (see work package (v)).

(iv) **Design and implementation of the FEC cooling:** The FECs will be cooled following the present NA61/SHINE scheme and even use the existing cooling plates. Another option is the use of fans to remove the heat. This will be decided once the mounting schemes have been developed and the space constraints are better known.

(v) **Production and tests of interface boards for the connection of the FEC output to the flexible buses:** Due to the different topologies the ALICE FECs cannot be read out via a rigid bus as in ALICE. Instead a more flexible readout using flat cables has to be used. Such a cable readout has been already developed for the PHOS detector in ALICE using the same FECs and RCUs as the TPC, see Fig. 32. This know-how can be directly applied to the future NA61 readout. Nevertheless, the

production and tests of the various adapter boards (to FEC and to RCUs) require a considerable effort, see Fig. 33 and Fig. 34.

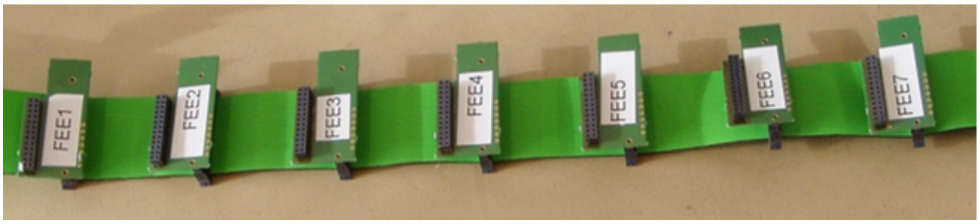

Figure 32: One of the three flexible readout bus cables with adapters.

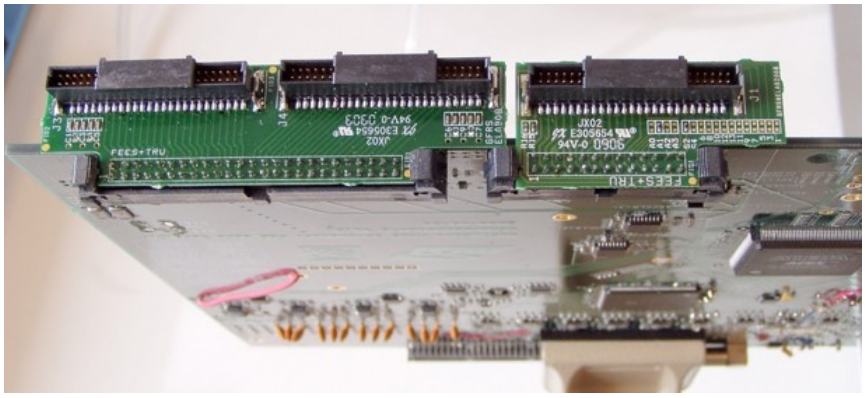

Figure 33: Front-end card with its two adapter cards to connect to the flexible readout buses.

(vi) **Development of read-out and DAQ for the new electronics:** The new readout requires a new DAQ system. A new modular system partly based on the ALICE HLT design is under investigation. The development and test of a new TPC DAQ system will be done in parallel to the development of the hardware components described above.

(vii) **Laboratory tests of the new readout chain:** Tests of the readout of several FECs in the lab using the full read-out chain (FECs, flexible cables, small adapter boards, RCU2s) will be performed in Bergen and at CERN and Warsaw University of Technology. These tests will be repeated with FECs connected to the upstream corner of one MTPC chamber with beam in order to see real track signals.

(viii) **Design and implementation of a new Low Voltage system:** The new readout system requires power supplies, bus bars and cables for the distribution of the low voltage (LV). It is foreseen to follow the design of the ALICE TPC LV system using power supplies from the company Wiener. For the distribution of the LV inside the chambers a system with bus bars running on one side of the chambers will be

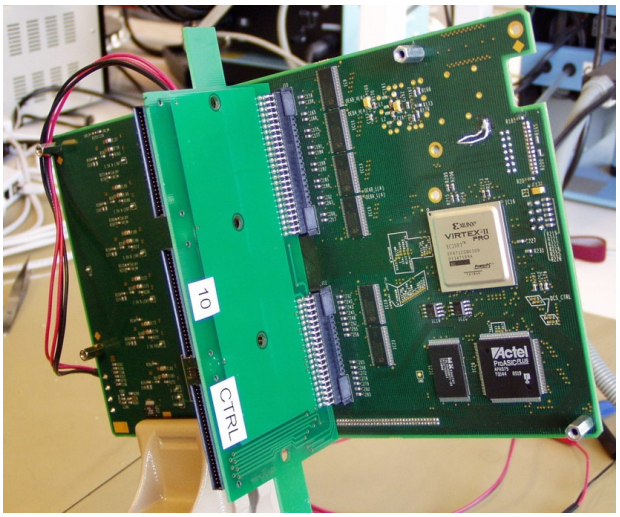

Figure 34: RCU with the adapter card plugged on.

used, very similar to ALICE. The connection between bus bars and FECs is then done by short patch cables.

(ix) **Development and implementation of new Detector Control System (DCS):** The new readout system requires a considerable extension of the existing NA61/SHINE DCS system to make full use of the information supplied by the FECs and the RCUs. It will follow the software design developed for ALICE.

(x) **Dismounting electronics from Alice and mounting in NA61/SHINE:** The last work package listed here deals with the actual dismounting, storage and transport and re-installation in NA61/SHINE of the ≈1700 FECs and ≈70 RCUs from ALICE requiring close coordination of the activities of the two experiments.

4.5.3 Trigger and DAQ upgrade

The key motivation for the readout system upgrade is the need to increase the event flow rate from 80 Hz to 1 kHz. This is possible thanks to the ALICE collaboration, which offers TPC front-end cards capable of collecting data with such rates. The cards were used with success to read out the ALICE TPCs and with small modification should be suitable for the NA61/SHINE experiment.

Furthermore, the evolution of the NA61/SHINE physics program requires adding new sub-detectors to the Data AcQuisition system (DAQ) easily without in-depth knowledge of the DAQ system. Also excluding sub-detectors from the DAQ system, which are not required for a particular run, would be beneficial to limit the event size.

The current DAQ system is already at the performance limit regarding the number of detectors as well as the bandwidth. Adaptation of the system would require substantial modifications. Consequently, it was decided to design a new system which meets the

future requirements of NA61/SHINE. The most fundamental requirements regarding the new DAQ system are:

- Speed – 1 kHz readout frequency
- Robustness – extended self diagnostic and adaptation algorithms of the DAQ core.
- Facile Control – shifter friendly interface to monitor and control data taking with algorithms detecting pre-failing states.
- Use of commercial off-the-shelf (COTS) components – profit from industry progress and competitive prices.
- Homogeneous Core – data from all subsystems treated in the same way.
- Inhomogeneous Nodes – each sub-detector readout system can be freely chosen by the sub-detector group.
- Extendibility – adding new detectors in plug-and-play manner. Self subscription (Nodes) and self adaptation (Core).
- Transparency – detector developers have well defined interface to pack, send and unpack data. The DAQ details will be hidden from sub-detector developers.

Currently, the raw event size is about 50 MB which after compression (zero-suppression algorithm) is reduced to about 1.5-5 MB depending on event multiplicity [85]. Adding new detectors will increase the event size and consequently the cost of hardware and data storage. To keep the overall cost within a reasonable range, an event size limit has to be introduced. A maximum size of 20 MB per event should be sufficient for the NA61/SHINE program beyond 2020.

$$1\,\text{kHz} \times 20\,\text{MB} = 20\,\text{GB/s} = 160\,\text{Gb/s} \tag{2}$$

In order to achieve such high readout speed, a network has to have a bandwidth of 20 GB/s as shown in Eq. 2. For the time being the 100 Gb Ethernet is being evaluated as the technology for the DAQ core. The attractive price, low number of links as well as flexibility due to high throughput makes 100 GbE a promising technology. Additionally, in order to use the full potential of this technology two techniques are explored: Remote Direct Memory Access (RDMA) and network package aggregation. The RDMA reduces CPU involvement in data transmission by bypassing the Linux kernel network stack. By so doing, the number of buffer copy operations between Open Systems Interconnection (OSI) layers is decreased and consequently the CPU time is saved. The latter technique – network package aggregation – prevents throughput degradation due to protocol overhead when dealing with very small packages. Therefore it improves performance greatly when small packages are aggregated into one big buffer and sent afterwards.

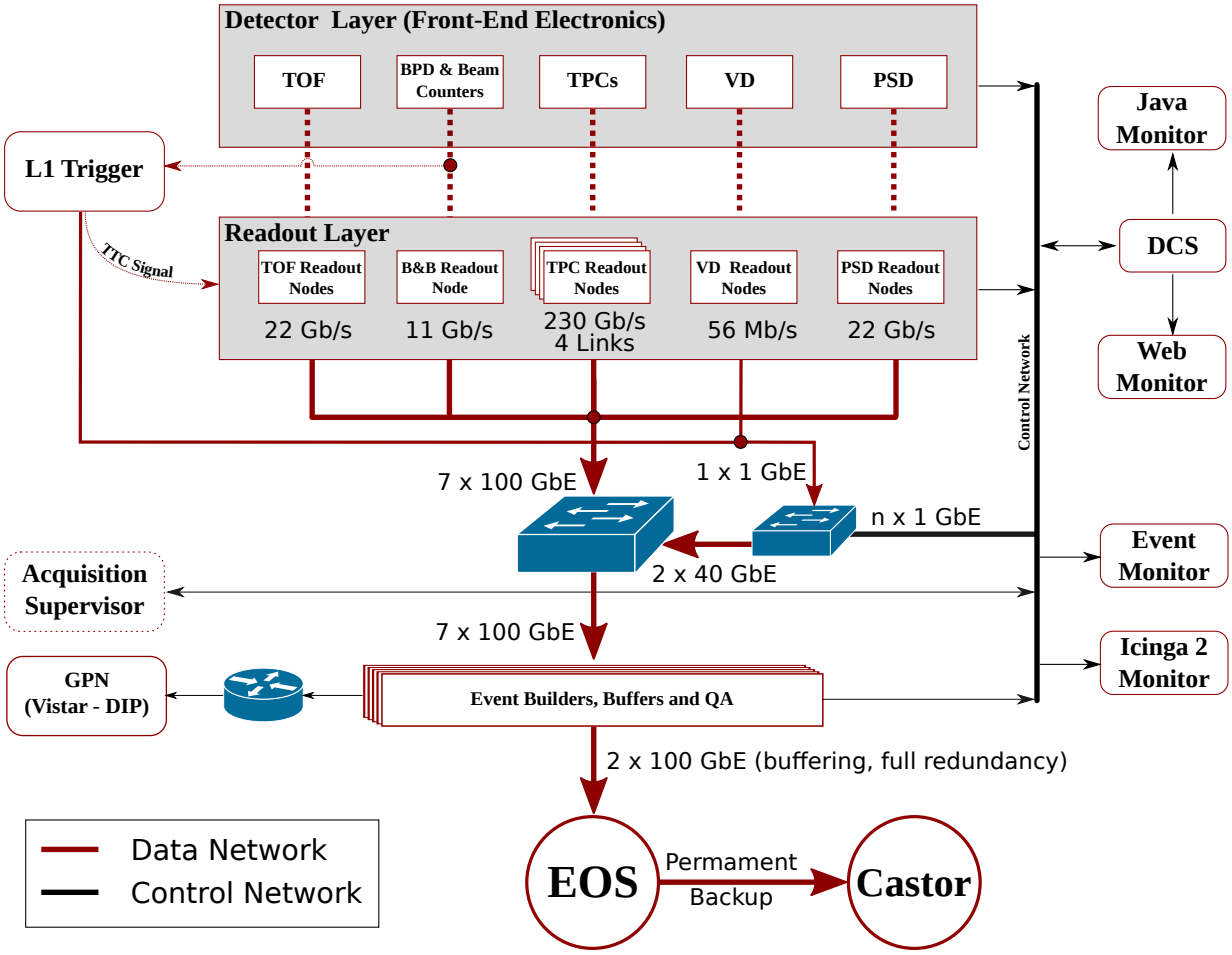

Figure 35: Overview of the planned NA61/SHINE data acquisition system.

The general schematic of the new readout system is depicted by Fig. 35. The **Detector Layer** is the starting point of data flow. This layer consists of front-end electronics, which sends data to the next layer – Readout Layer. The technology used to transport data between those layers as well as everything inside the Detector Layer are not part of the DAQ project. Thus sub-detector groups can freely choose the technologies they want to use. This design describes the data flow starting with the Readout Layer.

The **Readout Layer** consists of nodes, which are sub-event builders. In other words, a node collects data from the Detector Layer, builds sub-events and sends them to an Event Builder. Nodes are required to utilize x86-64 architecture and Ethernet technology for connection with Event Builders (through the Switching Network). The connection can be chosen as 1 GbE or 100 GbE depending on the amount of data produced by the sub-detector. The new DAQ system will provide a library to facilitate sending sub-events and communication with the Acquisition Supervisor as well as monitoring facility. Furthermore, the library will also implement a software RAM-based buffer. Therefore, nodes should have 8GB of RAM at minimum.

For the time being, the design foresees only a level 1 trigger (**L1 Trigger**). In order to improve the time response of the trigger, it has to take input signals directly from the front-end electronics of the beam counters. Signals from other sub-detectors can be used as additional trigger input signals, if needed.

The **Acquisition Supervisor** is an integral and central part of the DAQ system and, at the same time, the most crucial one. It is meant to perform the following functions:

(i) Sending/Updating LookUp Table (LUT) of Event Builder IP addresses.

(ii) Sending control commands such as START, STOP etc.

(iii) Collecting diagnostic data e.g. Buffer occupancy, CPU load etc.

(iv) Performing damage control tasks, e.g. abandoning non-responsive event builders

(v) Providing the DAQ User Interface (UI) for expert and non-expert users

The **Event Builders** receive sub-events from all nodes and form a final event. The event is stored in an internal RAM-based buffer until a chunk (set of events) is formed (1 GB size) which is then sent to the final storage.

The **Storage** will be delivered by CERN such as CASTOR, EOS etc. However, due to frequent network bandwidth problems between the experiment and the CERN storage services, an intermediate storage, which can buffer the data taking of up to three days, is under consideration

The **Vistar** [86] will publish the most crucial information about data taking so that experts can easily monitor the situation. In addition, the **Event Monitor** and the **DCS** will be integrated with the DAQ system.

In order to reduce required the data storage requirements, additionally to the trigger system, a partial online reconstruction (clustering) and an off-line filtration will be used. The online clustering is already implemented in the TPC readout electronics of

the ALICE readout system. The first test with one TPC sector is planned for the summer of 2018. The prototype of the off-line filtration system has already been implemented successfully on the OpenStack platform. Tests proved that the data can be filtered out with a low latency of around one hour after data had been collected. Furthermore, construction of the DAQ testbed has already started in November 2017, using more than 30 multi-core dual CPU machines. Before 2020, the testbed will be used for prototyping of the new data acquisition system. Afterwards, it is meant to be the DAQ replica, used for developing additional features and further improvement of the existing ones. Consequently, all developments will be done on the testbed, independently from the production DAQ, thus without a risk of jeopardizing data taking.

4.5.4 NA61/SHINE PSD upgrade

A forward hadron calorimeter, the Projectile Spectator Detector (PSD), measures forward energy (mostly from projectile spectators) and allows to reconstruct the event plane independently from the tracking in the Time Projection Chambers (TPCs). In addition, a fast analog signal from the PSD is used to select at the trigger level events based on the measured forward energy. The NA61/SHINE physics program beyond 2020 requires a tenfold increase of the beam and trigger rates. This necessitates an upgrade of the PSD. Details of this upgrade, performance studies, as well as the work schedule are presented below.

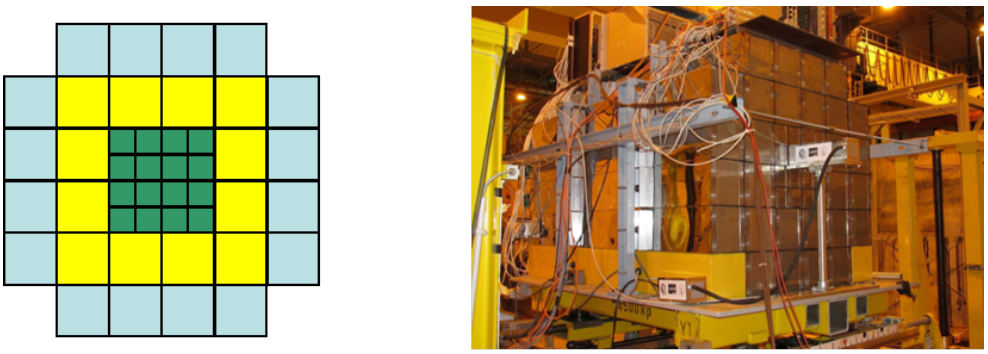

Figure 36: *Left:* schematic front view of the present PSD of NA61/SHINE. *Right:* Photo of the PSD placed on the beam line downstream of the NA61/SHINE detector. An additional small module (1.8 interaction length) is installed in the front of the PSD.

Performance of the present PSD of NA61/SHINE

The present PSD consists of 16 central small modules with transverse sizes of 10×10 cm^2 and 28 outer large modules with transverse sizes 20×20 cm^2 (Fig. 36 (*left*)). The length (depth) of the modules is 5.6 interaction lengths. The present PSD has no beam hole in

the centre. A small additional module is installed in front of the centre of the PSD to improve the energy reconstruction for heavy fragments (Fig. 36 (*right*)).

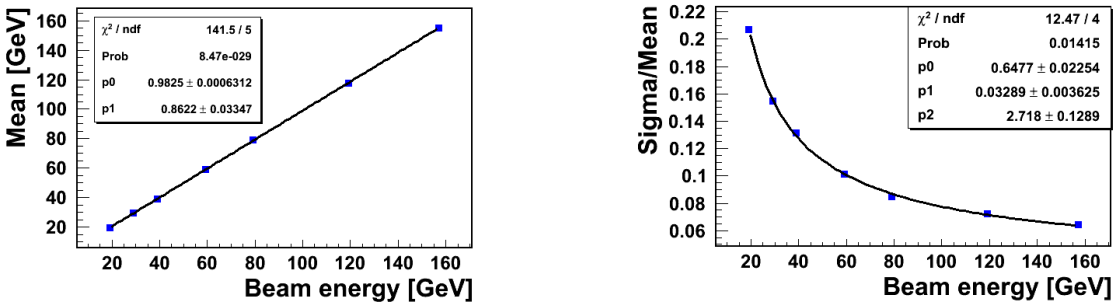

Figure 37: Response linearity *(left)* and energy resolution *(right)* of the PSD.

The present PSD has a good response linearity and energy resolution

$$\frac{\sigma_E}{E} = \sqrt{\left(\frac{0.65}{\sqrt{E}}\right)^2 + 0.033^2 + \left(\frac{2.7}{E}\right)^2} \tag{3}$$

according to measurements with proton beams in the energy range 20–158A GeV (see Fig. 37). Results are shown for the case when the proton beam hits one of the PSD central modules.

Motivation for the PSD upgrade.

The increase of the lead ion beam intensity by more than one order of magnitude (up to 10^5 ions per second) requires upgrades of the radiation hardness and protection as well as of readout rate of the PSD.

The radiation hardness problems with scintillator tiles, SiPMs, FEE and readout electronics in the central modules of the present PSD.

Figure 38 shows the radiation dose and neutron fluence simulated with the FLUKA code for the present PSD. The Pb beam rate was assumed as 5×10^4 ions per second. The accumulated radiation dose during one month of data taking significantly exceeds 10^3 Gy for the central part of the present PSD. Light transparency of the scintillator tiles degrades significantly above this dose. Moreover, the neutron fluence is of the order of 10^{12} n/cm^2 near the beam axis behind the calorimeter. This would cause degradation of the performance of the MPPC photo-detectors (increase of dark current, drop of gain, etc.) placed at the rear side of the calorimeter as well as of the commercial FPGAs used in the present readout electronics and also situated at the rear side of each module. Thus, the radiation hardness problems will lead to the deterioration of reliability and response of the calorimeter.

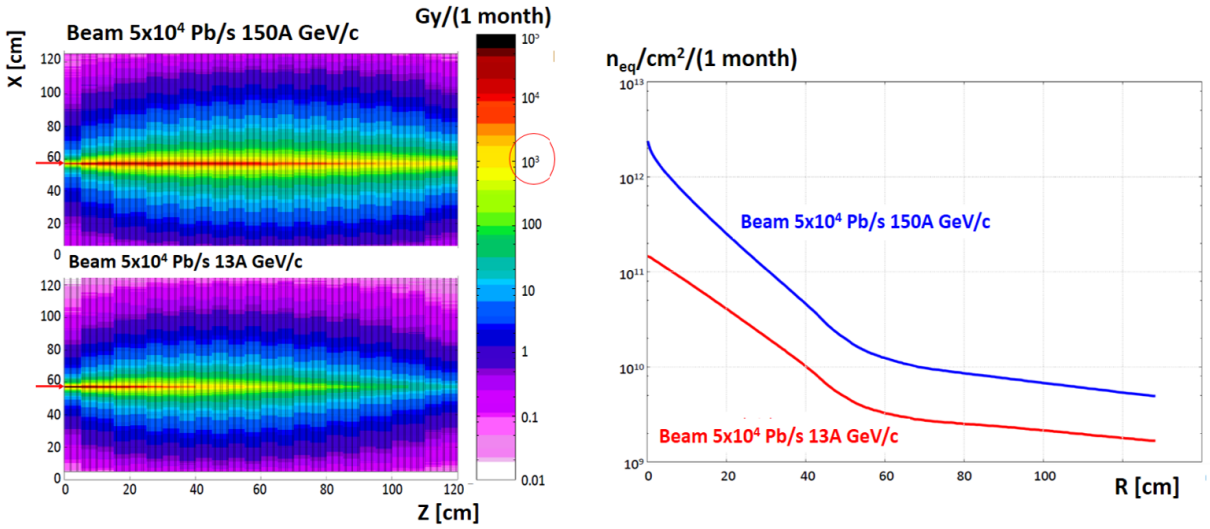

Figure 38: *Left:* radiation dose distribution along the PSD for Pb ions of 150A GeV/c and 13A GeV/c. *Right:* neutron fluence as function of distance from the beam axis at the rear side of the PSD for the same beam momenta.

PSD readout at high Pb beam rate.

In the present PSD only 16 small central modules use fast Hamamatsu MPPC photodetectors. Rather old MAPD-3A photodiodes with slow pixel recovery time are used in the other 28 large modules.

Figure 39 shows the dependence of the signal amplitude on the proton beam rate for one of the PSD sections. There is no reduction of the MPPC amplitude at a beam rate of 10^5 protons per second. The present readout electronics is based on 33 MSPS ADCs. Neither the slow photo-diodes nor the readout electronics are suitable for the higher beam intensity planned for NA61/SHINE beyond 2020.

Radiation shielding.

The increase of the Pb beam rate by more than one order of magnitude will lead to a radiation alarm in the experimental area of NA61/SHINE, because the present PSD serves as an active beam dump. Therefore, the PSD must be protected by additional concrete shielding. This is practically impossible for the present calorimeter because it is placed on a movable platform with large transverse size which is used to change the position of the PSD during data taking runs.

Planned upgrades of the NA61/SHINE PSD.

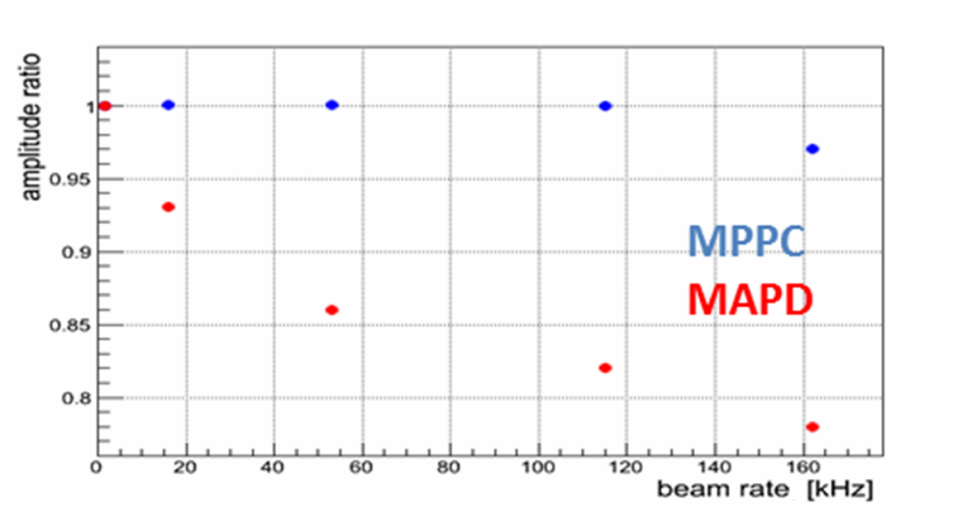

Figure 39: MPPC and MAPD signal amplitudes as a function of proton beam rate in one of the PSD sections.

Setup with two calorimeters.

To solve the problems mentioned above, it is proposed to use two calorimeters, the Main (M-PSD) and a Forward (F-PSD), see Fig. 40, instead of the present PSD. The M-PSD would be based on the present PSD with the 16 small central modules replaced by four new central modules with transverse sizes 20×20 cm^2 and with truncated edges forming a beam hole of 60 mm diameter at the center. In addition, 8 cm thick boron polyethylene blocks placed at the rear side of each of these modules will reduce the neutron fluence in the front of the MPPCs.

The F-PSD is an additional small calorimeter placed at a distance of 4.6 m downstream of the M-PSD, see Fig. 41. It consists of 9 modules with transverse sizes of 20×20 cm^2. All F-PSD modules will have 5.6 $\lambda_{\rm int}$ interaction lengths, the same as in the M-PSD, except for a longer central module of 7.8 $\lambda_{\rm int}$. As for the M-PSD, 8 cm thick boron polyethylene blocks will be placed at the rear side of each module. According to simulations, the two calorimeter setup will decrease the hadron shower leakage for Pb+Pb interactions at 150A GeV/c from 11 % for the present PSD to 4 %.

Radiation dose estimate.

The distribution of the radiation dose simulated with the FLUKA code for Pb+Pb collisions at 150A GeV/c are shown in Fig. 42 for the M-PSD and the F-PSD. The radiation dose and neutron fluence for the M-PSD are at an acceptable level even in the central modules. The expected radiation dose in the central module of the F-PSD is large, leading to loss of transparency of the scintillator tiles. But because the F-PSD will measure mainly heavy fragments producing a large amount of light, the attenuation can be compensated by increasing the MPPC bias voltages. The neutron fluences for the MPPCs in the F-PSD are at an acceptable level. Clearly, permanent monitoring is necessary for the

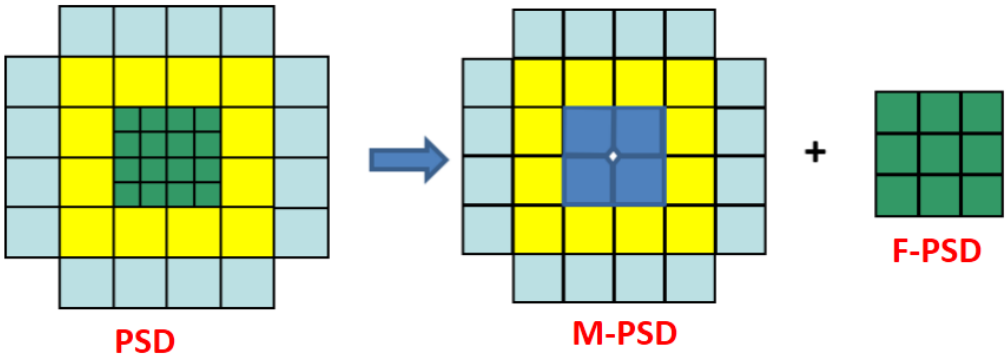

Figure 40: Schematic front view of the current PSD and the proposed new M-PSD and F-PSD calorimeters.

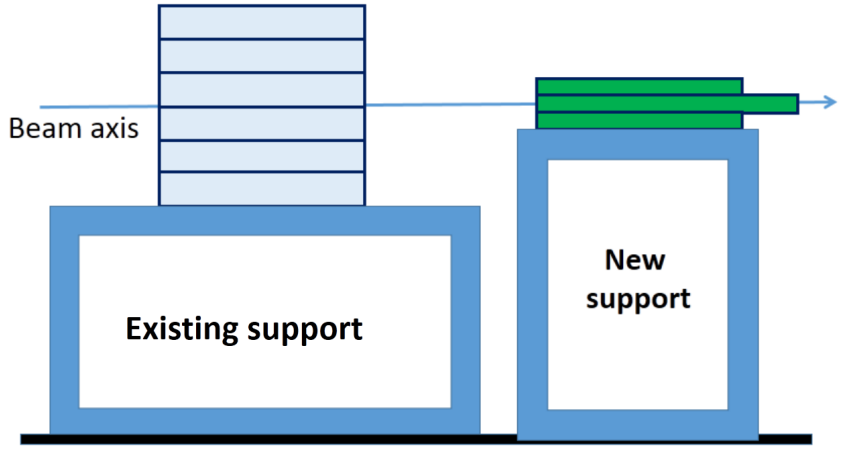

Figure 41: Horizontal cut of the proposed two calorimeter setup for NA61/SHINE.

F-PSD during data taking.

It is also important to take into account the activation of the M-PSD and F-PSD due to the high beam rate. Permitted activation for access is 0.5 μSv/h. According to simulations, the M-PSD activation will decrease to the permitted level already after one day without the beam. The activation of the F-PSD is significantly higher and decreases to the permitted level of activation only 6 months after stop of the beam. Additional concrete shielding of the F-PSD will be required for radiation protection.

Reaction plane determination.

The precision of the reaction plane determination for Pb+Pb collisions at 150A GeV/c with the present PSD and with the two calorimeter setup is shown in Figs. 43 *left* and *right*, respectively. One concludes that the precision of the reaction plane determination for semi-peripheral collisions remains almost unchanged.

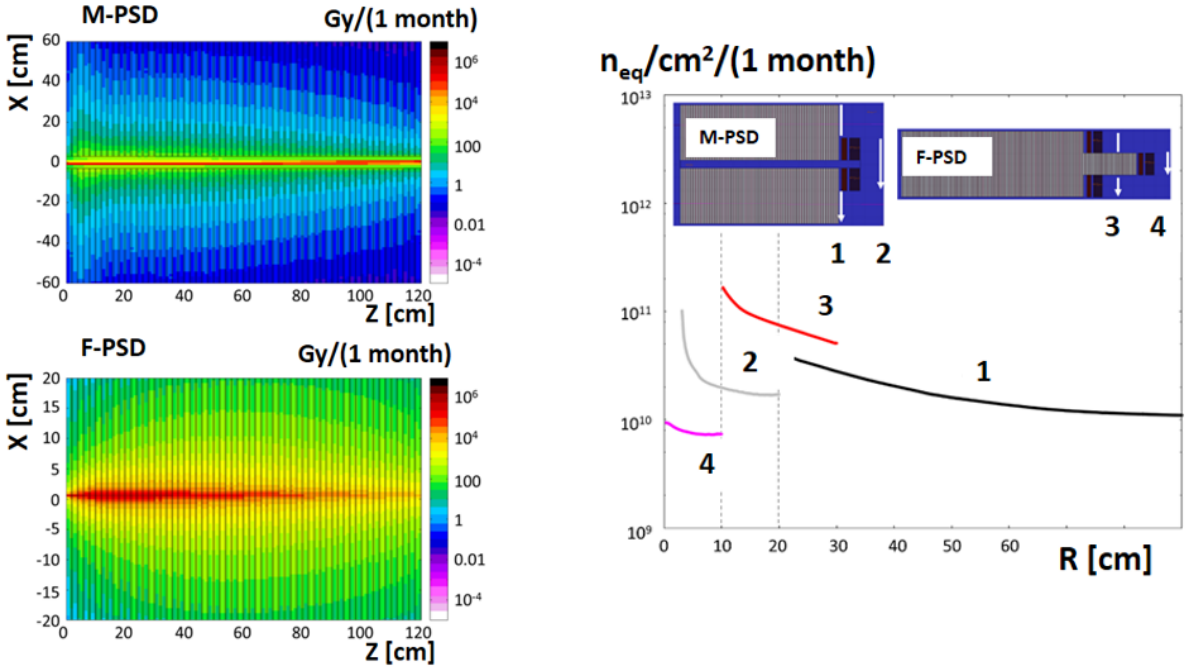

Figure 42: Radiation dose distributions along the M-PSD and the F-PSD (*left*) and neutron fluence distributions as a function of distance from the beam axis at the rear sides of the M-PSD and F-PSD (*right*) for the two calorimeter setup.

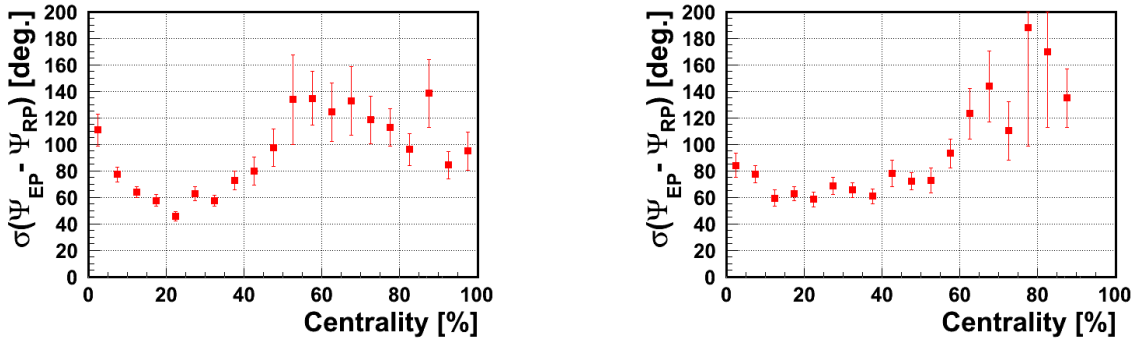

Figure 43: Reaction plane resolution as a function of centrality in Pb+Pb collisions at 150A GeV/c determined with the present PSD *(left)* and with the M-PSD and F-PSD setup *(right)*.

4.6 Beam Request for 2022

Measurements of charm production in Pb+Pb collisions as discussed in this section require 42 days of Pb beam at 150A GeV/c in 2022.

Beam requests for 2023 and 2024 will be the subject of future addenda.

5 Considered measurements with primary light ion beams

The results on the onset of fireball presented in Sec. 4.1.2 ask for precise measurements of hadron production properties in collisions of light ions with nuclear mass number between ^{7}Be and ^{40}Ar. This will allow to establish the nuclear mass number dependence in the transition region from p+p and Be+Be collisions to Ar+Sc and Pb+Pb collisions. Consequently a mechanism of the rapid change from non-statistical to statistical systems created in these collisions can be uncovered.

Data taking for C+C and Mg+Mg collisions at 13A GeV/c, 30A GeV/c and 150A GeV/c is considered. The measurements will require primary C and Mg beams. Secondary beams do not provide sufficient beam intensity and purity for the needed ions [87]. Measurements will be requested as soon as the corresponding results from the already recorded reactions will have been obtained. This is expected before the first data taking after the LS2 in 2022.

The measurements will require precise identification of charged kaons at mid-rapidity. This, in turn, requires new time-of-flight detectors with performance similar to that of the currently used ToF-L and ToF-R detectors.

5.1 The MRPC for the Time of Flight system

5.1.1 Introduction

The present Time of Flight (ToF) identification system of NA61/SHINE consists of two walls of 891 scintillation detectors each, designed and produced in 1997 at the University of Marburg and at the LHE JINR. It has a time resolution of about 75 ps, allowing to separate kaons from pions below 8 GeV/c [88].

After 20 years of operation all parts of the system require upgrades due to significant ageing of scintillators, photo-multipliers, power supplies as well as the obsolete readout electronics and cables. New ToF detectors based on multi-gap resistive plate chambers (MRPC) are proposed as replacement. At present, MRPCs are under construction for ToF identification in the BM@N experiment at the NICA facility [89]. In 2016 a BM@N type MRPC was tested next to the ToF-L wall of NA61/SHINE.

5.1.2 15-gap MRPC with strip readout

A schematic drawing of the triple-stack MRPC [90] is presented in Fig. 44. The detector consists of three stacks of 5 gas gaps each. Float glass was used for the resistive electrodes. The outer glass electrodes have a thickness of 400 μm. The internal glass electrodes have a thickness of 280 μm. A fishing line serves as a spacer and defines the 200 μm gap between the resistive electrodes. The outer surface of the external glass electrodes is covered by conductive paint with surface resistivity of about 10 M$\Omega/\square$ to allow applying the high voltage. All internal glass plates are floating. The overall dimensions of the detector (600$\times$300 mm^2) are determined by the available size of the

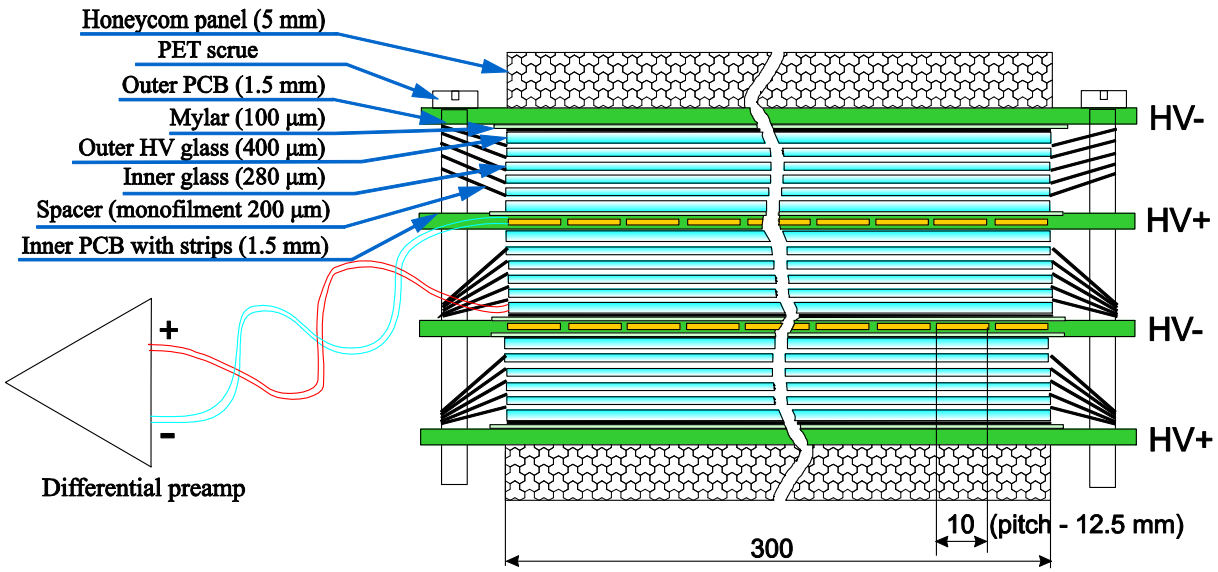

Figure 44: Cut view of the triple-stack MRPC.

Figure 45: Layout of the MRPC readout electrode.

glass sheets. The the inner layer of the readout PCB is covered by 48 pick-up strip electrodes with pitch of 12.5 mm as shown in Fig. 45. It is necessary for better electrical isolation of the strips from the high voltage layer.

The differential analogue signal is transferred from the PCB to the frontend electronics (FEE) board by doubled twisted pair cable. The FEEs based on the NINO ASIC were designed by JINR [91]. The signal is read out from both ends of the strip. This provides better time resolution and a determination of the coordinate of a particle along the strip. Digitization of the signal is provided by the VME based time-to-digital converter TDC72VHL [92] designed by JINR. The native time resolution of the readout electronics is below 20 ps.

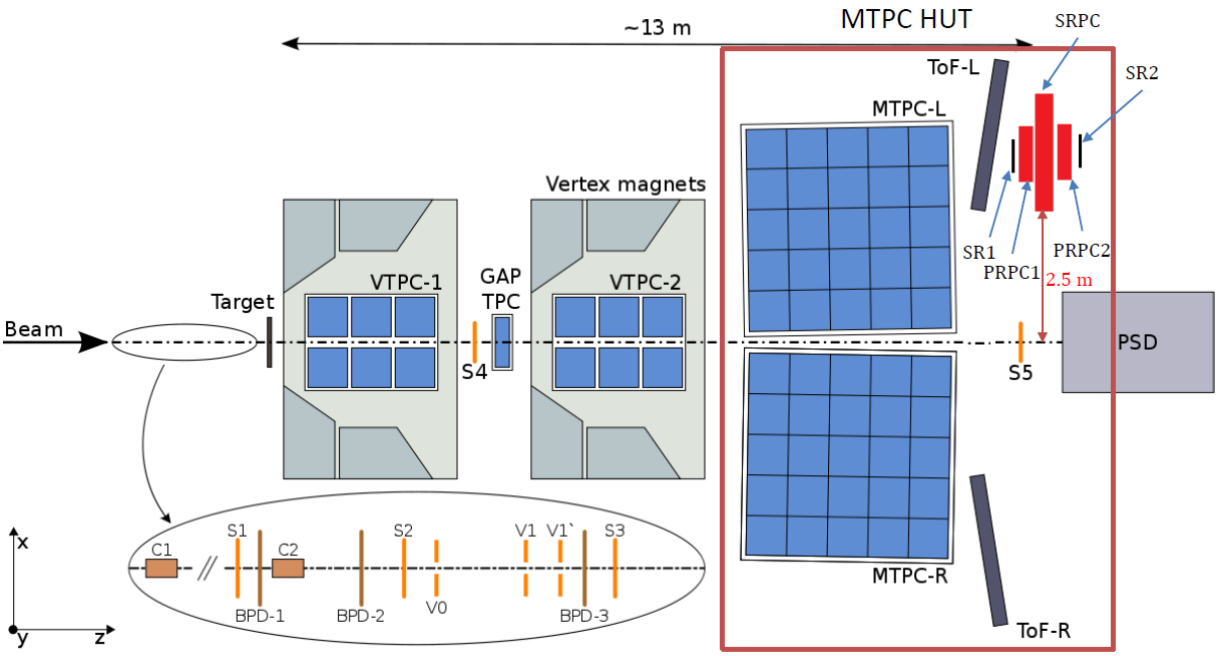

Figure 46: Location of the MRPC test setup in 2016: strip RPCs (SRPC,SR1,SR2) and pad RPCs (PRPC1 and PRPC2) were placed behind the ToF-L wall of NA61/SHINE.

5.1.3 MRPC test in NA61/SHINE

A full-scale prototype of a BM@N type triple stack MRPC was tested in NA61/SHINE in November 2016. The test set-up was positioned behind the ToF-L wall as shown in Fig. 46. It registered particles produced in Pb+Pb collisions at 30A GeV/c. The test data were recorded by a stand-alone data acquisition system. Two type of triggers were used in the test.

(i) coincidence of two scintillator counters before (SR1) and after (SR2) the MRPCs,

(ii) central interaction trigger (T2) from NA61/SHINE.

The two MRPCs (PRPC1 and PRPC2) with pad readout [93] were used as a reference to define the time resolution of the tested MRPC.

The time resolution of the MRPC was derived from the distribution of time differences between the tested MRPC and the two *start* MRPCs, as shown in Fig. 47 (*left*). As the time resolution of one pad MRPC is about 62 ps, the time resolution of the system of two detectors is $62/\sqrt{2} \approx 44$ ps. The time resolution of the tested MRPC is $\sqrt{66^2 - 44^2} \approx 50$ ps. The momentum spectrum of particles crossing the MRPCs was not measured, but its influence can be neglected as the distance between the tested MRPC and the *start* MRPCs is only 10 cm.

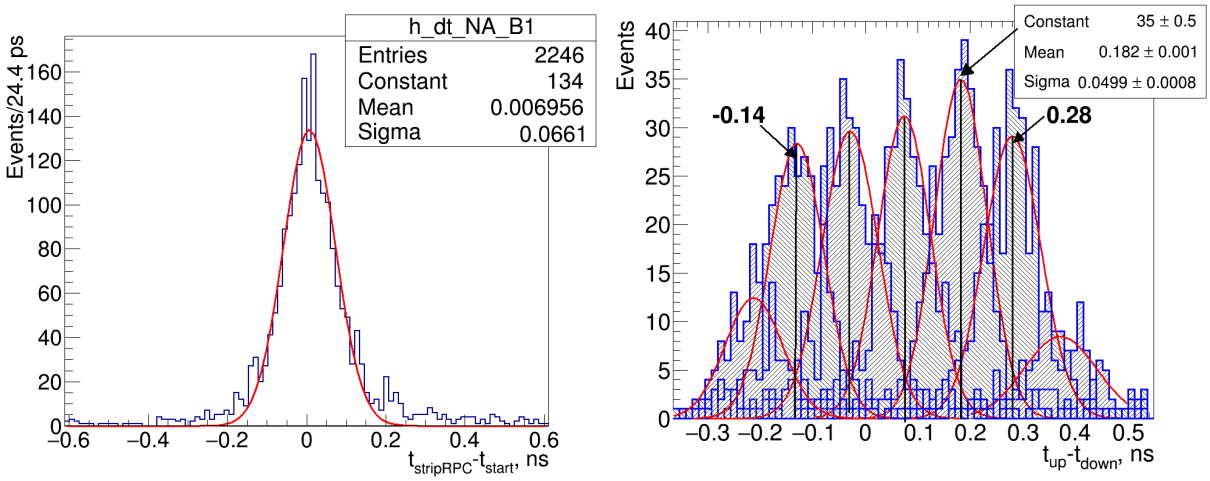

Figure 47: *Left:* Distribution of the time difference between the tested MRPC and the mean time of two reference MRPCs with pad readout. *Right:* Time difference between the signals from two ends of the strip of the MRPC for different positions of particles. Each peak represents the image of a pad on the strip.

The position of the particle impact point along the strip of the tested MRPC can be calculated from the time difference between the signals from the two opposite ends of the strip. The pad MRPCs were used as a rough tracking system. From Fig. 47 (*right*) one can estimate the velocity of the signal on the strip: $(0.28 + 0.14)/(4 \times 1.75) = 60$ ps/cm. If particles cross only one pad in each reference MRPC, one can evaluate the spatial resolution of the tested MRPC along the strip. For one pad with a pitch of 17.5 mm one expects the distribution of the time difference between the ends of the strip to be uniform with standard deviation of $1.75/\sqrt{12} = 0.51$ cm. In practice, the standard deviation of the distribution of pad projection on the strip is 50 ps (see Fig. 47 (*right*)) or $50/60 = 0.83$ cm. Hence, the position resolution along the strip can be calculated as $\sqrt{0.83^2 - 0.51^2} = 0.65$ cm.

From the data collected with central interaction trigger one can evaluate the multiplicity of particles hitting the ToF wall for 30A GeV/c Pb+Pb interaction. The resulting mean occupancy per strip is about 10% (Fig. 48). This means that this type of electrode was suitable in the region where the MRPC was tested. Most likely, shorter readout electrodes will be needed for regions located closer to the beam axis. It is planned to evaluate maximum occupancies for the whole ToF acceptance. Based on this information one will be able to design detectors with optimal size of readout electrodes and number of channels.

5.1.4 Possible layout of the MRPC ToF wall

One of the possible variants of the arrangement of the detectors in the ToF wall is shown in Fig. 49. A wall of 1008 strips of 15×1 cm^2 covers an area of about 1.9 m^2. The oc-

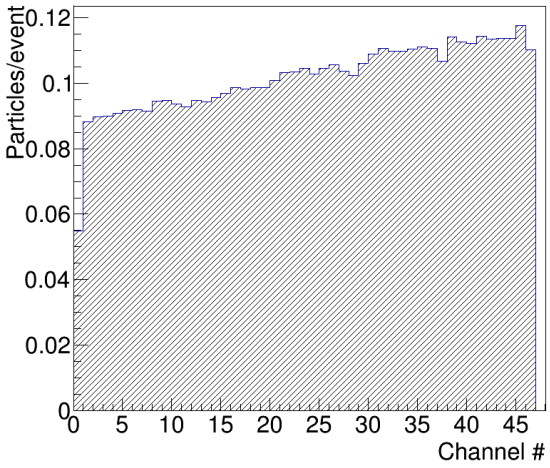

Figure 48: Mean number of hits per strip of the MRPC for one Pb+Pb interaction at 30A GeV/c. The beam line is at a distance of 250 cm to the right (See Fig. 44).

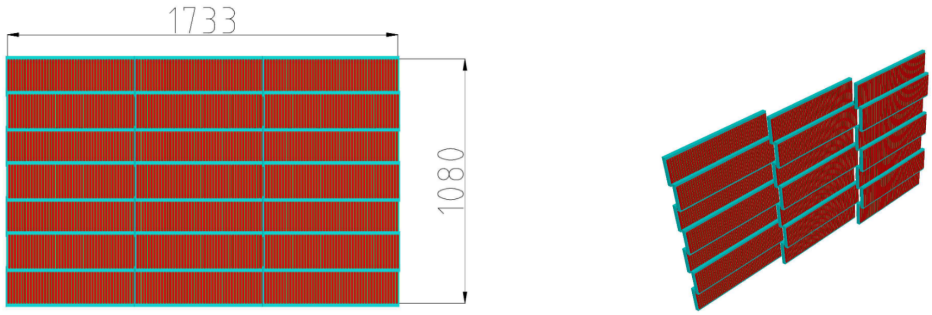

Figure 49: Possible arrangement of the MRPC ToF wall.

cupancy should stay below 10% for the maximum possible multiplicity of particles. Simulation-based optimization of the design is ongoing.

Considered measurements with primary light ion beams for the study of the onset of fireball do not lead to a beam request for 2022.

The measurements will be requested in a future addendum as soon as the corresponding results from the already recorded reactions will have been obtained. This is expected before the first data taking after the LS2 in 2022.

6 High statistics studies of spectator-induced effects in Pb+Pb collisions

The research programme proposed in this Addendum offers a unique opportunity for studies of electromagnetic as well as other effects induced by the spectator system in Pb+Pb collisions. Such effects are already under study in NA61/SHINE as they offer new, independent information on the longitudinal space-time evolution of the system of deconfined matter created in the collision. The presently available information covers the system size dependence of the electromagnetic (EM) distortion of π^+/π^- ratios (examples for intermediate multiplicity Ar+Sc and peripheral Pb+Pb collisions are shown in Figs 50 (a), (b)). The theoretical counterpart of this activity is described in Refs. [97,98] where the space-time observations from EM effects have been used to evaluate the role of local energy-momentum conservation rules in the longitudinal evolution of the system and to explain the centrality dependence of measured charged pion rapidity spectra and yields.

For the NA61/SHINE beyond 2020 programme, a new subject of presently increasing interest is the space-time evolution of the nuclear spectator remnant. From the point of view of "classical" (low energy) nuclear physics, the spectator system after abrasion[4] is quite an "exotic", highly deformed and excited state, its space-time evolution being affected by several different processes: evaporation, fission, multifragmentation, and vaporisation [99]. Recent theoretical work based on the multidimensional stochastic Langevin equation [95, 100] shows that the different state-of-the-art abrasion scenarios result in very different predictions for the spectator excitation energy (Fig. 50 (c)), but also that theoretical tools exist to compute the ensuing space-time evolution (Fig. 50 (d)). The experimental verification of these model predictions is, for the "extreme" case of the spectator system, the domain of ultrarelativistic heavy ion rather than classical nuclear physics. While momentum distributions and isotopic spectra of nuclear fragments for different systems and energies have been measured in the past, these give information only on the final state of the reaction, with no direct insight into its space-time evolution. EM effects, on the other hand, are known to be sensitive to the space-time evolution of spectator fragmentation. This is illustrated in Figs. 50 (e), (f), (g) which show that the EM distortion of π^+/π^- ratios in peripheral Pb+Pb collisions depends on spectator volume. Thus the hope emerges for using ultra-relativistic Pb+Pb collisions as a high statistics charged pion "factory" for spectator break-up time scale evaluation. EM effects have been applied to such purpose in the past [101].

The new measurements of spectator-induced EM effects will necessitate neither an improvement in detector set-up nor additional data with respect to those planned for open charm measurements. On the contrary, these "parasitic" studies will greatly benefit from the NA61/SHINE detector upgrades made for the latter purpose, with no extra requirements. Two main benefits should be pointed out:

[4] Abrasion is the process in which the spectator is torn off from the colliding nucleus.

(i) The inclusion of a new vertex detector will improve the event vertex reconstruction resolution, and consequently significantly decrease the beam-gas background contribution for peripheral Pb+Pb events. It is therefore to be expected that more peripheral Pb+Pb collisions will become available for analysis. This constitutes an important advantage over existing studies as it "anchors" the measurement of the centrality dependence of EM effects in the region of high spectator masses/charges, corresponding to low excitation energies (Fig. 50 (c)). This creates a useful reference point where a "maximally stable" spectator system simplifies any possible phenomenological analysis, see e.g. Ref. [102, 103].

(ii) High statistics is the decisive factor for this measurement. The requested data taking for the charm program should lead to $16 \cdot 10^7$ peripheral Pb+Pb collisions at 150A GeV/c, $16 \cdot 10^7$ mid-central Pb+Pb collisions at 150A GeV/c and $16 \cdot 10^7$ central Pb+Pb collisions at 150A GeV/c to be recorded. This will results in more than tenfold increase in statistics with respect to the analysis shown in Fig. 50 (b). This is of particular importance in view of the very steep structures created by EM effects in the $d^2n/dx_F dp_T$ spectra of final state particles. An example of such structures is given in Figs. 50 (h) and (i), where the Monte Carlo simulation of EM-induced enhancement of summed charged pion (mostly π^-) emission [98] in the vicinity of spectators (x_F=0.15, low p_T) is shown as a function of applied histogram binning. With a granularity increased by at least a factor of 3 x 3 with respect to the present measurement, a much better knowledge of these structures, and consequently a higher sensitivity to the space-time evolution of participant and spectator systems, is can be achieved.

The new measurements will not require new data analysis methods nor know-how with respect to what is already available in the NA61/SHINE Collaboration, evidently with the exception of software to be anyway developed in view of TPC upgrades and access to information from the Vertex Detector. The obtained new experimental data can, on the other hand, impose a challenge for existing models of nuclear dynamics both at low (MeV-scale) and high (GeV-scale) energies.

High statistics studies of spectator-induced effects in Pb+Pb collisions will be performed using data on Pb+Pb collisions recorded in 2022 for the charm program. Thus there is no beam request for 2022 specific to the physics of spectator-induced effects.

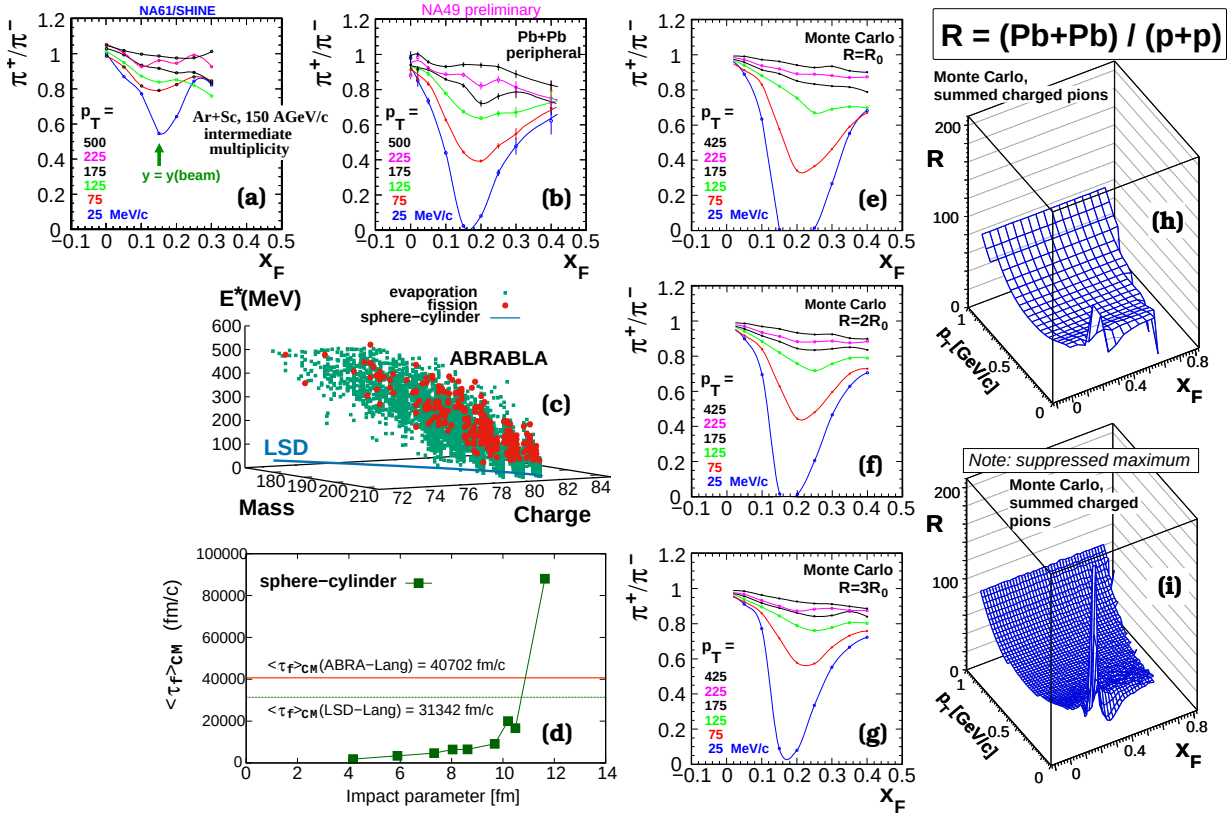

Figure 50: (a) Electromagnetic distortion of the π^+/π^- ratio measured in intermediate multiplicity Ar+Sc reactions at 150A GeV/c, drawn as a function of x_F at fixed values of p_T. (b) Same for peripheral Pb+Pb collisions at 158A GeV [94]. (c) Correlation between spectator mass, charge and excitation energy in two abrasion models (LSD, ABRABLA), for two deexcitation channels (evaporation, fission) in Pb+Pb reactions at 158A GeV [95]. (d) Corresponding mean fission time in collision centre-of-mass frame as a function of the collision impact parameter, in the LSD-Langevin model, as well as mean fission times averaged over all considered impact parameters for the LSD-Langevin and ABRA-Langevin models [95]. (e), (f), (g) Results of Monte Carlo simulation of peripheral Pb+Pb collisions at 158A GeV, for three different charged spectator volumes corresponding to its original, doubled and tripled radius R_0 (see text) [94]. (h) Enhancement of summed charged pion production in peripheral Pb+Pb over p+p reactions in the (x_F, p_T) binning corresponding to the present experimental analysis. (i) Same in finer (x_F, p_T) binning. Plots in panels (c) and (d) courtesy of Katarzyna Mazurek, 2017. Plots in panels (b)-(g) are redrawn from [96].

7 Measurements for Cosmic-Ray Research

7.1 Nuclear Fragmentation Cross Sections

7.1.1 Introduction

A wealth of new data on Galactic cosmic rays has recently been collected by the AMS and PAMELA space experiments. The fluxes of leptons, nuclei and antiprotons from GeV to TeV are now known to an unprecedented percent-level precision [104–112] and new detectors such as DAMPE, ISS-CREAM and CALET are pushing to even higher energies (see e.g. [113,114]). These new data sets provide a unique diagnostic of cosmic-ray propagation in the Galaxy [115,116] and an opportunity to find signatures of dark matter annihilation in the Galaxy [117,118].

Cosmic rays can be classified as being of primary or secondary origin. Primary cosmic-ray nuclei are assumed to be accelerated in supernova remnants (e.g., p, He, C, N, O, Fe), whereas secondary cosmic rays are created in nuclear interactions of primary cosmic rays with protons and helium nuclei of the interstellar medium (e.g. e^+, $\bar{p}$, d, Li, Be, B). The flux ratios of secondary to primary cosmic rays are key observables to determine the characteristics of propagation of cosmic rays in the Galaxy, such as the effective diffusion coefficient and its energy dependence, the column depth of material traversed by cosmic rays and the time they spend in the Galaxy before escaping. The most studied flux ratio is the B/C ratio because it is the experimentally most-accessible. The parameters of cosmic-ray diffusion in the Galaxy are estimated by analyzing the measured flux ratios of secondary and primary nuclei for an assumed propagation model. Using these parameters, the secondary background fluxes (e.g., positrons and antiprotons produced from interaction of primary cosmic rays with the interstellar medium) can be predicted. Unfortunately, this approach is severely hampered by uncertainties in the modeling of the propagation of cosmic rays in the Galaxy due to uncertainties of the cross sections for nuclear fragmentation on the level of 10–20% [119–123]. These uncertainties propagate directly to the flux predictions, i.e., if the integrated mass density is derived from the measured B/C ratio with 20% too low cross section for boron production, then the predicted secondary antimatter fluxes will be 20% too low as well (see e.g. [124]). A typical example of existing data relevant for cosmic-ray fragmentation is shown in Fig. 51. As can be seen, most of the previous measurements of Boron production in C+p interactions were performed at low energies. For the interpretation of cosmic-ray data, the asymptotic behavior of the fragmentation cross section above 10 GeV per nucleon is of major importance, since the current cosmic-ray measurements cover energies to up to several hundreds of GeV per nucleon. The measurement campaign proposed in the following will address the lack of precise measurements of fragmentation cross sections relevant to cosmic-ray transport in the Galaxy at high energies.

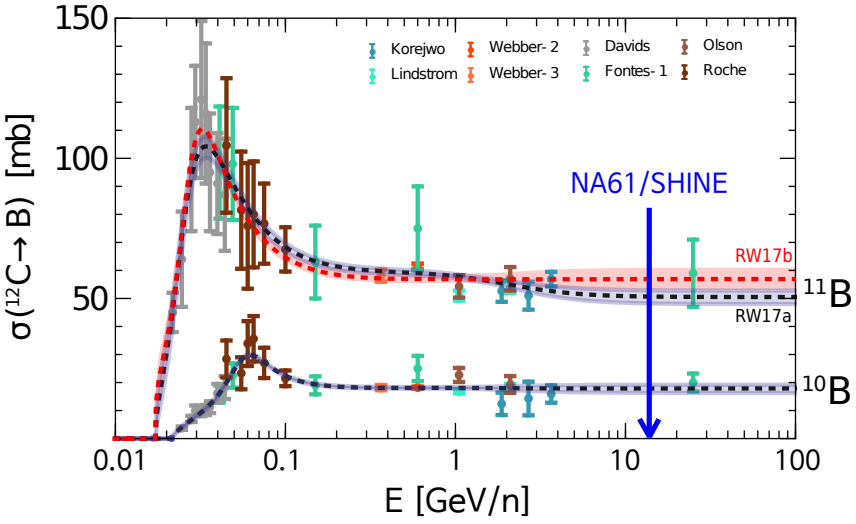

Figure 51: Current measurements of the fragmentation cross sections of $C + p \rightarrow {}^{11}B$ and $\rightarrow {}^{10}B$ as a function of energy per nucleon. Two different fits of the cross section data are shown by the red and black dashed lines. The light gray/red bands indicate the statistical uncertainty of the fits. The energy of the proposed NA61/SHINE measurements is shown as a vertical blue arrow. (Figure adapted from [123]). The energy range of main interest for cosmic-ray physics is above 1 GeV/n.

7.1.2 Proposed Measurements

We propose to measure fragmentation cross sections relevant for the production of Li, Be, B, C and N nuclei. These elements are of particular importance for the physics of cosmic rays in the Galaxy. Most of the studies of the cosmic-ray propagation are based on the B flux as mentioned above. In addition, Li provides a test of transport parameters complimentary to B. C and N are mostly primary nuclei, but the secondary fraction can reach ∼20-30%. Finally, different isotopes of Be are used to constrain the propagation time of cosmic rays ("cosmic-ray clock").

A detailed study of cross sections relevant for secondary cosmic rays has been performed in [125] using the semi-analytical propagation code USINE [126, 127] together with different cross section parametrizations. The impact of the fragmentation cross section of a given primary cosmic-ray species on the total flux is calculated by repeatedly running full propagation calculations in which a certain production channel is set to zero.

In these studies the most important reactions for secondary cosmic ray production were identified. These are visualized in Figs. 52 and 53 for Li, Be, B, C and N nuclei.

Here we propose to measure the n most important reactions needed to reduce the current uncertainties below desired uncertainty given by current space experiments, i.e. the reactions left of the intersection of the green benchmark curve and the dashed curve in Figs. 52 and 53. This leads to 13 reaction to be measured, 11 of which require a proton

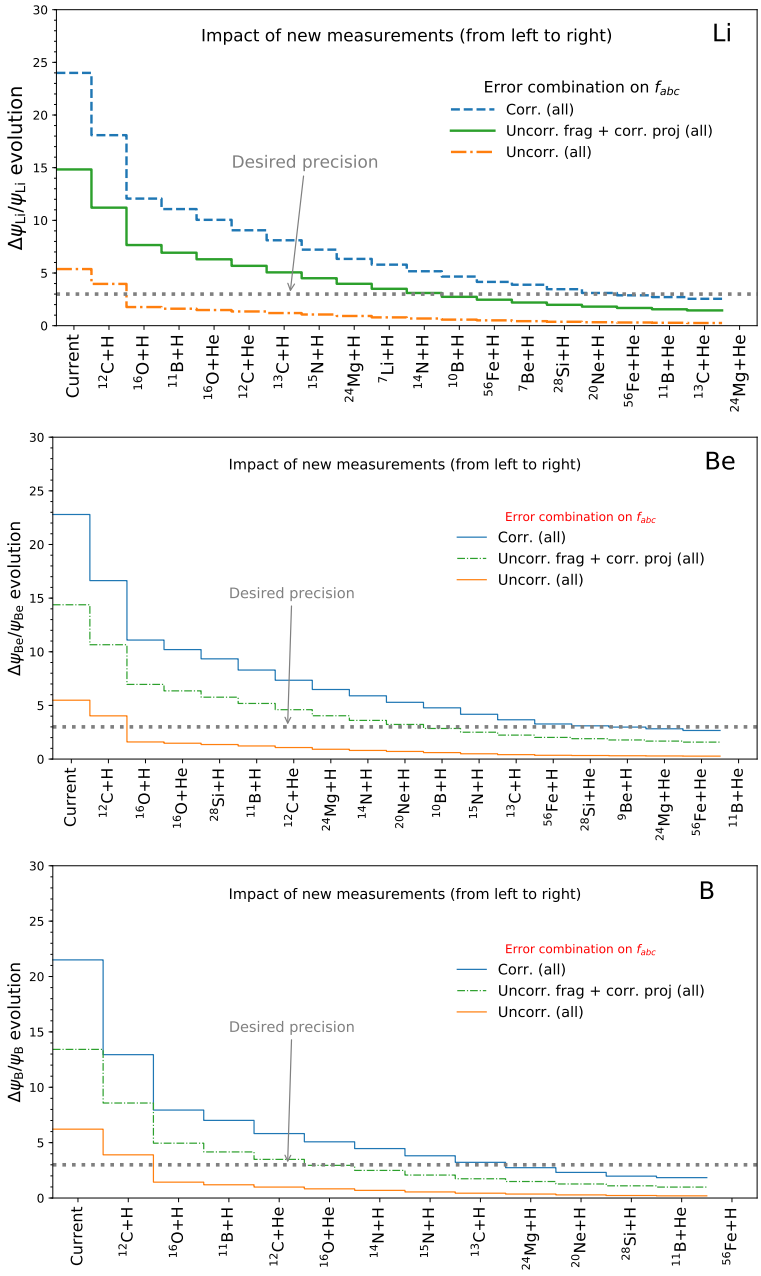

Figure 52: Evolution of uncertainty of predictions on the calculated Li, Be, and B fluxes at 10 A GeV/c as a function of reaction. The plot is to be read from left to right, with the first bin giving the currently estimated uncertainty on the flux (no new cross section measurement) and consecutive bins showing the remaining uncertainty from the reactions left to the bin. The three sets of curves correspond to three different assumptions made on the cross-section errors: correlated, uncorrelated, or a mixture of these two assuming $\Delta\sigma_r^{\text{current}} = 20\%$. (plots taken from [125]).

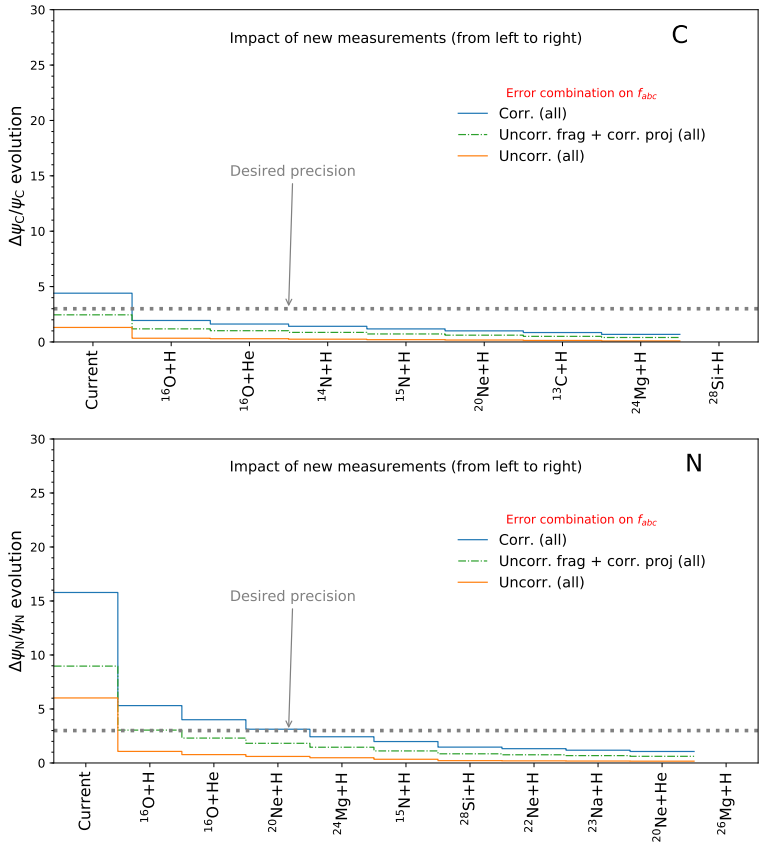

Figure 53: Evolution of uncertainty of predictions on the calculated C and N fluxes at 10 A GeV/c as a function of reaction. See Fig. 52 for further explanations. (plots taken from [125]).

target and 2 a helium target.

The statistical uncertainty of secondary cosmic-ray fluxes of type c depending on the number of recorded nuclear $a + b$ interactions can be determined via

$$\left(\frac{\Delta\psi^{\mathrm{sec}}}{\psi^{\mathrm{sec}}}\right)_{ab} = \frac{1}{\sqrt{N}}\,\mathcal{C}_{ab}. \tag{4}$$

where the constants $\mathcal{C}_{ab}$ were calculated in Ref. [125] taking into account the flux impacts and partial production cross sections. They are listed in Tab. 7 for the aforementioned 13 reactions. Each projectile and target combination needs to be measured until the individual uncertainty from the respective reaction becomes less than $\xi/\sqrt{n}$, where ξ is the desired accuracy of the sum of uncertainties of the considered reactions. The number of interactions to be recorded for each reaction is thus

$$N_{ab} \geq n\,(C_{ab}/\xi)^2. \tag{5}$$

Previous cross sections measurements of NA61/SHINE had a detector-related systematic uncertainty of 0.5% [128]. Aiming at a total uncertainty (statistical plus sys-

Table 7: C_{ab} coefficients (see text) for the fluxes of cosmic-ray nuclei as indicated in the table header. The first column list the reaction $a + b$ and the second column gives the C_{ab} coefficient.

Li	
$^{16}O + H$	1.057
$^{12}C + H$	0.773
$^{16}O + He$	0.615
$^{14}N + H$	0.410
$^{12}C + He$	0.158
$^{24}Mg + H$	0.152
$^{11}B + H$	0.134
$^{15}N + H$	0.120
$^{13}C + H$	0.115
$^{10}B + H$	0.066
$^{7}Li + H$	0.059

Be	
$^{16}O + H$	1.419
$^{12}C + H$	0.986
$^{16}O + He$	0.881
$^{14}N + H$	0.558
$^{28}Si + H$	0.202
$^{12}C + He$	0.192
$^{24}Mg + H$	0.192
$^{20}Ne + H$	0.130
$^{10}B + H$	0.083

C	
$^{16}O + H$	1.047

B	
$^{12}C + H$	0.808
$^{16}O + H$	0.656
$^{16}O + He$	0.609
$^{14}N + H$	0.574
$^{12}C + He$	0.148
$^{11}B + H$	0.108

N	
$^{16}O + H$	1.278
$^{16}O + He$	0.219
$^{20}Ne + H$	0.138

tematic added in quadrature) of 1% gives $\xi = 0.0087$ and the corresponding number of desired interactions from Eq. 5 is given in Table 8. For each reaction the maximum number needed for any of Li, Be, B, C and N is quoted.

7.1.3 Experimental Setup

The NA61/SHINE facility has already successfully taken data with light ion beams [129] and can be used with practically no modifications to perform the needed cross section measurements at isotope level (Fig. 54). Already in 2018, the NA61/SHINE facility will be used for a pilot run to establish the feasibility of fragmentation cross section measurements [130].

The main experimental components needed for the proposed measurement can be summarized as follows:

Table 8: Desired number of interactions, N_{inter} to be recorded for different reactions.

reaction	N_{inter}	A/Z
$^{16}\text{O} + \text{H}$	250k	2
$^{12}\text{C} + \text{H}$	150k	2
$^{16}\text{O} + \text{He}$	100k	2
$^{14}\text{N} + \text{H}$	40k	2
$^{10}\text{B} + \text{H}$	5k	2
$^{11}\text{B} + \text{H}$	5k	2
$^{12}\text{C} + \text{He}$	5k	2
$^{13}\text{C} + \text{H}$	5k	11/5
$^{15}\text{N} + \text{H}$	5k	13/6
$^{20}\text{Ne} + \text{H}$	5k	15/7
$^{24}\text{Mg} + \text{H}$	5k	2
$^{28}\text{Si} + \text{H}$	5k	2
$^{7}\text{Li} + \text{H}$	5k	7/3
	$\sum = 0.6\text{M}$	

(i) **secondary ion beam:** nuclear fragments from SPS, Pb on primary target, $p = 13A$ GeV/c at different A/Z settings. $p = 13A$ GeV/c is about the lowest energy for secondary ions at the SPS. This energy is well in the high energy region of Fig. 51 where new data is desperately needed and at the same time it is low enough to allow for a precise determination of the properties of the projectile and fragment with the NA61/SHINE setup.

(ii) **target:** the main data taking for X+H reactions will alternate between thin polyethylene (C_2H_4) and carbon targets and a small fraction of runs without any target. A systematic cross check of this measurement scheme will be performed by taking data with the standard NA61 liquid hydrogen target ($\rho \times l = 1.42$ g/cm^2, re-interaction probability $\sim 14\%$). The implementation of the helium target is still under study.

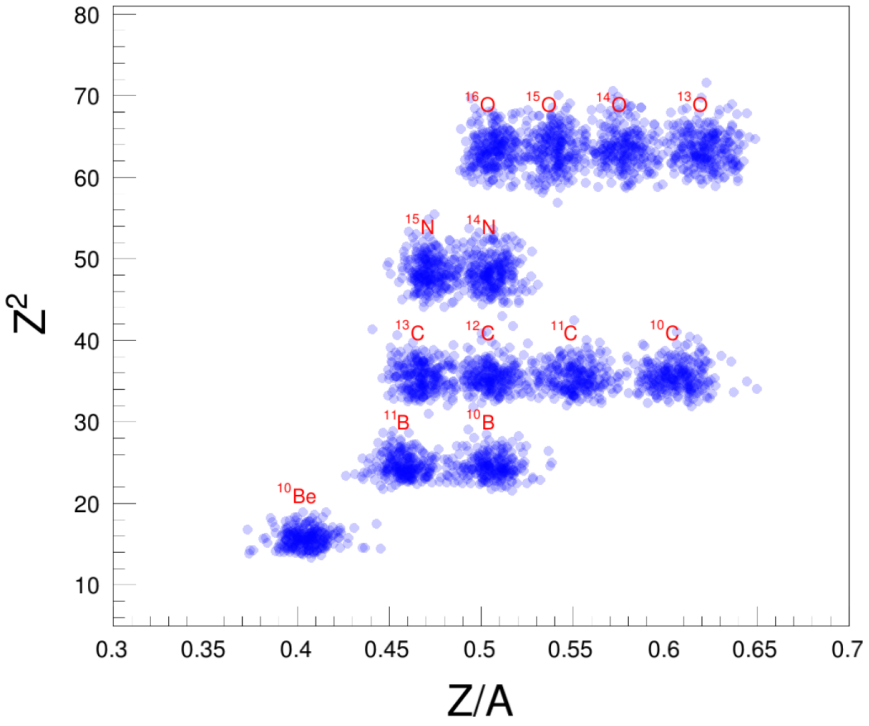

Figure 54: Simulation of the identification of isotopes of fragmented ions NA61/SHINE.

(iii) **beam pid:** Measurement of the projectile mass A_b from its time of flight over a distance of 240 m and determination of its charge Z_b from the energy deposit in a scintillator and amount of Cherenkov light produced in a quartz plate. Both techniques give a signal proportional to Z^2 of the particle.

(iv) **fragment pid:** Measurement of the charge of the fragment from the energy deposit in a scintillator downstream of the target and the energy deposit in the TPCs. Determination of the rigidity of the fragment (and thus mass given the measured charge) from the bending in the NA61 superconducting magnets with a maximum bending power of 9 Tm.

This experimental set-up is described in more detail in [130]. The ability to separate different isotopes from fragmentation interactions for a given charge was validated with simulations. Fragments were generated at the target position with a smeared momentum to mimic the momentum acceptance of the SPS beam line and then passed through a full GEANT4 description of the NA61/SHINE setup. The results of the simulation are displayed in Fig. 54. The individual ions are well separated, demonstrating the ability of the proposed setup to measure the production cross section of individual ions.

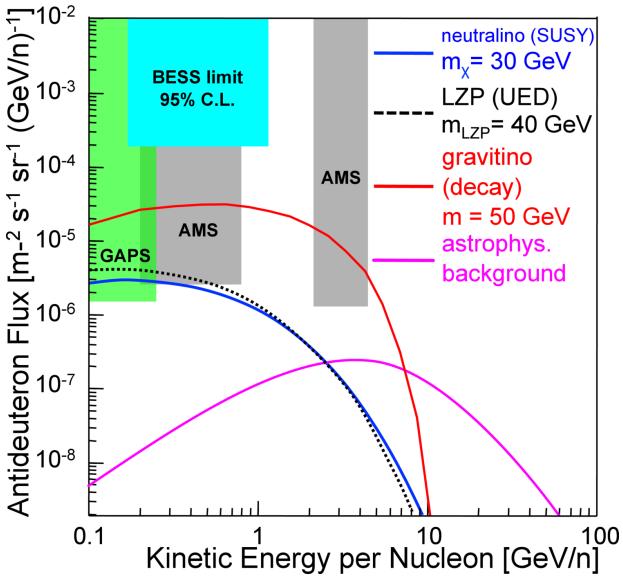

Figure 55: Predicted antideuteron fluxes from different dark matter models and astrophysical processes [131–134]. Also shown are limits from BESS [135] and the projected sensitivity of AMS-02 [136] (updated for measurement time, geomagnetic cutoff model, background fluxes) and GAPS [137, 138].

7.2 Dark Matter Searches with Cosmic-ray Antinuclei

The existence of dark matter is established on very different length scales from galaxies to galaxy clusters to the cosmic microwave background [139]. Little is known about dark matter particles except that they are gravitationally interacting, but other than that only very weakly interacting - if at all - with regular matter. Many theories trying to explain dark matter suggest a stable, relatively heavy particle - the weakly interacting massive particle (WIMP). All WIMPs invoke physics beyond the Standard Model of particle physics.

If dark matter was in thermal equilibrium in the early universe it is natural to assume that dark matter particles are able to annihilate with each other and produce Standard Model particles. These particles would contribute to the known cosmic rays, and thus an imprint of dark matter might be observable as an excess on top of the diffuse cosmic-ray flux. Dark matter models providing a very long-lived unstable candidate decaying into Standard Model particles might be detectable in a similar way. Cosmic-ray antiparticles without primary astrophysical sources are ideal candidates for such a dark matter search. The positron fraction results of PAMELA [140], Fermi [141], AMS-01 [142], AMS-02 [143, 144] show evidence of a structure that might be interpreted as induced by, e.g., dark matter or nearby pulsars [145]. Also the AMS-02 antiproton-to-proton ratio [107] is inconclusive: some models do not require any additional component [146], while others see potential evidence for dark matter annihilation [147]. The latter publication is especially interesting because it combines the antiproton measurements with a γ-ray excess

observed by Fermi in the Galactic Center region [148].

Anti-deuterons may also be generated in dark matter annihilations or decays, offering a potential breakthrough in unexplored phase space for dark matter. The unique strength of searching for low-energy anti-deuterons lies in the ultra-low astrophysical background [131, 132, 149–152]. The final report of the strategic planning for U.S. particle physics concludes that: "Future experiments sensitive to anti-deuteron fluxes at low energies may provide incisive tests of some WIMP dark matter candidates" [153]. Cosmic-ray anti-deuterons from any source have not been discovered so far and the best limits are given by the BESS experiment [135]. Fig. 55 reveals why low-energy anti-deuterons are such an important approach: the fluxes from a wide range of viable dark matter models [131–133] exceed the astrophysical background [134] by $\mathcal{O}(100)$ in the low-energy range below a few GeV/nucleon. This is in strong contrast to positrons, anti-protons, and γ-rays where only a small contribution on top of the background is expected in optimistic scenarios.

7.2.1 Anti-deuteron Formation

Although the predicted low-energy flux of antideuterons from dark matter annihilations or decays is much higher in many models, the uncertainties of anti-deuteron formation and propagation are on the order of a factor of 10 and should be reduced for a more powerful dark matter interpretation. The formation of nuclei in hadronic interactions is described by different models. It is an important question whether (anti)deuterons are produced at chemical freeze-out from a quark-gluon plasma or at a later stage via coalescence. The conclusion of the following short overview is that more experimental data and better modelling of (anti)deuteron formation are needed. This is in agreement with one outcome of the first dedicated cosmic-ray anti-deuteron workshop [154] that the measurement of (anti-)deuteron production in p+p interactions at $p_{\mathrm{LAB}} = 40 - 400$ GeV/c is of utmost importance.

The studies proposed in the following will have significant impact on dark matter searches with cosmic rays. It was pointed out by the authors of Refs. [155, 156] that more precise anti-proton data are needed to improve the modelling of the astrophysical anti-proton flux. Furthermore, the improved anti-deuteron coalescence modelling in the energy range that is most crucial for cosmic rays will decrease the uncertainties for the astrophysical background flux from about a factor of 10 [132] to about 2.

7.2.2 Coalescence Model

The fusion of an anti-proton and an anti-neutron into an anti-deuteron can be described by the simple coalescence model, which is based on the assumption that any pair of (anti-)proton and (anti-)neutron within a sphere of radius p_0 in momentum space will coalesce to produce an (anti)nucleus. The coalescence momentum p_0 is a phenomenological quantity and cannot be calculated from first principles. Therefore, it has to be determined through fits to experimental data [157]. In this approach, the (anti-)deuteron

spectrum is given by:

$$\gamma_d \frac{\mathrm{d}^3 N_d}{\mathrm{d}p_d^3} = \frac{\pi}{6} p_0^3 \left(\gamma_p \frac{\mathrm{d}^3 N_p}{\mathrm{d}p_p^3} \right) \left(\gamma_n \frac{\mathrm{d}^3 N_n}{\mathrm{d}p_n^3} \right), \tag{6}$$

where p_i and $\mathrm{d}N_i/\mathrm{d}p_i$ are, respectively, the momentum and the differential yield per event of particle i (d=(anti-)deuteron, p=(anti-)proton, n=(anti-)neutron). The coalescence momentum is a critical value because it enters to the third power and directly scales the yield, and as such the cosmic-ray flux. The state-of-the-art technique is to apply the coalescence condition to $\overline{\mathrm{pn}}$ pairs on a per-event basis in Monte Carlo simulations. Tuning to experimental data typically yields best-fit p_0 values in the range of about 100 MeV/c, which is smaller than the typical scale at which the perturbative theory of Quantum Chromodynamics breaks down. As a result, the coalescence model is sensitive to non-perturbative effects in the hadronic generators.

A recent study [158] combined results from existing anti-deuteron measurements. The left panel of Fig. 56 illustrates the best current understanding of the modified coalescence momentum, a slight redefinition compared to Eq. 6, for anti-deuteron production as a function of energy in the laboratory frame. The underlying data sets come from many different experiments, some dating back several decades. The different points are derived from mostly poorly constrained production cross section spectra. Due to the shape of the primary cosmic-ray spectrum, especially interesting for the understanding of cosmic-ray anti-deuterons is the steep increase of the coalescence momentum between 10 to 100 GeV/c of beam momentum.

7.2.3 Thermal model

The production of light nuclei in p+p interactions can also be discussed in a thermal model approach, where the hadronization happens in fireballs [159–161]. The resulting particle spectra can be used to examine the conditions at freeze-out. In this model, the particle yields depend approximately exponentially on the chemical freeze-out temperature T_{chem} and the mass m: $\mathrm{d}N/\mathrm{d}y \propto \exp\left(-m/T_{\mathrm{chem}}\right)$. Due to their large masses, the abundance of nuclei is very sensitive to T_{chem}. The value of T_{chem} obtained from data is about 170 MeV and shows a low energy dependence.

7.2.4 Anti-deuteron Formation Studies

The goal of this proposal is to improve the understanding of (anti-)deuteron formation by analysing large statistics p+p data sets in the range of 20–400 GeV/c. Therefore, it is proposed to collect 600 million collision each at 20, 158 and 400 GeV/c with NA61/SHINE. This request becomes feasible because of the about ten-times faster detector readout. It will have the big advantage of having precision data from a single modern experiment rather than relying on a number of different older experiments with partially unknown systematic effects. The right panel of Fig. 56 illustrates the impact on

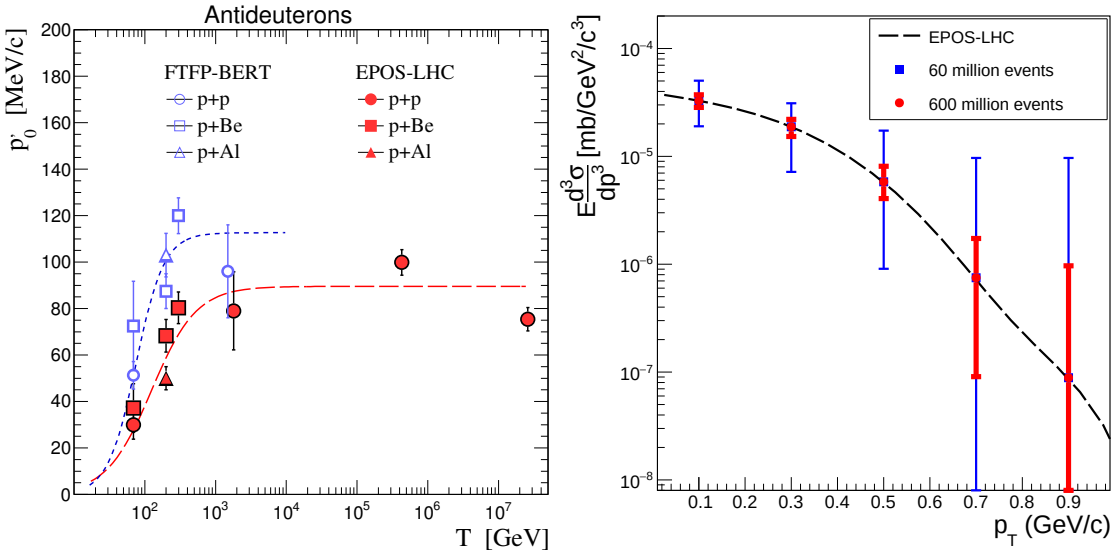

Figure 56: Left: Modified coalescence momentum p'_0 (see Ref. [158]) for anti-deuterons as function of kinetic energy for two different hadronic generators. The `Geant4` FTFP-BERT model could not be used to simulate the highest energies. Right: Estimates from EPOSLHC simulations for differential invariant anti-deuteron production cross sections in p+p interactions at 158 GeV/c for 60 and 600 millions, respectively.

the error bars of the anti-deuteron production cross section using EPOSLHC simulations and reasonable estimates for NA61/SHINE detection efficiencies. Overall, the error bars are roughly a factor of 4 smaller for 600 million collisions compared to the estimates for existing data from 2010/2011 with 60 million collisions. This directly translates into a better factor of 4 better understanding of the coalescence momentum, reducing an important uncertainty for the cosmic-ray anti-deuteron understanding significantly. The following paragraphs outline the different steps in the analysis that need to be taken to improve the anti-deuteron formation for hadronic event generators like EPOSLHC.

7.2.5 Measurement of Nucleon Production Channels

As mentioned above, a lot of the data that were used for the development of the modified coalescence model dates back several decades [158]. Therefore, it is important to add new results from experiments with up-to-date techniques in hardware and data analysis to reduce systematic errors. As was already started with lower statistics NA61/SHINE p+p data [162], detailed measurements of various (anti-)proton production channels will be performed to tune hadronic generators. The left panel of Fig. 57 shows the EPOSLHC prediction for the number of particles and particle pairs produced per collision in p+p interactions at 158 GeV/c. As (anti)deuterons are composed of two (anti-)nucleons, it is most interesting to study channels with at least two (anti-)nucleons in the final state.

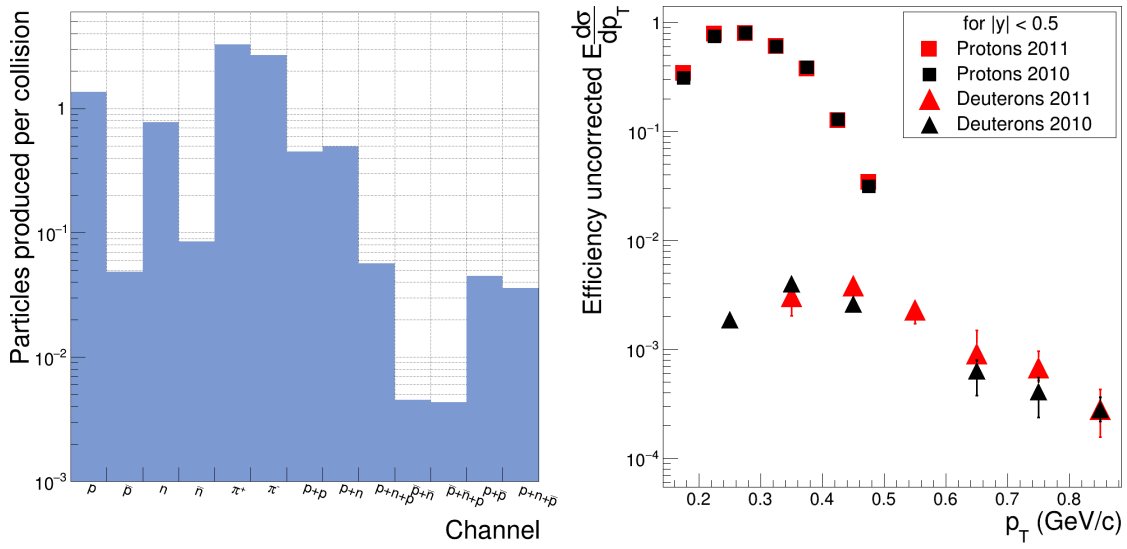

Figure 57: Left: EPOSLHC prediction for the number of particles and particle pairs produced per collision in p+p interactions at 158 GeV/c. Right: Efficiency uncorrected proton and deuteron differential invariant cross sections in p+p interactions at 158 GeV/c as measured with NA61/SHINE.

7.2.6 Correlation Studies

The underlying mechanisms of hadronic generators are very different and it cannot be expected that two-particle correlation models agree. There is also no a-priori reason to expect the two-particle correlations from one generator to be more reliable than from another. Therefore, an important study is to compare angular correlations between (anti-)protons and (anti-)neutrons for different generators. For this purpose the differences in azimuthal angle $\Delta\phi$ and in pseudo-rapidity $\Delta\eta$ of nucleon pairs will be investigated. Like many fixed-target experiments, NA61/SHINE does not have experimental access to (anti-)neutron spectra. Therefore, only pp, $p\overline{p}$, and $\overline{p}\overline{p}$ correlations will be studied experimentally and compared to simulations. This is a crucial step for validating and/or tuning the underlying hadronic models. EPOSLHC simulations indicate that small $\Delta\eta$ and $\Delta\phi$ differences are favoured for deuteron coalescence. Additionally, the same study also showed that pp pairs exhibit a similar behaviour as pn pairs, serving as additional motivation to use pp, $p\overline{p}$, and $\overline{p}\overline{p}$ pairs for correlation studies relevant to (anti-)deuterons.

7.2.7 (Anti-)deuteron Cross Section Measurements

The Pb+Pb data of NA49 were already analysed for anti-deuterons and successfully demonstrated that anti-deuterons can be identified in the experimental set-up [163]. However, the large number of nucleons in heavy-ion collisions cause different formation conditions than in p+p interactions or light-ion collisions and are not directly transferable.

Between 2009 and 2011, nearly 60 million events on p+p interactions with the target inserted and about 5 million events with the target removed were recorded. The identification of low-momentum deuterons is based on the truncated mean of the energy depositions in the TPCs along the track. Combining estimates for the detection efficiency with the EPOSLHC simulations, about 300 000 protons, 13 000 anti-protons, 1100 deuterons, and 10 anti-deuterons are expected in the low-momentum range.

More than 1000 clean low-momentum deuterons were detected with high statistical significance in the 2009 to 2011 p+p data sets. A preliminary step for the cross section calculation (without acceptance correction) is shown in the right panel of Fig. 57. The optimization of selection and quality criteria is ongoing. Further momentum range widening will be achieved by using time-of-flight information. Measuring charge, momentum, and velocity, mass reconstruction in NA61/SHINE is possible up to a maximum momentum of about 10 GeV/c (restricted by timing resolution), which corresponds to the momentum range accessible for deuterons by the cosmic-ray experiment AMS-02.

7.2.8 (Anti-)deuteron Production Channels

Deuteron production is dominated by production in association with pions (p+p $\rightarrow$ p+n+π^+above $\sqrt{s} \approx 2.0$ GeV) while anti-deuteron production requires at least six final-state nucleons (p+p $\rightarrow$ $\overline{\text{p}}$+$\overline{\text{n}}$+n+p+p+p above $\sqrt{s} \approx 5.6$ GeV). Production of anti-deuterons in association with only pions is not possible for interactions of (anti-)protons with the interstellar medium. Therefore, a detailed accounting of the number of pions, protons, anti-protons, etc. in association with deuterons will be carried out to study if and how the deuteron spectrum changes. Two channels are especially important: The deuteron production in association with one proton (p+p $\rightarrow$ d+$\overline{\text{n}}$+p) is relevant because the production of anti-deuterons in $\overline{\text{p}}$+p $\rightarrow$ $\overline{\text{d}}$+n+p should show the same energy dependence. In addition, production of deuterons in association with a single anti-proton (p+p $\rightarrow$ d+$\overline{\text{p}}$+$\overline{\text{n}}$+p+p) will be searched for. Clean anti-deuteron events should have three additional protons in the final state (p+p $\rightarrow$ $\overline{\text{d}}$+n+p+p+p).

7.2.9 Ratios

The d/p and $\overline{\text{d}}/\overline{\text{p}}$ ratios as a function of transverse momentum will be determined and used as tools to tune hadronic generators as well as to test the coalescence and thermal model approach. The analysis of ALICE data [164] suggests that the thermal model works well for Pb+Pb interactions, but that the d/p ratio is over-predicted for p+p interactions. As it is more relevant to cosmic rays, this finding will be tested with the lower SPS energies.

7.3 Beam Request for 2022

Measurements for cosmic-ray research require 24 days of secondary ion beam at 13 A GeV/c in 2022. This beam request is needed to start measurements of nuclear fragmentation cross sections as discussed is Sec. 7.1.

The total number of interactions to record is about 0.6×10^6 (cf. Table 8) and a similar amount of auxiliary measurements ($C + C$ and target-removed) are needed in addition corresponding to about 19 days of uninterrupted data taking at a recorded interaction rate of 62k/day (cf. Sec. 9.2). Additional time needs to be reserved for changing the different targets (polyethylene/C, liquid hydrogen, helium) and the setup of trigger and beam-line for different beam-rigidities. Assuming one day of setup for each rigidity a total of 24 days of data taking are needed. The request for continuation of the measurements in 2023 and 2024 will be subject of a future addendum.

The proton beam request related to measurements of light nuclei and anti-nuclei in p+p interactions will be subject of a future addendum.

8 Hadron production measurements for neutrino physics

During the recent 'NA61 beyond 2020' workshop [165] the importance of hadron production measurements for on-going and future neutrino experiments was strongly emphasized by all neutrino physics speakers. Many accelerator and atmospheric neutrino experiments expressed interest in new additional thin-target measurements. These range from very low beam momenta up to 120 GeV/c.

Published NA61/SHINE thin-target measurements [128, 166–168] have been crucial for T2K to reduce (anti-)neutrino flux uncertainties down to $\approx$ 10%, and further improvements - by a factor of two - are expected soon [169], as the T2K replica-target results [170, 171] are added to the T2K's flux model.

The SPS beam group has discussed constructing a tertiary hadron beam-line for beams at very low momenta ($<$ 10 GeV/c). Measurements with these low-energy particles could be very important for future high-precision T2K physics.

T2K is considering hybrid and alternative target materials for high-power operation in the T2K-II/Hyper-K era. Hadron production measurements with these new target materials are a priority for the early post-LS2 NA61 operation. Whether new measurements with the existing T2K replica target are needed will be concluded after introducing the NA61/SHINE 2010 replica-target results [172] in the T2K beam simulation. The design of new targets for the future high-intensity long-baseline neutrino experiment DUNE is in progress now. Prototype long targets could possibly be available in 2022 and beyond.

Additional tracking detectors will improve the precision of long-target measurements, especially for the very long targets for DUNE. The target could be surrounded by a set of tracking detectors to pinpoint low-angle tracks from the upstream end of the target.

8.1 Measurements for T2K, T2K-II and HyperK

NA61/SHINE hadron production measurements play an important role in the T2K long baseline neutrino oscillation programme because precise knowledge of production distribution of the hadrons which are the neutrino parents is crucial to predict the neutrino flux and its uncertainty [173]. Neutrino flux of T2K is currently calculated based on the published results of NA61/SHINE thin target measurements [128, 166–168]. The uncertainty on the absolute flux at the T2K neutrino energy peak at 0.6 GeV is around 10 % in total at both near and far neutrino detectors and the largest source of this uncertainty is the imprecise knowledge of hadron production spectra, as shown in Fig. 58. Improvement of the flux uncertainty using the NA61/SHINE 2009 replica target data is expected soon and promises to reduce the uncertainty from hadron production down to 4 % [169, 171, 172]. Moreover, further improvement is expected with the 2010 replica target data in particular the uncertainty in high neutrino energy region because of significant improvement of the knowledge of the kaon yield from the replica target data.

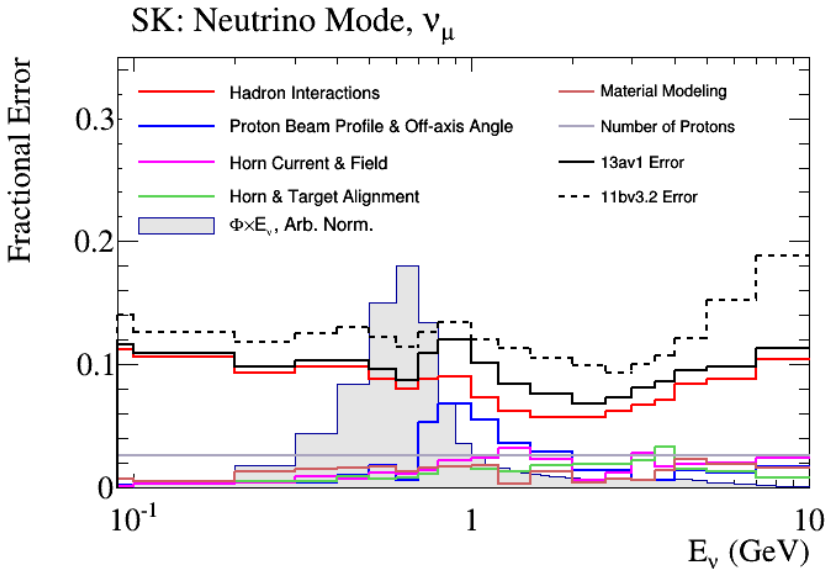

Figure 58: T2K flux uncertainty as a function of the neutrino energy. Black and red line show the total error and the error from hadron interactions, respectively.

Neutrino oscillation measurements at T2K indicate neutrino CP violation and a maximal mixing angle θ_{23} [174, 175]. For higher sensitivity measurements of these indications, an extension of T2K data taking (T2K-II) was proposed by increasing the beam power of the J-PARC Main Ring (MR) as well as by improving the T2K analyses and their systematic uncertainties [176]. The J-PARC MR beam power is planned to be increased from the current 475 kW to 1.3 MW and some upgrades of the neutrino beam facility are also planned. The neutrino production target will be upgraded by enhancing the cooling capability by increasing the pressure of the cooling helium gas and re-optimization of its titanium window geometry while the shape of core graphite target part will not be changed. The same J-PARC neutrino beam-line will also be utilized for the Hyper-K experiment.

For T2K-II and Hyper-K a reduction of the total flux uncertainty down to 3–4 % is desired. The major uncertainty in the replica target tuning is still hadron production. Further improvement of the hadron production data can be expected from the following measurements:

(i) Improved measurement of hadron production with the T2K replica target

(ii) Hadron production with low momentum beams

Moreover, a new design of the neutrino production target is being discussed. Motivating the new target is an increase of the neutrino flux while reducing the wrong sign neutrino flux for better significance of neutrino CP violation measurements.

8.1.1 Improved measurement of hadron production with the T2K replica target

As mentioned in the previous subsection, the major uncertainty on the T2K flux predicted with the NA61/SHINE replica target data is still from the lack of precise data on hadron interactions. In 2009 replica target measurements, the production momentum and angle distribution of the charged pion is measured individually for five longitudinal parts of the T2K replica target and directly used to tune the yield of pions on the surface of the target in the T2K flux calculation. The statistical and systematic uncertainties of the these yields are used to evaluate the T2K flux uncertainties. It was found that the uncertainties of the NA61/SHINE results are a large source of the hadron interaction uncertainty in the T2K flux while the uncertainty of the interaction length is the second largest contribution.

One potential improvement is expected from further precise measurements with the replica target. As discussed in the published literature [171,172], a discrepancy between the charged pion data and the model prediction was observed in particular for the first three upstream longitudinal parts of the target although the published NA61/SHINE thin target results were probably used in the FLUKA model. For the upstream longitudinal parts, a large systematic uncertainty was assigned. In order to achieve better precision of the T2K flux prediction, it is desired to understand and improve these uncertainties.

One significant source of uncertainty in the 2010 long-target data is the backward pointing of tracks to the target surface. This, and the overall tracking efficiency uncertainty, may be addressed by the addition of tracking planes near the target (as described in Sec. 8.3). Moreover, it was found necessary to take data with empty target and changed magnetic field/beam momentum in addition to data taking with the nominal condition, in order to

(i) eliminate sources of fake tracks from interactions in the target support,

(ii) measure precisely the transmission of the target for incoming beam particles.

Once these sources of uncertainty are reduced to the few 0.1% level, the uncertainties due to the replica target measurements themselves should be well below $\pm 2\%$.

The run plan should be similar to that of 2010, with 14 days of normal magnetic field with 31 GeV/c proton beam and 7 days at full field. In addition 6 days of empty target at normal field and one day at full field should be foreseen, for a total of 28 days of beam. Given the improved data acquisition rate of NA61/SHINE, the data so acquired should allow an improvement of statistical uncertainties by a factor of 3.

8.1.2 Hadron production with low momentum beams

Neutrino CP violation is explored by measuring $\nu_\mu \rightarrow \nu_e$ and $\overline{\nu}_\mu \rightarrow \overline{\nu}_e$ appearance modes. In these measurements, intrinsic ν_e or $\overline{\nu}_e$ are a major background contribution. Moreover, some fraction of the wrong sign components are contributed from the

Table 9: Fraction of the T2K flux from different hadronic interaction chains producing neutrinos at the far detector in the neutrino mode beam. (a) the number of inelastic proton beam interactions is one and the interaction occurred in the target, (b) other than the case (a), (c) the number of inelastic hadronic interactions outside the target is greater than or equal to one which is a part of (b).

type	(a)	(b)	(c)
ν_μ	63.2%	36.8%	12.4%
$\overline{\nu}_\mu$	41.5%	58.5%	45.1%
ν_e	61.7%	38.3%	12.7%
$\overline{\nu}_e$	54.0%	46.0%	27.2%

hadronic interactions outside the target, as summarized in Table 9. Those interactions outside the target occur in the magnetic horn, the wall of the decay volume, the helium gas in the decay volume, and the beam dump (the materials are Al,Fe,He and C, respectively). Therefore, it is important to understand the interactions outside the target to precisely predict the wrong sign ν_e backgrounds.

Recently, it was realized that better measurements of the following hadron production reactions are necessary to improve the precision of the T2K flux calculation, in particular of the wrong sign flux, because there are no available data (NA61/SHINE, HARP etc.) at present. The following reactions are of primary interest:

(i) 1-5 GeV/c pions on aluminum

(ii) 1-5 GeV/c pions on carbon

(iii) 1-5 GeV/c kaons on carbon

(iv) 1-5 GeV/c pions on helium

The low momentum (less than 12 GeV/c) hadron production data is also useful for improvement of the atmospheric neutrino flux prediction for future neutrino experiments such as Hyper-K and DUNE.

Based on simulation studies, new measurements of the above interactions with 10 % uncertainty are required in order to reduce the flux uncertainty from the above interactions to less than 2 %. New measurements of hadron production distributions and total inelastic cross sections are proposed with thin targets and the beam momenta mentioned above. Possibilities to realize such low momentum beams at the SPS by constructing a tertiary hadron beam-line was discussed during the 'NA61 beyond 2020' workshop [165].

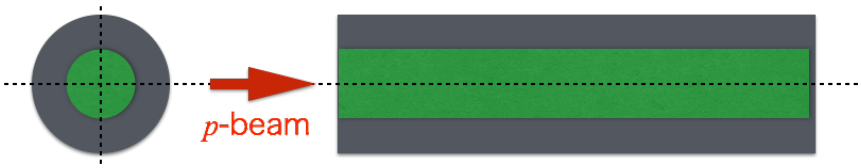

Figure 59: Schematic diagram of a new potential J-PARC hybrid target.

8.1.3 Measurements for T2K-II and HyperK Hybrid Target

Present and future J-PARC long-baseline neutrino oscillation experiments, T2K, T2K-II, and Hyper-K, predict the number of ν_e and $\overline{\nu}_e$ appearance events based on simulated neutrino beam fluxes. The major background contribution for a measurement of $\overline{\nu}_e$ appearance from a $\overline{\nu}_\mu$ beam is the intrinsic wrong sign component (ie ν_e's in a $\overline{\nu}_e$ appearance search). In order to improve the significance of a CP violation measurement, it is essential to reduce this intrinsic wrong sign component.

One possibility for reducing the wrong-sign component is to increase the density of the material used for the neutrino production target, which is presently made of graphite. Figure 59 shows a cartoon of the new target idea, where the new target consists of a dense core surrounded by a less dense graphite sheath. Potential advantages of this target design are :

(i) Hadron production is increased in the higher-density core without increasing hadron absorption in the target's lower-density sheath

(ii) Forward-going hadrons outside of the horn acceptance are decreased by absorption in the higher density core

(iii) The hadron production source becomes point-like (such that better horn focusing is expected)

(iv) Even if the target core is damaged, fragments would be contained by the graphite sheath

The candidate core material currently under investigation is Super-Sialon ($Si_3N_4Al_2O_3$), which has a density of 3.2 g/cm^3, 1.8 times larger than the current graphite target. Although further studies of mechanical stress and radiation damage of this design are necessary, it is believed that this material could lead to a viable new target design.

Results of a Monte Carlo study of the predicted neutrino flux using the new hybrid target design are shown in Fig. 60, indicating a 10% increase of the right-sign neutrino flux at the flux peak, with a 10$\sim$25% reduction of the wrong sign component.

In order to study the feasibility of this new target idea, new hadron production measurements with the new target material are proposed. The precision of the neutrino flux

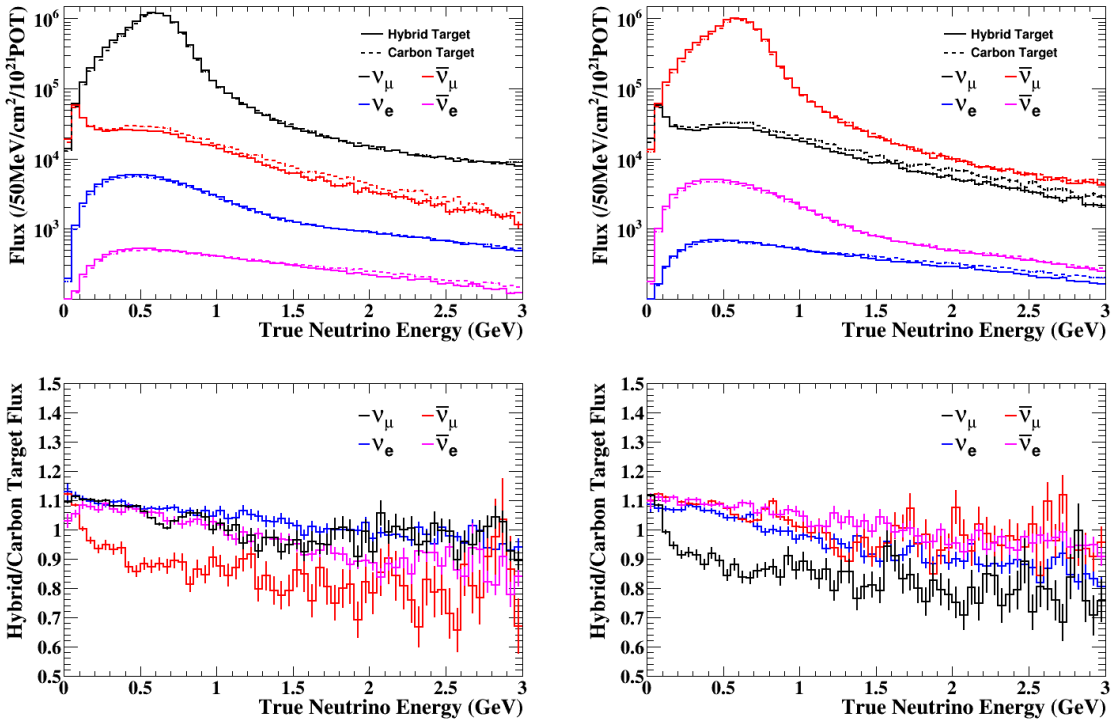

Figure 60: The neutrino flux at Super-K in neutrino-mode (top left) and anti-neutrino-mode (top right) for the current graphite target and new hybrid target designs, as well as the ratio of the flux for the hybrid/graphite target (bottom left in neutrino-mode and bottom right in anti-neutrino-mode).

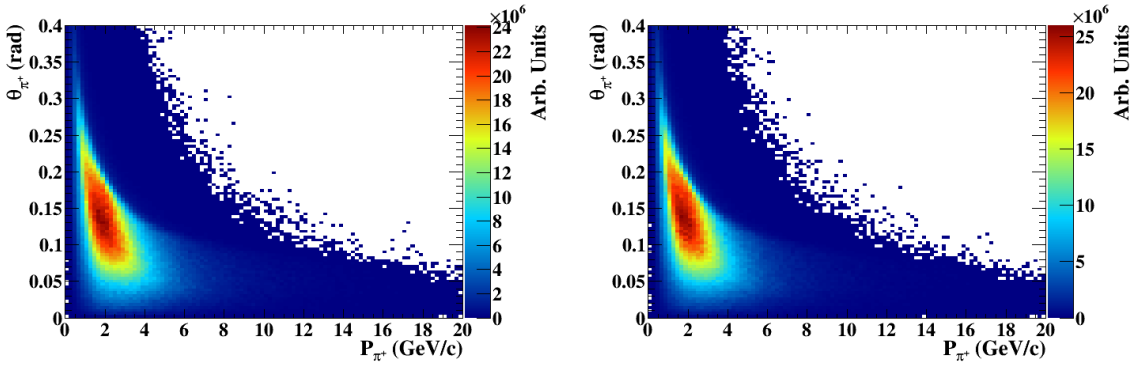

Figure 61: The phase space of π^+'s contributing to the neutrino flux in neutrino-mode for the current graphite target (*left*) and the proposed hybrid target (*right*). The phase space of other hadrons for the hybrid target is similarly consistent with that of the graphite target.

using this new hybrid target must be similar to the precision of the flux from the T2K target (systematic uncertainties arising from hadron production uncertainties of 5% at the near detector and <0.2% on the far-to-near detector flux extrapolation [169, 173]). In order to achieve this precision, new measurements with 30 GeV protons incident on a thin (∼2 cm) target made of the new material are proposed. Following preliminary studies of the new material, if all properties are viable, measurements with 31 GeV/c protons incident on a replica (90 cm) hybrid target will also be proposed. The replica target design would depend on the initial thin target hadron production measurement results, as well as mechanical design concerns.

The phase space of π^+'s contributing to the neutrino flux for the current graphite target and the new hybrid target is shown in Fig. 61. Since the phase space of hadrons contributing to the flux for the new target is similar to that of the graphite target, NA61/SHINE data can cover a significant region. Previous NA61/SHINE measurements for T2K consist of 6×10^6 triggers on a thin graphite target and 10×10^6 triggers on a T2K replica target. Similar measurements are proposed for the new target material in order to achieve a similar precision. This requires one week of proton beam at 31 GeV/c.

8.2 Measurements for LBNF/DUNE

Hadron production measurements will be particularly important for DUNE [177] which aims to make an accurate determination of the CP violating phase of the neutrino mixing matrix, which requires a precise prediction for the electron neutrino event rate in the far liquid argon detector. Since DUNE will not have identical near and far detectors, DUNE will need precise knowledge of the flux in the neutrino beam generated by the future Long-Baseline Neutrino Facility Beam (LBNF) being planned for DUNE [178]. The secondary SPS hadron beams available to NA61/SHINE (13–400 GeV/c) are well suited to the LBNF beam-line, where the neutrinos originate from high-intensity proton

beams in the energy range 60-120 GeV/c that impinge upon graphite and/or beryllium targets.

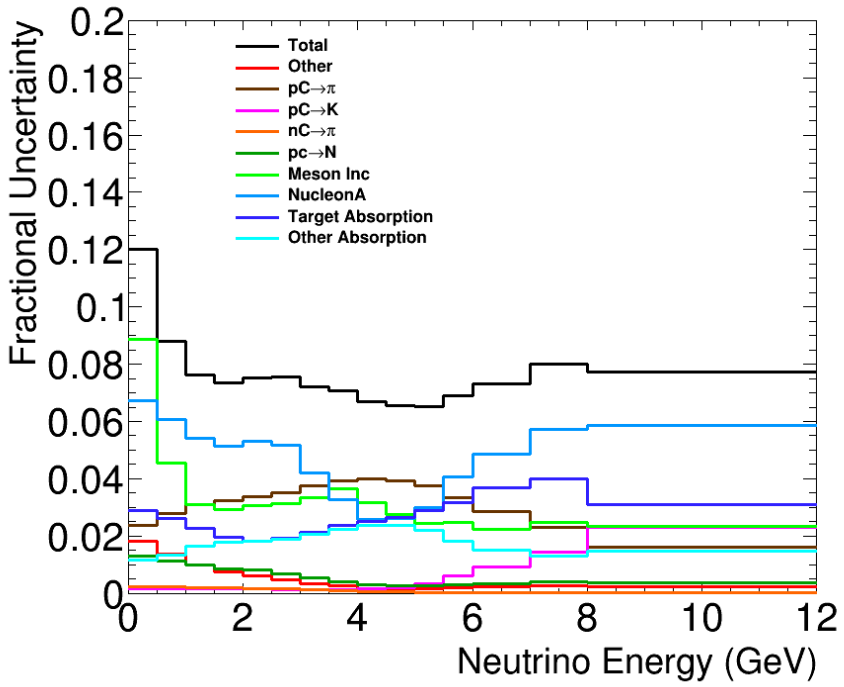

Figure 62: Current estimated uncertainties on the LBNF neutrino mode ν_μ flux at the DUNE far detector due to hadron production. This is for the optimized 3-horn beam configuration with an 80 GeV/c primary proton beam [179]. These errors are expected to be similar for a 120 GeV/c primary proton beam.

Figure 62 shows the current estimates of the hadron production uncertainties. The biggest contributions are due to uncertainties in existing measurements of pion production from proton interactions with carbon (shown in brown as p+C $\rightarrow$ π+X in Fig. 62), pion and kaon re-interactions (shown in bright green as Meson Inc), nucleon interactions not covered by existing data (shown in blue as NucleonA), and the uncertainty on the total probability of interactions in other materials (shown in cyan and labeled as "Other Absorption"). In the DUNE optimized beam, it is estimated that there will be an average of $\approx$1.7 interactions occurring in the beam-line for each neutrino that will reach the near detector [179]. So in addition to the primary proton interactions, the re-interactions of lower-energy protons, pions, neutrons, and kaons make a very significant contribution to the neutrino flux.

A campaign is currently under-way in NA61/SHINE to make thin target (a few percent of λ_i) measurements using proton, pion, and possibly kaon beams on carbon, beryllium and aluminium to measure the products of the primary proton interactions in the

target, as well as the secondary re-interactions of those hadrons in the target material and aluminium horns. These will have more incident hadron species over a more suitable range of incident hadron momenta, additional target materials, higher statistics, and better coverage of particle production in the forward direction compared to the existing data, and should dramatically reduce the flux uncertainties coming from hadron production uncertainties at DUNE in the region of interest for neutrino oscillations.

Beyond 2020 the highest priority measurements for DUNE will be to expand from the current suite of thin target measurements to measurements on a full-scale replica LBNF target (as was done for T2K). NA61/SHINE will pursue LBNF long target measurements in 2022–2024 if a prototype target is available. The LBNF target is still under design and the exact time scale for the availability of a prototype target is uncertain.

In addition to the replica target measurements, additional thin target measurements should be performed in 2022 (if possible even in 2021), especially with kaon beams. There is little high-quality hadron production data for kaon beams in this energy range. Since the kaons will re-interact in the graphite target and in the aluminium horns, K^+ +C at 60 GeV/c and K^+ +Al at 60 GeV/c would be a high priority for future data taking beyond 2020. Each measurement would likely required 2 weeks of beam time.

8.3 Additional tracking detectors for long targets

To maximize the reach of long-target measurements in the future, especially for LBNF/DUNE where the target could be twice as long as T2K's, we propose to develop a set of tracking detectors surrounding the target to aid in pointing tracks backward to their origin at the surface of the target.

An analysis of the present uncertainties of the replica target measurements identifies the following dominant sources:

(i) The overall track reconstruction uncertainty of $\pm 2\%$. This is surprisingly large for a TPC-based spectrometer. It is evaluated by varying the setup, in particular by using or not the GAP TPC, and varying geometrical cuts. Such variations are useful to estimate uncertainties but the method can be blind to overall common effects, which explains the somewhat conservative estimate. Adding redundancy by adding a tracking device near the target would allow a more deterministic approach, which typically should lead to more typical reconstruction efficiency uncertainties at the few 0.1% level.

(ii) The backward extrapolation uncertainty results from tracking errors, magnetic field errors, multiple scattering and nuclear interactions of particles from the spectrometer back to the origin of the particles on the surface of the replica target. The lack of measured points near the target is again the main source of these uncertainties, which were estimated in the replica target paper to amount to $\pm 10\%$ of the yields for low-angle tracks originating from the upstream part of the target or for large-angle, low-momentum tracks originating from the most downstream parts of the target.

A search for an affordable and flexible tracking device for long target measurements has led us to consider a setup based on micromegas detectors with 1 mm-pitch strip readout in two dimensions, positioned as sketched in Fig. 63. The point resolution of such a device is about 350 microns. The most important requirements are the following:

(i) There should be a full set of three tracking devices (with $xy/uv/xy$ readout) downstream of the target covering the acceptance of the spectrometer ($\pm$400 mrad in horizontal plane, $\pm$150 mrad in the vertical plane).

(ii) There should be measured points a few cm downstream of each of the four locations of the longitudinal binning along the target, in order to provide precise extrapolation of particles to the target surface.

(iii) A similar device should be placed upstream of the target to include the beam particle measurement in the same geometrical reference.

(iv) All tracking elements as well as the target should be mounted on a single precise mechanical frame.

The figures shown are for a set of detectors specific to the T2K target, as its shape is known. The detector system should be designed in a way that is modular and flexible to accommodate additional target geometries such as LBNF/DUNE. As the detector planes themselves are not expected to be particularly expensive, the planes that have a hole for the target may be built specifically for each target geometry. The design would allow them to be easily swapped out when using different targets, while keeping the same front-end electronics.

8.4 Beam Request for 2022

Measurements for neutrino physics require:

(i) 35 days of proton beam at 31 GeV/c in 2022. This beam request is needed to improve measurements of hadron flux from the T2K replica target (28 days) and measurements of hadron production on a Super-Sialon thin target (7 days) as discussed in Secs. 8.1.1 and 8.1.3

(ii) 28 days of K^+ beam at 60 GeV/c in 2022 to gather missing data on hadron production by K^+ mesons relevant for simulations of hadron flux from long targets.

Some or all of these measurements could take place in 2021 as well, if beam and detector conditions permit. Beam requests related to other possible measurements for neutrino physics discussed in this section will be the subject of future addenda.

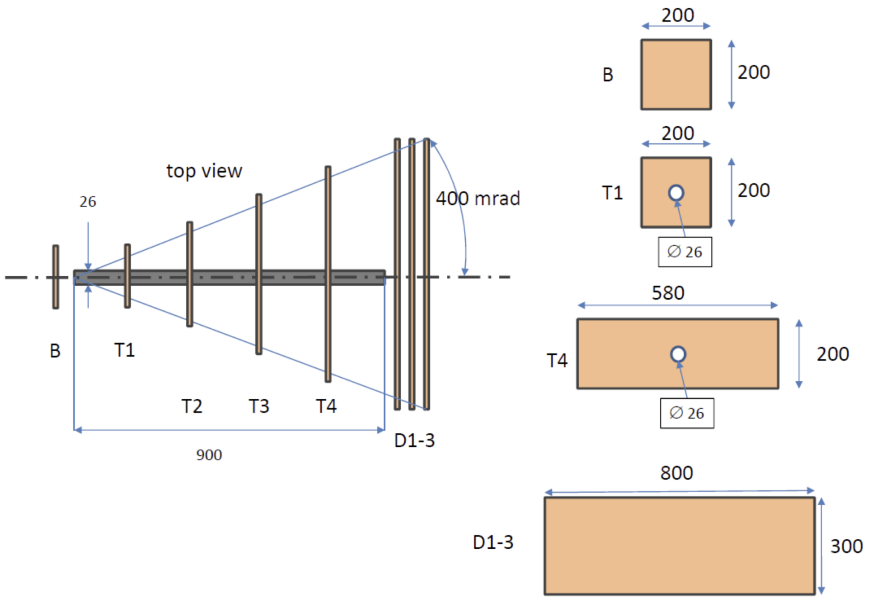

Figure 63: Layout of the proposed long target tracker set-up. On the left is the top view ($x - z$ horizontal plane); on the right is the $x - y$ view of some of the detectors. Dimensions are in millimeters. Detector B is measuring the incoming particle; detectors T1 to T4 are situated around the target to precisely measure the location of the exit point of particles from the target surface; detectors D1 to D3 are situated downstream of the target to resolve possible ambiguities and determine the track angles, thus allowing a redundant evaluation of tracking efficiencies.

9 Data taking parameters

Basic parameters of data taking requested in 2022 (see Sec. 10) are summarized below.

9.1 Data taking for charm in Pb+Pb collisions

Data is planned to be recorded under following conditions:

(i) SPS cycle length: from 26.4 s to $\approx$ 70 s, flat top: 8.5 s,
average duty cycle (based on the Xe+La data taking): $\approx$ 0.15,

(ii) Pb beam intensity at the NA61/SHINE target: $\approx 10^5$ ions/s,

(iii) Pb target: $\approx$ 5% interaction probability (about 0.25 cm thickness), rate of all inelastic events 5000 Hz, rate of 30% most violent collisions 1500 Hz,

(iv) recorded event rate during the spill: 800 Hz,

(v) fraction of time for physics data taking
(includes beam, detector, and trigger set-up time, as well as planned and unplanned machine stops based on Xe+La data taking in 2017): $\approx$ 80%,

(vi) mean number of recorded events: $\approx$ 8M events/day.

Mean number of recorded Pb+Pb collisions after off-line quality cuts (mostly off-time rejection) is expected to be about 6M events/day.

Data on Pb+Pb collisions 150A GeV/c will be recorded using two on-line event selections:

(i) minimum bias event selection (95% events) and

(ii) Pb beam selection (5% events).

Data on Pb+Pb collisions 40A GeV/c will be recorded using three on-line event selections:

(i) selection of 30% of inelastic collisions with the smallest energy recorded in the PSD (80% events),

(ii) minimum bias event selection (15% events) and

(iii) Pb beam selection (5% events).

The minimum bias event selection will be provided by anti-coincidence of the incoming beam particle with the signal from a scintillator detector located just downstream of the Vertex Detector. This should minimize the contamination by non-target interactions. The detector will work as a threshold detector with the threshold set just below the Pb-ion signal.

The maximum beam intensity on NA61/SHINE target is limited by following reasons:

(i) Data quality of the PSD is reduced at beam intensities > 100 kHz,

(ii) Probability of off-time beam particles increases reducing number of events useful for analysis, at beam intensities > 100 kHz more than 30% of events could not be used during analysis,

(iii) Radiation shielding of the beam-line limits maximum beam intensity.
Even with increase of intensity to 100 kHz the shielding have to be upgraded.

9.2 Data taking for nuclear fragmentation cross section

Data is planned to be recorded with secondary ion beam produced by fragmentation of primary Pb beam on the T2 target.

Estimated data taking conditions:

(i) SPS cycle length: from 26.4 s to ≈ 70 s, flat top: 8.5 s,
average duty cycle (based on Xe+La data taking): ≈ 0.15,

(ii) fraction of wanted ions within secondary beam hitting the NA61/SHINE target: 2–4%,

(iii) target: $\approx 2\%$ interaction probability,

(iv) maximum intensity of the secondary beam: 100 kHz
(limited by off-time beam particles),

(v) intensity of wanted ions on the NA61/SHINE target: 2–4 kHz,

(vi) recorded event rate during the spill: 800 Hz,

(vii) number of recorded interactions per second: 16,

(viii) inefficiency due to low frequency time structure of the low momenta beams: 50%,

(ix) number of recorded interactions: 62k events/day,

(x) fraction of time for physics data taking
(includes beam, detector, and trigger set-up time, as well as planned and unplanned machine stops based on Xe+La data taking in 2017): $\approx 90\%$,

(xi) mean number of recorded interactions including typical data taking efficiency: 56k events/day,

The low frequency time structure of the low momenta beams causes the most severe loss of statistics. The solution for this problem was discussed between NA61/SHINE and SPS operators on "NA61/SHINE beams beyond LS2" meeting [180].

An on-line event selection will accept all events with a wanted beam particle (interacting or not). This selection is due to a low fraction of wanted ions in the secondary ion beam. Using an interaction trigger with would not saturate the DAQ, therefore the increase of the number of recorded interactions would be at most by a factor of two. The disadvantage of the interaction trigger is an increase of systematic uncertainty of final results. For example the systematic uncertainty of the Be+Be cross section measurement related to the interaction trigger is $\approx 1\%$.

9.3 Data taking for neutrino physics

The neutrino physics programme assumes two sets of measurements: 31 GeV/c proton beam and 60 GeV/c K^+ beam.

The data taking conditions for 60 GeV/c K^+ beam are estimated as follow:

(i) SPS cycle length: from 26.4 s to $\approx$ 70 s, flat top: 8.5 s,
average duty cycle (based on Xe+La data taking): ≈ 0.15,

(ii) fraction of wanted hadrons within secondary beam hitting the NA61/SHINE target: 3%,

(iii) target: $\approx 5\%$ interaction probability,

(iv) maximum intensity of the secondary beam: 200 kHz
(limited by off-time beam particles),

(v) intensity of wanted hadrons on the NA61/SHINE target: 6 kHz,

(vi) minimum bias interaction rate: 300 Hz

(vii) recorded event rate during the spill: 60 Hz,

(viii) fraction of time for physics data taking
(includes beam, detector, and trigger set-up time, as well as planned and unplanned machine stops based on Xe+La data taking in 2017): $\approx 90\%$,

(ix) mean number of recorded interactions: 600k events/day,

(x) number of recorded interactions without off-time particles: 250k events/day.

The data taking conditions for 31 GeV/c proton beam are estimated as follow:

(i) SPS cycle length: from 26.4 s to $\approx$ 70 s, flat top: 8.5 s,
average duty cycle (based on Xe+La data taking): ≈ 0.15,

(ii) fraction of wanted hadrons within secondary beam hitting the NA61/SHINE target: 14%,

(iii) target: $\approx$ 5% interaction probability,

(iv) maximum intensity of the secondary beam: 200 kHz
(limited by off-time beam particles),

(v) intensity of wanted hadrons on the NA61/SHINE target: 28 kHz,

(vi) minimum bias interaction rate: 1200 Hz

(vii) recorded event rate during the spill: 240 Hz,

(viii) fraction of time for physics data taking
(includes beam, detector, and trigger set-up time, as well as planned and unplanned machine stops based on Xe+La data taking in 2017): $\approx$ 90%,

(ix) mean number of recorded interactions: 2.5M events/day,

(x) number of recorded interactions without off-time particles per day: 1.2M events/day.

10 Summary of beam requests

In view of the Memorandum of the CERN DRC (see Appendix B), in this document we request a beam time for physics data taking only in 2022, namely:

(i) 42 days of primary Pb beam at 150A GeV/c for data taking on charm hadron production in Pb+Pb collisions (heavy ion physics).

(ii) 24 days of secondary light ion beam at 13A GeV/c for data taking on nuclear fragmentation cross section (cosmic ray physics).

(iii) 35 days of proton beam at 31 GeV/c for data taking on hadron production from the T2K replica target and the Super-Sialon thin target (neutrino physics).

(iv) 28 days of K^+ beam at 60 GeV/c for data taking on hadron production by induced K^+ mesons. (neutrino physics)

In addition we plan a commissioning and calibration of the upgraded detector in 2021. Two weeks of secondary hadron beams at 13–400 GeV/c will be needed for this purpose. Finally, we request a feasibility study of very low energy (1-5 GeV/c) hadron beams needed for neutrino physics.

Acknowledgments

We would like to thank the CERN EP, BE and EN Departments for the strong support of NA61/SHINE.

This work was supported by the Hungarian Scientific Research Fund (Grants NK-FIH 123842–123959), the János Bolyai Research Scholarship of the Hungarian Academy of Sciences, the Polish Ministry of Science and Higher Education (grants 667/N-CERN/2010/0, NN 202 48 4339 and NN 202 23 1837), the Polish National Center for Science (grants 2011/03/N/ST2/03691, 2013/11/N/ST2/03879, 2014/13/N/ST2/02565, 2014/14/E/ST2/00018, 2014/15/B/ST2/02537 and 2015/18/M/ST2/00125, 2015/19/N/ST2/01689, 2016/23/B/ST2/00692), the Foundation for Polish Science – MPD program, co-financed by the European Union within the European Regional Development Fund, the Russian Science Foundation, grant 16-12-10176, the Russian Academy of Science and the Russian Foundation for Basic Research (grants 08-02-00018, 09-02-00664 and 12-02-91503-CERN), the Ministry of Science and Education of the Russian Federation, grant No. 3.3380.2017/4.6, the National Research Nuclear University MEPhI in the framework of the Russian Academic Excellence Project (contract No. 02.a03.21.0005, 27.08.2013), the Ministry of Education, Culture, Sports, Science and Technology, Japan, Grant-in-Aid for Scientific Research (grants 18071005, 19034011, 19740162, 20740160 and 20039012), the German Research Foundation (grant GA 1480/2-2), the Bulgarian Nuclear Regulatory Agency and the Joint Institute for Nuclear Research, Dubna (bilateral contract No. 4418-1-15/17), Bulgarian National Science Fund (grant DN08/11), Ministry of Education and Science of the Republic of Serbia (grant OI171002), Swiss Nationalfonds Foundation (grant 200020117913/1), ETH Research Grant TH-01 07-3 and the U.S. Department of Energy.

References

[1] N. Abgrall *et al.*, [NA61/SHINE Collab.] *JINST* **9** (2014) P06005, arXiv:1401.4699 [physics.ins-det].

[2] M. Gazdzicki, M. Gorenstein, and P. Seyboth *Acta Phys.Polon.* **B42** (2011) 307–351, arXiv:1006.1765 [hep-ph].

[3] N. Abgrall *et al.*, [NA61/SHINE Collab.], "Hadron Production Measurements for Fermilab Neutrino Beams," 2014. Addendum to the NA61/SHINE proposal submitted to the SPSC on October 14, 2014.

[4] M. van Leeuwen, "Kaon and open charm production in central lead-lead collisions at the CERN SPS," 2015.

[5] R. Arnaldi *et al.*, [NA60 Collab.] *Eur. Phys. J.* **C59** (2009) 607, arXiv:0810.3204 [physics.nucl-ex].

[6] E. V. Shuryak *Phys. Rept.* **61** (1980) 71–158.

[7] D. D. Ivanenko and D. F. Kurdgelaidze *Astrophysics* **1** (1965) 251–252. [Astrofiz.1,479(1965)].

[8] N. Itoh *Prog. Theor. Phys.* **44** (1970) 291.

[9] J. C. Collins and M. J. Perry *Phys. Rev. Lett.* **34** (1975) 1353.

[10] N. Cabibbo and G. Parisi *Phys. Lett.* **59B** (1975) 67–69.

[11] R. Hagedorn *Nuovo Cim. Suppl.* **3** (1965) 147–186.

[12] R. Hagedorn and J. Rafelski, "From Hadron Gas to Quark Matter. 1.," in *NUCLEAR PHYSICS. PROCEEDINGS, INTERNATIONAL CONFERENCE, BERKELEY, CALIFORNIA, USA, AUGUST 24-30, 1980*, pp. 237–251. 1980.

[13] M. I. Gorenstein, V. K. Petrov, and G. M. Zinovev *Phys. Lett.* **106B** (1981) 327–330.

[14] T. Bhattacharya *et al. Phys. Rev. Lett.* **113** no. 8, (2014) 082001, arXiv:1402.5175 [hep-lat].

[15] M. Asakawa and K. Yazaki *Nucl. Phys.* **A504** (1989) 668–684.

[16] A. Barducci, R. Casalbuoni, S. De Curtis, R. Gatto, and G. Pettini *Phys. Lett.* **B231** (1989) 463–470.

[17] U. W. Heinz and M. Jacob arXiv:nucl-th/0002042 [nucl-th].

[18] M. Gazdzicki and D. Roehrich *Z.Phys.* **C65** (1995) 215.

[19] M. Gazdzicki and D. Rohrich *Z.Phys.* **C71** (1996) 55–64, arXiv:hep-ex/9607004 [hep-ex].

[20] E. Fermi *Prog. Theor. Phys.* **5** (1950) 570–583.

[21] L. Landau *Izv.Akad.Nauk Ser.Fiz.* **17** (1953) 51–64.

[22] M. Gazdzicki *Z. Phys.* **C66** (1995) 659–662.

[23] M. Gazdzicki and M. I. Gorenstein *Acta Phys.Polon.* **B30** (1999) 2705, arXiv:hep-ph/9803462 [hep-ph].

[24] S. Afanasiev *et al.*, [NA49 Collab.] *Phys. Rev.* **C66** (2002) 054902.

[25] C. Alt *et al.*, [NA49 Collab.] *Phys. Rev.* **C77** (2008) 024903.

[26] L. Adamczyk *et al.*, [STAR Collab.] *Phys. Rev.* **C96** no. 4, (2017) 044904, arXiv:1701.07065 [nucl-ex].

[27] A. Rustamov *Central Eur.J.Phys.* **10** (2012) 1267–1270, arXiv:1201.4520 [nucl-ex].

[28] A. Aduszkiewicz, [NA61/SHINE Collaboration Collab.], "Report from the NA61/SHINE experiment at the CERN SPS," Oct, 2014.

[29] N. Antoniou *et al.*, [NA49-future Collaboration Collab.], "Study of Hadron Production in Hadron-Nucleus and Nucleus-Nucleus Collisions at the CERN SPS," Tech. Rep. SPSC-P-330. CERN-SPSC-2006-034, CERN, Geneva, Nov, 2006. https://cds.cern.ch/record/995681. revised version submitted on 2006-11-06 12:38:20.

[30] N. Antoniou *et al.*, [NA49-future Collaboration Collab.], "Study of Hadron Production in Collisions of Protons and Nuclei at the CERN SPS," Tech. Rep. CERN-SPSC-2006-001. SPSC-I-235, CERN, Geneva, Jan, 2006. https://cds.cern.ch/record/919966. revised version submitted on 2006-03-31 17:22:05.

[31] A. Aduszkiewicz, [NA61/SHINE Collaboration Collab.], "Report from the NA61/SHINE experiment at the CERN SPS," Tech. Rep. CERN-SPSC-2017-038. SPSC-SR-221, CERN, Geneva, Oct, 2017. https://cds.cern.ch/record/2287091.

[32] F. Becattini, J. Manninen, and M. Gazdzicki *Phys.Rev.* **C73** (2006) 044905, arXiv:hep-ph/0511092 [hep-ph].

[33] V. V. Begun, M. Gazdzicki, M. I. Gorenstein, M. Hauer, V. P. Konchakovski, and B. Lungwitz *Phys. Rev.* **C76** (2007) 024902, arXiv:nucl-th/0611075 [nucl-th].

[34] G. Baym *Physica A* **96** (1979) 131–135.

[35] T. Celik, F. Karsch, and H. Satz *Phys. Lett.* **97B** (1980) 128–130.

[36] M. Braun and C. Pajares *Nucl. Phys.* **B390** (1993) 542–558.

[37] N. Armesto, M. A. Braun, E. G. Ferreiro, and C. Pajares *Phys. Rev. Lett.* **77** (1996) 3736–3738, arXiv:hep-ph/9607239 [hep-ph].

[38] L. Cunqueiro, E. G. Ferreiro, F. del Moral, and C. Pajares *Phys. Rev.* **C72** (2005) 024907, arXiv:hep-ph/0505197 [hep-ph].

[39] J. M. Maldacena *Int. J. Theor. Phys.* **38** (1999) 1113–1133, arXiv:hep-th/9711200 [hep-th]. [Adv. Theor. Math. Phys.2,231(1998)].

[40] E. Shuryak *Prog. Part. Nucl. Phys.* **62** (2009) 48–101, arXiv:0807.3033 [hep-ph].

[41] S. Lin and E. Shuryak *Phys. Rev.* **D79** (2009) 124015, arXiv:0902.1508 [hep-th].

[42] J. Wosiek *Acta Phys. Polon.* **B19** (1988) 863–869.

[43] A. Bialas and R. Hwa *Phys.Lett.* **B253** (1991) 436–438.

[44] M. A. Stephanov, K. Rajagopal, and E. V. Shuryak *Phys.Rev.* **D60** (1999) 114028, arXiv:hep-ph/9903292 [hep-ph].

[45] M. Gorenstein and M. Gazdzicki *Phys. Rev.* **C84** (2011) 014904.

[46] A. Snoch, [NA61/SHINE Collab.] arXiv:1803.01692 [nucl-ex].

[47] R. V. Gavai, S. Gupta, P. L. McGaughey, E. Quack, P. V. Ruuskanen, R. Vogt, and X.-N. Wang *Int. J. Mod. Phys.* **A10** (1995) 2999–3042, arXiv:hep-ph/9411438 [hep-ph].

[48] P. Braun-Munzinger and J. Stachel *Phys. Lett.* **B490** (2000) 196–202, arXiv:nucl-th/0007059 [nucl-th].

[49] O. Linnyk, E. L. Bratkovskaya, and W. Cassing *Int. J. Mod. Phys.* **E17** (2008) 1367–1439, arXiv:0808.1504 [nucl-th].

[50] T. Song.

[51] A. P. Kostyuk, M. I. Gorenstein, H. Stoecker, and W. Greiner *Phys. Lett.* **B531** (2002) 195–202, arXiv:hep-ph/0110269 [hep-ph].

[52] M. C. Abreu *et al.*, [NA50 Collab.] *Phys. Lett.* **B477** (2000) 28–36.

[53] P. Levai, T. S. Biro, P. Csizmadia, T. Csorgo, and J. Zimanyi *J. Phys.* **G27** (2001) 703–706, arXiv:nucl-th/0011023 [nucl-th].

[54] R. V. Poberezhnyuk, M. Gazdzicki, and M. I. Gorenstein *Acta Phys. Polon.* **B48** (2017) 1461, arXiv:1708.04491 [nucl-th].

[55] J. Rafelski and B. Muller *Phys. Rev. Lett.* **48** (1982) 1066. [Erratum: Phys. Rev. Lett.56,2334(1986)].

[56] A. P. Kostyuk, M. I. Gorenstein, and W. Greiner *Phys. Lett.* **B519** (2001) 207–211, arXiv:hep-ph/0103057 [hep-ph].

[57] p. c. R. V. Poberezhnyuk.

[58] T. Matsui and H. Satz *Phys. Lett.* **B178** (1986) 416–422.

[59] H. Satz *Adv. High Energy Phys.* **2013** (2013) 242918.

[60] M. C. Abreu *et al.*, [NA50, NA38 Collab.] *Eur. Phys. J.* **C14** (2000) 443–455.

[61] R. Arnaldi *et al.*, [NA60 Collab.] *Phys. Rev. Lett.* **99** (2007) 132302.

[62] H. Satz *EPJ Web Conf.* **71** (2014) 00118.

[63] "Mimosa26 user manual." https://www.google.de/url?sa=t&rct=j&q=&esrc=s&source=web&cd=1&cad=rja&uact=8&ved=0ahUKEwi4udLhuOHYAhWE1iwKHQ5QC38QFggnMAA&url=http%3A%2F%2Fwww.iphc.cnrs.fr%2FIMG%2Fpdf%2FM26_UserManual_light.pdf&usg=AOvVaw3TtHsmtXtnFO57_rFSqXIM.

[64] B. Abelev *et al.*, [ALICE Collaboration Collab.], "Technical Design Report for the Upgrade of the ALICE Inner Tracking System," Tech. Rep. CERN-LHCC-2013-024. ALICE-TDR-017, Nov, 2013. https://cds.cern.ch/record/1625842.

[65] Z.-W. Lin *et al. Phys. Rev.* **C72** (2005) 064901.

[66] A. Aduszkiewicz *et al.*, [NA61/SHINE Collaboration Collab.], "Beam momentum scan with Pb+Pb collisions," Tech. Rep. CERN-SPSC-2015-038. SPSC-P-330-ADD-8, CERN, Geneva, Oct, 2015. https://cds.cern.ch/record/2059811.

[67] L. Zi-Wei *et al. Phys. Rev.* **C72** (2005) 064901, arXiv:nucl-th/0411110 [physics.nucl-th].

[68] E. Linnyk, Bratkovskaya and W. Cassing *Int. J. Mod. Phys.* **E17** (2008) 1367.

[69] M. Gazdzicki *Phys. Rev.* **C60** (1999) 054903, arXiv:hep-ph/9809412 [hep-ph].

[70] E. Meninno, [ALICE Collab.] *EPJ Web Conf.* **137** (2017) 06018.

[71] G. W. S. Hou, [ATLAS, CMS Collab.] *PoS* **CHARM2016** (2016) 088.

[72] M. Simko, [STAR Collab.] *J. Phys. Conf. Ser.* **832** no. 1, (2017) 012028.

[73] K. Nagashima, [PHENIX Collab.] *Nucl. Phys.* **A967** (2017) 644–647, arXiv:1704.04731 [nucl-ex].

[74] G. Odyniec *J. Phys. Conf. Ser.* **455** (2013) 012037.

[75] C. Yang, [STAR Collab.] *Nucl. Phys.* **A967** (2017) 800.

[76] K. C. Meehan, [STAR Collab.] *Nucl. Phys.* **A956** (2016) 878.

[77] V. Kekelidze, A. Kovalenko, R. Lednicky, V. Matveev, I. Meshkov, A. Sorin, and G. Trubnikov *Nucl. Phys.* **A967** (2017) 884.

[78] V. Kekelidze, "Why are we building the nica ?." https://indico.cern.ch/event/638553/contributions/2771587/attachments/1554737/2444516/KekelidzeNICAdays.pdf.

[79] H. Sako *et al.*, [J-PARC Heavy-Ion Collab.] *Nucl. Phys.* **A956** (2016) 850.

[80] M. Kitazawa, "Search for qcd critical point at j-parc-hi." https://kds.kek.jp/indico/event/25425/session/7/contribution/20.

[81] B. Friman, C. Hohne, J. Knoll, S. Leupold, J. Randrup, R. Rapp, and P. Senger *Lect. Notes Phys.* **814** (2011) 1.

[82] V. Friese, "Studying dense matter with the cbm experiment." http://www.ectstar.eu/sites/www.ectstar.eu/files/talks/ECT_Nov17_Friese.pdf.

[83] N. Abgrall *et al.*, [NA61/SHINE Collab.], "Beam momentum scan with Pb+Pb collisions by NA61/SHINE at the CERN SPS," 2015. CERN-SPSC-2015-038; SPSC-P-330-ADD-8.

[84] G. Aglieri Rinella, [ALICE Collab.] *Nucl. Instrum. Meth.* **A845** (2017) 583.

[85] A. Laszlo, E. Denes, Z. Fodor, T. Kiss, S. Kleinfelder, C. Soos, D. Tefelski, T. Tolyhi, G. Vesztergombi, and O. Wyszynski *Nucl. Instrum. Methods Phys. Res., A* **798** (May, 2015) 1. 14 p.

[86] "Vistars - OP Webtools." https://op-webtools.web.cern.ch/vistar/vistars.php.

[87] M. Gazdzicki, [NA61/SHINE Collaboration Collab.], "The 2010 test of secondary light ion beams," Tech. Rep. CERN-SPSC-2011-005. SPSC-SR-077, CERN, Geneva, Jan, 2011. https://cds.cern.ch/record/1322135.

[88] S. V. Afanasev, A. Isupov, V. I. Kolesnikov, A. I. Malakhov, G. L. Melkumov, and A. Yu. Semenov *JINR rapid communications* **5[85]-97** (1997) 69–90.

[89] V. Kekelidze, V. Kolesnikov, and A. Sorin *EPJ Web Conf.* **171** (2018) 12001. https://doi.org/10.1051/epjconf/201817112001.

[90] V. Babkin *et al. Nucl. Instrum. Meth.* **A824** (2016) 490–492.

[91] M. G. Buryakov, V. A. Babkin, V. M. Golovatyuk, S. V. Volgin, and M. M. Rumyantsev *Phys. Part. Nucl. Lett.* **13** no. 5, (2016) 532–534.

[92] http://afi.jinr.ru/TDC72VHL.

[93] V. Babkin, et al. *Bulgarian Chemical Communications, 47, Special Issue B* **47** (2015) 215.

[94] A. Rybicki *Acta Phys. Polon.* **B42** (2011) 867–876.

[95] K. Mazurek, A. Szczurek, C. Schmitt, and P. N. Nadtochy arXiv:1708.03716 [nucl-th].

[96] A. Marcinek *et al.* to appear in Acta Phys. Polon. B (2018).

[97] A. Szczurek, M. Kiełbowicz, and A. Rybicki *Phys. Rev.* **C95** no. 2, (2017) 024908, arXiv:1612.06694 [nucl-th].

[98] A. Rybicki, A. Szczurek, and M. Kłusek-Gawenda *Acta Phys. Polon.* **B46** no. 3, (2015) 737.

[99] K. Mazurek. private communication.

[100] K. Mazurek, A. Szczurek, and P. N. Nadtochy *Acta Phys. Polon. Supp.* **10** (2017) 113, arXiv:1612.05397 [nucl-th].

[101] V. A. Karnaukhov *et al. Phys. Atom. Nucl.* **69** (2006) 1142.

[102] A. Rybicki and A. Szczurek *Phys. Rev.* **C75** (2007) 054903, arXiv:nucl-th/0610036 [nucl-th].

[103] A. Rybicki and A. Szczurek *Phys. Rev.* **C87** no. 5, (2013) 054909, arXiv:1303.7354 [nucl-th].

[104] M. Aguilar *et al.*, [AMS Collab.] *Phys. Rev. Lett.* **120** no. 2, (2018) 021101.

[105] M. Aguilar *et al.*, [AMS Collab.] *Phys. Rev. Lett.* **119** no. 25, (2017) 251101.

[106] M. Aguilar *et al.*, [AMS Collab.] *Phys. Rev. Lett.* **117** no. 23, (2016) 231102.

[107] M. Aguilar *et al.*, [AMS Collab.] *Phys. Rev. Lett.* **117** no. 9, (2016) 091103.

[108] M. Aguilar *et al.*, [AMS Collab.] *Phys. Rev. Lett.* **115** no. 21, (2015) 211101.

[109] M. Aguilar *et al.*, [AMS Collab.] *Phys. Rev. Lett.* **114** (2015) 171103.

[110] M. Aguilar *et al.*, [AMS Collab.] *Phys. Rev. Lett.* **113** (2014) 221102.

[111] M. Aguilar *et al.*, [AMS Collab.] *Phys. Rev. Lett.* **113** (2014) 121102.

[112] L. Accardo *et al.*, [AMS Collab.] *Phys. Rev. Lett.* **113** (2014) 121101.

[113] G. Ambrosi *et al.*, [DAMPE Collab.] *Nature* **552** (2017) 63–66, arXiv:1711.10981 [astro-ph.HE].

[114] O. Adriani *et al.*, [CALET Collab.] *Phys. Rev. Lett.* **119** no. 18, (2017) 181101, arXiv:1712.01711 [astro-ph.HE].

[115] A. W. Strong, I. V. Moskalenko, and V. S. Ptuskin *Ann. Rev. Nucl. Part. Sci.* **57** (2007) 285–327.

[116] E. Amato and P. Blasi arXiv:1704.05696 [astro-ph.HE].

[117] T. A. Porter, R. P. Johnson, and P. W. Graham ARA&A **49** (2011) 155–194.

[118] J. Lavalle and P. Salati *Comptes Rendus Physique* **13** (2012) 740–782.

[119] W. R. Webber, A. Soutoul, J. C. Kish, and J. M. Rockstroh *The Astrophysical Journal Supplement Series* **144** no. 1, (2003) 153. http://stacks.iop.org/0067-0049/144/i=1/a=153.

[120] D. Maurin, A. Putze, and L. Derome *Astronomy and Astrophysics* **516** (June, 2010) A67, arXiv:1001.0553 [astro-ph.HE].

[121] Y. Genolini, A. Putze, P. Salati, and P. D. Serpico *Astronomy and Astrophysics* **580** (Aug., 2015) A9, arXiv:1504.03134 [astro-ph.HE].

[122] N. Tomassetti *Phys. Rev.* **D96** no. 10, (2017) 103005, arXiv:1707.06917 [astro-ph.HE].

[123] A. Reinert and M. W. Winkler arXiv:1712.00002 [astro-ph.HE].

[124] K. Blum, K. C. Y. Ng, R. Sato, and M. Takimoto arXiv:1704.05431 [astro-ph.HE].

[125] Y. Genolini, D. Maurin, I. Moskalenko, and M. Unger *submitted to PRC* (2018) , arXiv:1803.04686 [astro-ph.HE].

[126] Putze, A., Derome, L., and Maurin, D. *Astronomy & Astrophysics* **516** (2010) A66. https://doi.org/10.1051/0004-6361/201014010.

[127] D. Maurin, "USINE propagation code and associated tools," in *Proceedings of the 34th International Cosmic Ray Conference*. 2015.

[128] N. Abgrall *et al.*, [NA61/SHINE Collab.] *Eur. Phys. J.* **C76** no. 2, (2016) 84, arXiv:1510.02703 [hep-ex].

[129] E. Kaptur, [NA61/SHINE Collab.] *Proceedings of Science* **CPOD2014** (2015) 053.

[130] A. Aduszkiewicz *et al.*, [NA61/SHINE Collab.], "Feasibility Study for the Measurement of Nuclear Fragmentation Cross Sections with NA61/SHINE at the CERN SPS," 2017. CERN-SPSC-2017-035 ; SPSC-P-330-ADD-9.

[131] H. Baer and S. Profumo *Journal of Cosmology and Astroparticle Physics* **0512** (2005) 008, arXiv:astro-ph/0510722 [astro-ph].

[132] F. Donato, N. Fornengo, and D. Maurin *Physical Review D* **78** (2008) 043506, arXiv:0803.2640 [hep-ph].

[133] L. Dal and A. Raklev *Physical Review D* **89** (2014) 103504, arXiv:1402.6259 [hep-ph].

[134] A. Ibarra and S. Wild *Physical Review D* **88** (2013) 023014, arXiv:1301.3820 [astro-ph.HE].

[135] H. Fuke *et al. Physical Review Letters* **95** no. 8, (Aug., 2005) 081101, astro-ph/0504361.

[136] V. Choutko and F. Giovacchini *International Cosmic Ray Conference* **4** (2008) 765–768.

[137] C. J. Hailey *New Journal of Physics* **11** no. 10, (Oct., 2009) 105022+.

[138] T. Aramaki *et al. Astroparticle Physics* **74** (Feb., 2016) 6–13, arXiv:1506.02513 [astro-ph.HE].

[139] K. Freese *EAS Publications Series* **36** (2009) 113–126, arXiv:0812.4005 [astro-ph].

[140] O. Adriani *et al. Nature* **458** (Apr., 2009) 607–609, arXiv:0810.4995.

[141] M. Ackermann *et al. Physical Review Letters* **108** no. 1, (Jan., 2012) 011103, arXiv:1109.0521 [astro-ph.HE].

[142] M. Aguilar *et al. Physics Letters B* **646** no. 4, (2007) 145 – 154.

[143] M. Aguilar *et al. Physical Review Letters* **110** (Apr, 2013) 141102.

[144] L. Accardo *et al.*, [(AMS Collaboration) Collab.] *Physical Review Letters* **113** (Sep, 2014) 121101.

[145] M. Boudaud, S. Aupetit, S. Caroff, A. Putze, G. Belanger, Y. Genolini, C. Goy, V. Poireau, V. Poulin, S. Rosier, P. Salati, L. Tao, and M. Vecchi *Astronomy & Astrophysics* **575** (Mar., 2015) A67, arXiv:1410.3799 [astro-ph.HE].

[146] R. Kappl, A. Reinert, and M. W. Winkler *JCAP* **1510** no. 10, (2015) 034, arXiv:1506.04145 [astro-ph.HE].

[147] A. Cuoco, J. Heisig, M. Korsmeier, and M. KrÃd'mer *JCAP* **1710** no. 10, (2017) 053, arXiv:1704.08258 [astro-ph.HE].

[148] V. Vitale, A. Morselli, and for the Fermi/LAT Collaboration *ArXiv e-prints* (Dec., 2009) , arXiv:0912.3828 [astro-ph.HE].

[149] F. Donato, N. Fornengo, and P. Salati *Physical Review D* **62** (2000) 043003, arXiv:hep-ph/9904481 [hep-ph].

[150] N. Fornengo, L. Maccione, and A. Vittino *Journal of Cosmology and Astroparticle Physics* **1309** (2013) 031, arXiv:1306.4171 [hep-ph].

[151] R. Duperray, B. Baret, D. Maurin, G. Boudoul, A. Barrau, L. Derome, K. Protasov, and M. Buénerd *Physical Review D* **71** no. 8, (Apr., 2005) 083013, astro-ph/0503544.

[152] A. Ibarra and S. Wild *Journal of Cosmology and Astroparticle Physics* **1302** (2013) 021, arXiv:1209.5539 [hep-ph].

[153] S. Ritz *et al.*, "Building for discovery: Strategic plan for u.s. particle physics in the global context," 2014. http://science.energy.gov/~/media/hep/hepap/pdf/May%202014/FINAL_P5_Report_Interactive_060214.pdf.

[154] T. Aramaki *et al. Physics Reports* **618** (Mar., 2016) 1–37, arXiv:1505.07785 [hep-ph].

[155] R. Kappl, A. Reinert, and M. W. Winkler *Journal of Cosmology and Astroparticle Physics* **10** (Oct., 2015) 034, arXiv:1506.04145 [astro-ph.HE].

[156] M. Kachelriess, I. V. Moskalenko, and S. S. Ostapchenko *Astrophysical Journal* **803** no. 2, (2015) 54, arXiv:1502.04158 [astro-ph.HE].

[157] A. Schwarzschild and Č. Zupančič *Physical Review* **129** (Jan, 1963) 854–862.

[158] D.-M. Goemz-Coral *et al. in preparation* (2018) .

[159] F. Becattini and U. W. Heinz *Zeitschrift fÃijr Physik C Particles and Fields C* **76** (1997) 269–286, arXiv:hep-ph/9702274 [hep-ph]. [Erratum: Z. Phys.C76,578(1997)].

[160] A. Andronic, P. Braun-Munzinger, J. Stachel, and H. StÃűcker *Physics Letters B* **697** no. 3, (2011) 203 – 207.

[161] J. Cleymans, S. Kabana, I. Kraus, H. Oeschler, K. Redlich, and N. Sharma *Physical Review C* **84** no. 5, (Nov., 2011) 054916, arXiv:1105.3719 [hep-ph].

[162] A. Aduszkiewicz *et al.*, [NA61/SHINE Collab.] *European Physical Journal* **C77** no. 10, (2017) 671, arXiv:1705.02467 [nucl-ex].

[163] T. Anticic *et al. Physical Review C* **85** no. 4, (Apr., 2012) 044913, arXiv:1111.2588 [nucl-ex].

[164] M. Floris *Nuclear Physics A* **931** no. 0, (2014) 103 – 112.

[165] "Workshop *NA61 beyond 2020*," 2017. https://indico.cern.ch/event/629968/timetable/. 26-28 July 2017, Geneva, Switzerland.

[166] N. Abgrall *et al.*, [NA61/SHINE Collab.] *Phys. Rev.* **C84** (2011) 034604.

[167] N. Abgrall *et al.*, [NA61/SHINE Collab.] *Phys. Rev.* **C85** (2012) 035210.

[168] N. Abgrall *et al.*, [NA61/SHINE Collab.] *Phys.Rev.* **C89** no. 2, (2014) 025205, arXiv:1309.1997 [physics.acc-ph].

[169] T. Vladisavljevic, [T2K Collab.], "Estimating the T2K Neutrino Flux with NA61/SHINE 2009 Replica-Target Data," 2017. https://meetings.triumf.ca/indico/event/6/session/31/contribution/160/material/poster/0.pdf. Poster at the NuInt workshop, 25-30 June 2017, Toronto, Ontario, Canada.

[170] N. Abgrall *et al.*, [NA61/SHINE Collab.] *Nucl. Instrum. Meth.* **A701** (2013) 99.

[171] N. Abgrall *et al.*, [NA61/SHINE Collab.] *Eur. Phys. J.* **C76** no. 11, (2016) 617, arXiv:1603.06774 [hep-ex].

[172] M. Pavin, "Measurements of hadron yields from the T2K replica target in the NA61/SHINE experiment for neutrino flux prediction in T2K," 2017. PhD. Thesis, University of Paris VI, France, CERN-THESIS-2017-233.

[173] K. Abe *et al.*, [T2K Collab.] *Phys. Rev.* **D87** (2013) 012001.

[174] K. Abe *et al.*, [T2K Collab.] *Phys. Rev.* **D96** no. 9, (2017) 092006, arXiv:1707.01048 [hep-ex].

[175] M. Hartz, [T2K Collab.], "T2K neutrino oscillation results with data up to 2017 Summer," 2017. http://www.kek.jp/en/NewsRoom/Release/pressrelease20170808en.pdf. Talk at KEK colloquium.

[176] K. Abe *et al.* arXiv:1609.04111 [hep-ex].

[177] R. Acciarri *et al.*, [DUNE Collab.] arXiv:1512.06148 [physics.ins-det].

[178] J. Strait *et al.*, [DUNE Collab.] arXiv:1601.05823 [physics.ins-det].

[179] L. Fields, "LBNF hadron production needs and plans," in *NA61 Beyond 2020 Workshop, University of Geneva, July 26-28, 2017*. 7, 2017. Slides available at https://indico.cern.ch/event/629968/timetable/.

[180] E. Kaptur *et al.*, 2018. Minutes of the NA61/SHINE beams beyond LS2 meeting, https://edms.cern.ch/document/1936777/1.

Appendices

A Supporting letters

Universität Bielefeld
Department of Physics
Theoretical Physics

Bielefeld University | P.O. Box 10 01 31 | 33501 Bielefeld | GERMANY

Prof. Jordan Nash
Chairperson of the SPS and PS Experiments Commitee (SPSC)
Imperial College London, UK

Prof. Eckard Elsen
Director for Research and Computing
CERN, Geneva, Switzerland

Prof. Dr. Helmut Satz

Telephone: +49 (521) 106-6208
Secretariat: +49 (521) 106-6223
Facsimile: +49 (521) 106-2961
satz@physik.uni-bielefeld.de
www.physik.uni-bielefeld.de

Bielefeld, September 1, 2017

Dear Colleagues,

I am writing you to point out a very promising physics opportunity for the CERN SPS after the coming shut-down, in the context of the heavy ion program and specifically addressed to the continuation of the present experiment NA61/SHINE.
Over the years, charmonium production has proven to be one of the crucial probes for quark-gluon plasma (QGP) production in high energy nuclear collisions. It was noted some twenty years ago [Matsui and HS, PL B 178 (1986) 416] that color screening in the plasma would reduce and eventually prevent the binding of charm quarks and antiquarks to produce charmonia, thus suppressing charmonium production in nuclear collisions as evidence for deconfinement.
The $c\bar{c}$ pairs produced in energetic proton-proton collisions are converted into open charm (D mesons) and charmonia; below LHC energies, one finds about 90 % open charm production, with the remaining 10 % giving charmonia (J/ψ and excited charmonium states). Color screening reduces charm production, so that at a given collision energy, the relative fraction going into charmonia should in nuclear collisions be less than it is in proton-proton collisions at the same energy.
Due to shadowing, parton energy loss etc., the overall scaled number of $c\bar{c}$ produced in nuclear collisons may well be less than it is proton-proton interactions, and this of course will reduce the charmonium production rate in AA relative to pp collisions, even if there is no medium effect on $c\bar{c}$ binding. Hence the effect of the medium on $c\bar{c}$ binding can only be determined by comparing the ratio charmonium production / open charm production in nuclear collisions to that in proton-proton collisions.
To illustrate: if the overall scaled $c\bar{c}$ production in nuclear collisions is reduced by a factor two relative to that in pp collisions, the charmonium production rate is expected to be reduced by the same factor if the medium has no effect whatsoever on the binding process. Hence a simple comparison of only J/ψ production in Pb-Pb collisions to that in pp interactions is completely inconclusive. To see if the production of a hot, deconfining medium has, as predicted, an effect on J/ψ production, it is essential to compare the ratio of J/ψ rates/open charm rates in AA to that in pp collisions.
Up to now, such a comparison has not been possible at the SPS, since the measurement of open charm production requires that of low transverse momentum charmed

Bielefeld University
Universitätsstraße 25
33615 Bielefeld
Germany

mesons, which has so far encountered severe difficulties. Preliminary measurements are only available from RHIC, where it is indeed found that in Au-Au collisions, the rates of J/ψ production at low transverse momenta drop up to 80 % with centrality, compared to the D production rates. In pp collisions, the relative rates are those found at low centrality in nuclear collisions.
At the LHC, such a comparison is not yet possible, again due to difficulties in measuring low momentum D mesons. It may, moreover, be hindered in principle by the possibility of J/ψ production through regeneration. At extreme energies, there is an oversaturation of charm in the produced medium, and this may lead to secondary J/ψ production at hadronisation, preventing a study of medium effects on direct J/ψ formation.
For this reason, the ideal energy range for a precision study of medium effects on J/ψ production is that of the SPS. Here regeneration effects are excluded, since charm production is on the whole too small. Thus $c\bar{c}$ production is essentially due to direct parton interactions, so that any modifications of charmonium/open charm in going from pp to AA interactions is the result of in-medium binding modifications. From this point of view, the ideal experiment would measure at top SPS energy as function of centrality and down to low transverse momenta

- charmonium production (J/ψ, χ_c, ψ')
- open charm production (D mesons)

both in nuclear collisions and in pp interactions at the same energy.
This data should provide a detailed study of charmonium survival in the medium produced in nuclear collisions and hence specify the onset of deconfinement for the different charmonium states, allowing a quantitative study of sequential charmonium suppression [F. Karsch et al., B 637 (2006) 75].
The preliminary results on charmonium production at the SPS formed a significant basis for the CERN conclusions presented in the year 2000, claiming the observation of a new state of matter. As we have shown, such conclusions remain preliminary, as long as the correspond ding open charm data are not available. The proposed measurements of open charm production in nuclear collisions at the SPS energies would allow NA61/SHINE to fill the missing gap and thus to complete an absolutely crucial part of the CERN heavy ion program. I hope that these remarks are of use to you and that the proposed NA61/SHINE program can be realized.

With best regards, sincerely yours,

Prof. Helmut Satz
Fakultät für Physik, Universität Bielefeld
Bielefeld, Germany

НАЦІОНАЛЬНА АКАДЕМІЯ НАУК УКРАЇНИ
ІНСТИТУТ ТЕОРЕТИЧНОЇ ФІЗИКИ
ім. М.М. БОГОЛЮБОВА

NATIONAL ACADEMY OF SCIENCES OF UKRAINE
BOGOLYUBOV INSTITUTE FOR
THEORETICAL PHYSICS

вул. Метрологічна, 14-б,
Київ, 03680, Україна
Tel: 38 (044) 526-5362
E-mail: itp@bitp.kiev.ua
Fax: 38 (044) 526-5998
www.bitp.kiev.ua
14-b Metrologichna St.
Kyiv, 03680, Ukraine

28.09.2017 № 69/01-12/336

Prof. Jordan Nash
Chairperson of the SPS
and PS Experiments Commitee (SPSC),
Imperial College London, UK

Prof. Eckard Elsen
Director for Research and Computing,
CERN, Geneva, Switzerland

Dear Colleagues,

In 1986 Matsui and Satz (Phys. Lett. B 178 (1986) 416) formulated a conjecture that color screening in the deconfined phase would reduce the binding of charm quarks and antiquarks to produce charmonia. Thus, a suppression of charmonia production in nuclear collisions was suggested as the evidence of deconfinement. Results obtained on J/ψ yield at the CERN SPS following the conjecture served as the basic argument for the CERN press release on the observation of a new state of matter in 2000. However, this conclusion remains preliminary, as long as data on open charm are not available.

I am writing this letter to emphasize a very interesting physics opportunity for the CERN SPS. It is given by a possibility to measure open charm production by the upgraded NA61/SHINE experiment. Color screening reduces charmonia production, so that at a given collision energy, the relative fraction of charm going into charmonia should in nuclear collisions be less than it is in proton-proton interactions at the same energy. However, to support this interpretation measurements of open charm (D mesons) in Pb+Pb collisions and proton-proton interactions are evidently needed. Up to now, these measurements have not been possible at the CERN SPS. Note that the ideal energy range for a study of medium effects on J/ψ production is that of the SPS. The low number of produced c and anti-c quarks reduces the probability of their recombination into a charmonium (Braun-Munzinger, Stachel, Phys.Lett. B490 (2000) 196) – in comparison to the LHC case – dramatically.

Thus the lower limit of charmonia yield is given by their statistical production at hadronization (Gazdzicki, Gorenstein, Phys.Rev.Lett. 83 (1999) 4009). As a consequence the proposed measurements of open charm production in nuclear collisions at the SPS energies would allow NA61/SHINE to complete a crucial part of the CERN heavy ion program.

I was also suggested by Kostyuk, Gorenstein, and Greiner (Phys. Lett. B 519 (2001) 207) that the enhancement of open charm production in Pb+Pb collisions may appear due to the broadening of the available phase space caused by the presence of strongly interacting medium. Consequently, an enhancement of open charm yield in nucleus-nucleus collisions with respect to the direct extrapolation of proton-proton data may signal the creation of quark-gluon medium. The c – anti-c pair created with an invariant mass below the open charm threshold, $2\ m_D = 3.7$ GeV, can be nevertheless transformed to a D – anti-D pair in nucleus-nucleus collisions, where missing energy can be taken from the quark-gluon plasma. In proton-proton interactions this is not possible, the subthreshold c – anti-c pairs must be transformed into non-charmed states. The enhancement of open charm yield at the CERN SPS energies due to deconfined medium may be large; a factor of about 5 is expected.

I hope that all these remarks will be useful while you consider the NA61/SHINE proposal to measure open charm.

Kind regards,

Prof. Mark Gorenstein

S.Perepelytsya
Scientific Secretary
of the Bogolyubov Institute for Theoretical Physics

JUSTUS-LIEBIG-
UNIVERSITÄT
GIESSEN

FACHBEREICH 07
Mathematik
und Informatik,
Physik, Geographie

Institut für Theor. Physik Heinrich-Buff-Ring 16 ▪ D-35392 Gießen

Prof. Jordon Nash
Chairperson of the SPS and PS (SPSC)
Imperial College, London, UK

Prof. Eckhard Elsen
Director of Research and Computing
CERN, Geneva, Switzerland

Institut für Theoretische Physik
Prof. Dr. Dr. Wolfgang Cassing
Heinrich-Buff-Ring 16
D-35392 Gießen

Tel.: +49-641 / 99 – 3 33 10
Fax.: +49-641 / 99 – 3 33 09
Email: Wolfgang.Cassing@theo.physik.uni-giessen.de
07.09.2017

Letter of support for the measurements of open charm production at CERN SPS energies

Dear Colleagues,

I had the pleasure to participate in the ***NA61 Beyond 2020*** workshop in July in Geneva and was impressed by the scientific potential in reach for the NA61 detector system. This letter is written in support of proposals for the SPS heavy-ion program and in particular for the measurement of open charm production in heavy-ion collisions. Let we explain my point of view in more detail.

Whereas the properties of partonic systems at vanishing baryon chemical potential have been explored with ultra-relativistic heavy-ion beams at RHIC and the LHC in the past and a strong program has been launched for the next years the properties of partonic and hadronic systems at large chemical potentials are widely unknown as well as the phase boundary in the plane of temperature versus baryon chemical potential. Present lattice QCD calculations provide valuable information at vanishing chemical potential and allow to extrapolate to small chemical potentials via susceptibilities, however, the phase boundary and the order of the phase transition cannot be calculated with present techniques or algorithms. This calls for experimental studies of heavy-ion collisions in the SPS energy regime since the extrapolations of effective models lead to very different predictions. This is partly related to the fact that together with the deconfinement phase transition the restoration of chiral symmetry might go along – in terms of a cross over at low baryon chemical potential – or not at all. At high baryon densities another phase might exist where chiral symmetry is restored to a large extent, however, the degrees of freedom are still confined (quarkyonic matter). Probably these phases become separated at a critical endpoint in the phase diagram which should be characterized by large fluctuations. Accordingly the suggestion has been to look experimentally for fluctuations in observables for low transverse momentum as a function of bombarding energy and system size, i.e. from pp to central Pb+Pb reactions. Although the systematics are far from being completed by now the present data do not show evidence for the appearance of unusual fluctuations.

The quest, therefore, is to look for additional observables that incorporate a different (mass) scale. Here open charm mesons and intermediate mass dilepton pairs (between 1.2 GeV and 2.8 GeV of invariant mass) provide additional information in particular on the charm quark dynamics and angular correlations as well as on the light quark annihilation to lepton pairs from the approximately thermalized partonic system. Angular correlations

between D-meson pairs appear promising probes since the variation of the correlation with system size – from pp to Pb+Pb - will provide information on the interaction rates in the medium complementing traditional R_AA systematics. The intermediate mass dileptons are essentially sensitive to the partonic phase since here the contribution from hadronic decays is practically absent. However, there is a background of lepton pairs from the semileptonic decay of open charm hadrons which has to been to measured independently in order to allow for a clean subtraction.

At SPS energies the probability for charm-pair production is below 15% even in central Pb+Pb collisions at 158 A GeV such that the correlations between open charm hadrons are rather free from background once the D-mesons are properly identified. I should mention that the spectra and angular correlations of D-mesons are important observables on their own. Additionally, they are necessary ingredients for a determination of the dilepton contribution from semileptonic decays and extraction of the electromagnetic emissivity of the QGP at moderate/high baryon chemical potential.

Furthermore, apart from science aspects, we need a timely heavy-ion program and actual experiments in the near future since the Compressed-Baryonic-Matter (CBM) program at FAIR as well as the BES II and fixed-target program at RHIC will not provide experimental information in the near future. The education of young researches needs experiments, actual data and their analysis in order to guarantee the success of heavy-ion research on the long run.

Sincerely yours,

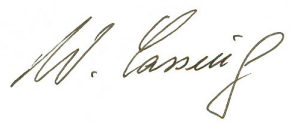

Wolfgang Cassing

(Professor of Theoretical Physics and Senator of the University of Giessen)

cc: Marek Gazdzicki

The Henryk Niewodniczański
INSTITUTE OF NUCLEAR PHYSICS
POLISH ACADEMY OF SCIENCES

Kraków, 16 February 2018

Prof. Adam MAJ
Tel.:+4812 6628141
Fax.:+4812 6628423
Mob.: +48 606 291 860
e-mail: Adam.Maj@ifj.edu.pl

Prof. Jordan Nash,
Chairperson of the SPS
and PS Experiments Committee
Imperial College London, UK

Prof. Eckard Elsen
Director for Research and Computing,
CERN, Geneva, Switzerland

Dear Colleagues,

this letter is to support the physics program of extension of Pb+Pb data taking by the improved NA61/SHINE experiment at the CERN SPS in the period 2021-2024.

In particular, I wish to draw your attention to studies of spectator-induced electromagnetic (EM) effects proposed by the NA61/SHINE Collaboration as an auxiliary measurement with respect to its principal aim of studying open charm in Pb+Pb reactions. For non central collisions of large nuclei, the latter EM effects on charged pion ratios do not only trace the space-time evolution of the system of hot and dense matter created in the course of the reaction, but may also offer a chance to investigate the space-time evolution of the spectator remnant itself. Following the recent theoretical developments the spectator remnant after abrasion is to be considered as a highly excited nuclear system, with different assumed model scenarios resulting in very different predictions for its initial excitation energy.

For me, the low-energy nuclear physicist, this aspect is of high interest. Namely the corresponding high statistics measurements of EM effects as a function of Pb+Pb collision centrality would offer a chance to probe the nuclear system space-time evolution, as a function of spectator mass which is the main observable governing its model-dependent excitation energy. A recent work based on state-of-the-art theoretical tools (Mazurek *et al.*, Phys. Rev. C**97**, 2018, 024604) addresses this issue of EM-distorted charged pion spectra measurements at spectator velocity, as a possible independent way of probing the space-time expansion (abrasion + ablation) of the spectator system as obtained therein from 3D Langevin equation calculations. Such measurements, possibly correlated with those of nuclear fragments which are also doable for the improved NA61/SHINE experiment, would then be a first step towards providing us with insight on poorly known issues such as abrasion friction, energy propagation through the nuclear fragment, and corresponding relaxation times. This could bridge the domain of high energy (GeV-scale) and lower energy (MeV-scale) nuclear

ul. Radzikowskiego 152, 31-342 Kraków, POLAND
www.ifj.edu.pl
switchboard: +48 12 662 8000

physics by falsification of the corresponding models, in extreme experimental conditions (that is, high excitation energies) not available to conventional nuclear physics detectors.

Thanks to its large fixed target TPC system NA61/SHINE would offer a unique opportunity of charge pion tracking and identification in a very extended coverage of available phase space, up to and above spectator remnant velocities, which is a necessary condition to perform measurements of spectator-induced EM effects at least in the charged pionic sector. To the best of my knowledge, no other high energy experiment has that possibility, which leaves NA61/SHINE as the only detector possibly able to explore this problematics in the near future.

I hope these remarks may be useful to you while you consider the NA61/SHINE proposal for high statistics Pb+Pb data taking after 2020.

With kind regards,

Adam Maj

Professor in the Institute of Nuclear Physics Polish Academy of Sciences (IFJ PAN)
and the member of the Nuclear Physics European Coordination Committee (NuPECC)

ul. Radzikowskiego 152, 31-342 Kraków, POLAND
www.ifj.edu.pl
switchboard: +48 12 662 8000

Letter of support for NA61/SHINE cross-section measurements for cosmic-ray physics

January 17, 2018

From

Fiorenza Donato (Professor at Università di Torino, Italy)
David Maurin (CNRS researcher at LPSC, France)
Igor Moskalenko (Senior Staff Scientist at Stanford University, USA)
Pierre Salati (Professor at Université Savoie Mont Blanc, France)
Nicola Tomassetti (MSCA researcher at Università di Perugia, Italy)
Martin Winkler (Postdoctoral fellow at NORDITA, Stockholm, Sweden)

To

NA61/SHINE board

The purpose of this letter is to support a physics program of cross-section measurements at NA61/SHINE that is essential for the investigation and eventual resolution of important questions in galactic cosmic ray (CR) and dark matter physics.

The accuracy of the new generation of cosmic ray experiments, such as AMS-02, PAMELA, DAMPE, CALET, and ISS-CREAM, is now reaching ~1–3% in a wide energy range from GeV/n (per nucleon) to multi-TeV/n. Such a precision could lead to discoveries of new physics and subtle effects that were unthinkable just a decade ago. However, this requires accurate knowledge of several cross sections that regulate production and destruction of CRs in the interstellar matter. The sparseness of precision data on these cross sections currently poses the most limiting element in the interpretation of CR spectra. Furthermore, our present understanding of CR fragmentation relies heavily on extrapolations of semiempirical formulae that have never been tested at the relevant energies. The current uncertainty in the production cross sections can be as high as 20–50% or larger in some cases. There is a consensus in the astroparticle physics community that new measurements of cross sections are of vital importance, as was discussed at the dedicated CERN conference "*XSCRC2017: Cross sections for Cosmic Rays*" (https://indico.cern.ch/event/563277/) organized by some of us. The goal of the conference was to bring together different communities (astrophysicists, cosmic-ray, nuclear, and particle physics theorists and experimentalists) to discuss the perspectives for new particle/isotopic production cross section measurement campaigns. The conference was very successful as it triggered many discussions and paved the way for possible collaborations, which are at the core of this letter of support.

More than a century after the discovery of CRs, their studies are more active than ever. Thanks to new instruments launched into space, the last decade has recorded major breakthroughs and discoveries of primary importance for the astrophysics and particle physics communities, and new measurements of composition and spectra of CR species are eagerly awaited. Many efforts are dedicated to understanding of CR sources, the origin of measured antimatter positrons and antiprotons employed also as dark matter messenger, charged particle acceleration and their transport in the Galaxy. Production cross sections is a cornerstone of all CR propagation calculations. Isotopically resolved cross sections are mandatory to derive propagation parameters. These parameters provide the basis for many other studies, including a search for signatures of the dark matter and new physics, for which new measurements of antimatter production cross sections are strongly required. The most wanted cross sections are:

- fragmentation of O, N, and C into Li, Be, and B isotopes for the study of transport parameters;
- the production of anti-protons, anti-neutrons, anti-deutons, positrons, pions, and kaons from H and He targets for the dark matter and new physics searches.

As was presented at the CERN "*XSCRC2017*" conference, the NA61/SHINE Collaboration has the potential to perform some of these measurements for a variety of reactions and energies that are otherwise inaccessible by other facilities. Subsequent discussions with members of the collaboration triggered further efforts from some of us, to better characterize the needs and in turn, to define realistic goals. The measurements that could be performed with NA61/SHINE at SPS energies would probably be game-changing for our community.

For these reason, we fully and strongly support the initiatives to establish the feasibility of these measurements in pilot runs and to establish longer term programs in the context of NA61/SHINE beyond 2020.

Fiorenza Donato

David Maurin

Igor Moskalenko

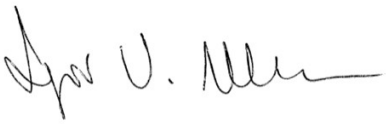

Pierre Salati

Nicola Tomassetti

Martin Winkler

Istituto Nazionale di Fisica Nucleare
SEZIONE DI TRIESTE

Laboratori –Area di Ricerca
Padriciano 99 – 34149 Trieste (I)

Att.ne:
NA61/SHINE board

Letter of support for NA61/SHINE cross-section measurements for cosmic-ray physics

The purpose of this letter is to support a physics program of cross-section measurements at NA61/SHINE that will provide necessary information to answer fundamental questions concerning cosmic rays physics and dark matter searches.

Cosmic rays (CRs) are a direct sample of solar, galactic, and extragalactic matter that includes all known nuclei and their isotopes, as well as electrons and antiparticles. Their energy spectrum extends for many orders of magnitude from energies lower than 10^6 eV up to about ~10^{21} eV. The origin of CRs, their acceleration mechanisms, and their subsequent propagation toward Earth are still unresolved questions. Moreover, CRs are strictly connected with fundamental physics topics such as the nature of dark matter (DM) or the unexplained asymmetry between antimatter and matter in our Universe.
Cosmic-ray antiparticles are particularly intriguing since they may be the result of annihilation or decay of DM particles. The nature of the DM is one of the unsolved problems in modern astrophysics and this has motivated the search for antiparticles in many CR experiments. However, a claim of DM signature from these indirect measurements is very challenging, because antiparticles are also created by collisions of ordinary CRs with the nuclei of the interstellar medium (ISM). This astrophysical background has to be carefully predicted and these calculations critically depend on our knowledge of CR acceleration and propagation processes through the Galaxy, which are as yet not well understood. It is believed that CRs at least up to about 10^{17} eV are accelerated by Galactic sources, such as supernova remnants, and subsequently diffuse in the turbulent magnetic fields of the Galaxy. During this propagation, CRs interact with the ISM and produce lighter elements including CR particles that should be scarce in the cosmic radiation such as ^{2}H or ^{3}He isotopes, Li-Be-B and nuclei just lighter than iron, and antiparticles.

In recent years, a large number of state-of-the art CR space- and satellite- borne experiments have been developed and operated, namely AMS-02, DAMPE, CALET, ISS-CREAM, PAMELA in space, and BESS, CREAM, TIGER and SuperTIGER in stratospheric balloons. Furthermore, space agencies and scientists are designing next generation experiments (e.g. HERD, GAPS) that will further extend the energy reach as well as the statistics on the CR flux and composition measurements.
These experiments, using novel methodologies and instrumentations adopted from high energy particle physics, have greatly improved on previous cosmic-ray measurements providing results spanning several decades in energy with enormous increase of the statistical precision. Moreover, detailed on-ground calibrations and redundant instrumentation have allowed a great reduction of the

Istituto Nazionale di Fisica Nucleare
codice fiscale 84001850589

Sezione di Trieste – Laboratori – Loc. Padriciano, 99 - 34149 Trieste (Italia) - https://www.ts.infn.it
tel. +39 040 3756220/59/75 - fax +39 040 3756258 - email: infn@ts.infn.it - PEC: trieste@pec.infn.i

systematical uncertainties down to a few per-cent level. This has been convincingly shown for various CR particle species, from the most abundant proton and helium nuclei to the rarer positrons and antiprotons, which fluxes measured by different experiments (e.g. PAMELA and AMS-02) agree at the per-cent level. However, only a detailed comparison between these experimental data and theoretical predictions provide the needed information to answer fundamental questions concerning the origin and propagation of cosmic rays as well as search for new physics. To this day, these theoretical calculations are affected by uncertainties that are significantly larger than the experimental ones. For example, tantalizing indications of larger than expected positron and antiproton fluxes cannot be convincingly interpreted as signatures of new physics (e.g. DM annihilation or decay) or novel astrophysical sources (e.g. pulsars) because of the large uncertainties on the prediction of the antiparticle fluxes produced by CRs interacting with the ISM.

One of the largest uncertainties in these theoretical calculations results from the insufficiency and limited precision of the cross sections related to CR interaction with the ISM. NA61/SHINE has the potentiality to fundamentally contribute to CR studies measuring the cross sections that are most needed. These are:

- fragmentation of O, N, and C into Li, Be, and B isotopes;
- production of antiprotons, antineutrons, antideutons, positrons, pions and kaons from H and He targets.

For this reasons, I strongly support the initiatives to establish the feasibility of these measurements in pilot runs and to establish longer term program in the context of NA61/SHINE beyond 2020.

Trieste, 28 February 2018.

Yours Sincerely .

Dr. Mirko Boezio .
INFN Senior Staff Scientist
PAMELA Data Analysis Coordinator and Italian PI

Istituto Nazionale di Fisica Nucleare
codice fiscale 84001850589

Sezione di Trieste – Laboratori – Loc. Padriciano, 99 - 34149 Trieste (Italia) - https://www.ts.infn.it
tel. +39 040 3756220/59/75 - fax +39 040 3756258 - email: infn@ts.infn.it - PEC: trieste@pec.infn.i

Letter of support for NA61/SHINE cross-section measurements for cosmic-ray physics

February 27, 2018

From

Shoji Torii (Professor at Waseda University and CALET PI, Japan)
Katsuaki Kasahara (Invited senior researcher at Waseda University, Japan)

To

NA61/SHINE board

With the CALorimetric Electron Telescope (CALET) on board the International Space Station, we are currently observing high energy cosmic rays ranging from 1 to 10^6 GeV. The observation will continue few years more.

Nowadays precision measurements are required for judging various possible scenarios of origin, propagation mechanism etc of various cosmic ray components. For this, we need detailed hadronic interaction information in large phase space in a wide energy range. This is also true when we observe cosmic gamma rays and electrons for separating them from p, He, etc. So far NA61/SHINE has been providing important information for such purposes. To keep upscaling the situation, it will be better to fill the gaps in existing data.

Below we list our hopes independently of how they are difficult or not, and we understand so many combinations cannot be realized in a short time.

1. We need basically the cross-section as a function of generated particle type, angle and energy for various targets, projectile and energies.

2. Projectiles: p, pion, (kaons), heavy ions (Be, C, Ar, Fe...). Energy: as high as possible. But need 10 GeV region too.

3. Produced particle ID and momentum $\vec{p}$ measurement : p, pi, K. heavy ions.

4. Covering wide angle: Even back scattered particle information is useful for us.

This type of information should also be very useful for many cosmic ray experiments such as the Tibet ASg experiment. Atmospheric neutrino observation will be benefited for detailed study of neutrino oscillation and leptonic cp violation.

Although it will be not easy, a very big step will be achieved if NA61/SHINE collaboration can realize extraction of beam particles from the LHC beam pipe and make it possible to study >few TeV particle interactions with various fixed targets.

Shoji Torii

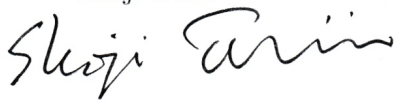

Katsuaki Kasahara

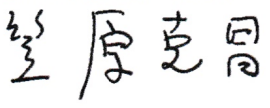

中国科学院紫金山天文台
PURPLE MOUNTAIN OBSERVATORY, CAS

Jin Chang
2nd West Beijing Road
Nanjing, Jiangsu, 210008 China
Email: chang@pmo.ac.cn

February 18, 2018

To whom it may concern,

I am a professor and the deputy director of Purple Mountain Observatory (PMO), Chinese Academy of Sciences, and also the PI of the DArk Matter Particle Explorer (DAMPE) mission, the first Chinese space mission for science. The objectives of DAMPE is to search for dark matter particles and study cosmic ray physics via high precision observations of high-energy cosmic ray electrons, nuclei, and gamma-rays.

I am very glad to hear about that the NA61/SHINE collaboration is preparing a proposal for dedicated measurements of cross sections of antiprotons, antideuterons, and a series of nuclei, which are crucial for understanding the fundamental questions of cosmic rays such as their propagation and interaction in the Galaxy and the indirect detection of dark matter particles. It is the right time to so do now, since more and more measurements of cosmic rays with significantly improved precision are available in recent years, and the uncertainties of particle (nuclear) physics become dominant usually. These measurements are also expected to be very helpful in interpreting the DAMPE results. I thus fully support such a proposal, and am looking forward to seeing the new data in the near future. Please let me know if there is anything else I can be helpful.

Sincerely yours

Jin Chang

中国南京市北京西路 2 号 邮政编码:210008 2 West Beijing Road,Nanjing 210008,China

COLUMBIA UNIVERSITY
IN THE CITY OF NEW YORK

COLUMBIA ASTROPHYSICS LABORATORY

February 28, 2018

To the NA61/Shine Collaboration:

I am the principal investigator of the General Antiparticle Spectrometer Experiment (GAPS). GAPS is a balloon-based, indirect dark matter search to be flown from Antarctica in 2020. It searches for antideuterons and antiprotons produced in the annihilation or decay of dark matter. It will be the first low energy antideuteron experiment ever flown, and the most sensitive search for low energy antiprotons. GAPS is a multi-national collaboration involving some 17 institutions in the USA, Japan and Italy, as well as NASA and the Japanese Space Agency (JAXA).

I am writing a letter of support for the NA61/SHINE collaboration for their fixed-target experiment at CERN. This experiment will provide data I consider absolutely crucial to the interpretation of data obtained with GAPS, and to the maximization of the GAPS science return. Antideuterons and antiprotons can be produced through conventional hadronic processes as well as through dark matter channels, and understanding these conventional processes for production is crucial to disentangling dark matter antideuterons and antiprotons (the primaries) from those produced in normal cosmic-ray interactions in the interstellar medium (ISM). In addition, and especially in low energy antimatter searches, understanding transport of particles through the ISM is vital, since low energy particles are particularly sensitive to parameters used in cosmic-ray transport models. Our ability to accurately constrain various beyond Standard Model physics theories is crucially dependent on our ability accurately assess particle loss during transport, and how transport modifies the particle spectrum from point of creation to detection at the earth.

The proposed NA61/SHINE experiment addresses all the issues I have mentioned above, and which are so important for GAPS. Antiproton and antideuteron production cross-sections are directly relevant to assessing secondary/tertiary particle fluxes, and to better understanding the process by which protons and neutrons coalesce into hadrons. This is a large source of uncertainty in understanding fluxes of antideuterons from dark matter, and there is a great need for the improved measurements which NA61/SHINE would provide. The experiment will also provide data useful to constraining the B/C ratio. This is a key factor in normalizing the cosmic-ray transport codes are another major source of uncertainty in constraining beyond Standard Model physics. GAPS also has significant capability to improve our understanding of conventional cosmic-ray processes in the ISM through its unprecedented sensitivity to low energy antiprotons (<~ 150 MeV). But to fully exploit these antiprotons requires better constrained transport parameters, which the NA61/SHINE experiment can provide with its ability to help better constrain the crucial B/C ratio.

550 West 120th Street Pupin Hall Mail Code 5247 New York, NY 10027 212-854-7815 Fax 212-854-8121

I think it has been recognized for many years that there is a great need for an experiment like NA61/SHINE because its relevance to the AMS experiment, which is also measuring antiproton and potentially antideuteron fluxes. With the flight of GAPS in the not-too-distant future, there is greater urgency in both acquiring and understanding the data NA61/SHINE can provide, prior to the flight of GAPS.

With Best Regards,
Chuck Hailey
Pupin Professor of Physics
Co-Director, Columbia Astrophysics Laboratory

Prof. M. Nakahata
Prof. M. Shiozawa
Prof. F. Di Lodovico

PROF. ALAIN BLONDEL

UNIVERSITY OF GENEVA

DEPARTMENT OF PHYSICS

NAKAHATA@SUKETTO.ICRR.U-TOKYO.AC.JP
MASATO@SUKETTO.ICRR.U-TOKYO.AC.JP
F.DI.LODOVICO@QMUL.AC.UK

Dear Alain,

We are the spokesperson, Masayuki Nakahata, of the Super-Kamiokande experiment, the project leader, Masato Shiozawa, and co-leader, Francesca Di Lodovico, of the Hyper-Kamiokande proto-collaboration.

Super-Kamiokande is a water Cherenkov neutrino experiment in Kamioka, Japan. It works both as the far detector for the long baseline neutrino experiment T2K and as neutrino observatory for atmospheric and astrophysics neutrinos as well as rare decays. Hyper-Kamiokande is a water Cherenkov detector starting to take data in the middle of the next decade and 10 times larger than Super-Kamiokande. It is located in the same prefecture as Super-Kamiokande and will also work as far detector for the upgrade beam from J-PARC and as a neutrino observatory.

The physics goals of T2K are to be sensitive to the values of $\sin^2 2\theta_{13}$ down to 0.006 and to measure the neutrino oscillation parameters with precision of $\delta(\Delta m^2_{32}) \sim 10^{-4}$ eV^2 and $\delta(\sin^2 2\theta_{23}) \sim 0.01$. To achieve these, the near-to-far extrapolation of the flux, i.e., the far-to-near flux ratio as a function of energy has to be known to better than 3%. To achieve this objective is vital to reduce the absolute flux uncertainty. To predict the neutrino flux, T2K relies primarily on the measurements of pion and kaon yields by the NA61/SHINE experiment at the CERN SPS. These data were initially taken with a thin (2 cm) graphite target and the same proton beam energy as that of T2K and subsequentially with a T2K replica target.

Studies are currently ongoing for the Hyper-Kamiokande beam target, but more statistics as well as lower systematic errors for the experiment increase the demand to NA61/SHINE for Hyper-Kamiokande from measuring the pion and kaon distributions with the

Hyper-Kamiokande target to increasing the phase-space and to study the interactions with the out-of-target materials.

Atmospheric neutrino measurements and searches for nucleon decay at Super-Kamiokande and its planned successor, Hyper-Kamiokande, are subject to uncertainties in the prediction of the atmospheric neutrino flux. Uncertainties in the proton interaction cross section on nuclei in the air as well as uncertainties on the type and multiplicity of particles produced from such interactions lead directly to systematic errors affecting programs to address open questions in neutrino mixing and the quest for grand unification.

Measurements of the relative production of pions and kaons from protons, as well as their interaction rates, on target nuclei similar to those found in the atmosphere are particularly important for understanding the impact of the atmospheric flux and its uncertainty on these measurements. Possible low energy extensions of NA61 can provide critical measurements for constraining the atmospheric neutrino flux at sub-GeV energies, where the atmospheric neutrinos carry information on the CP phase of the standard neutrino oscillation paradigm. While next-generation experiments seek to establish or refute the existence of neutrino CP violation using accelerator neutrinos, if uncertainties in the flux can be reduced in this way, atmospheric neutrinos will provide an independent measurement with complementary sensitivity.

Proton decay searches suffer backgrounds from atmospheric neutrinos and similarly benefit from improved flux modelling. While the flux uncertainties have a modest impact on searches at Super-Kamiokande, at the megatonyear-scale exposures envisioned for Hyper-Kamiokande, where the current background model predicts a handful of events, they are roughly 20% of the error budget. For this reason, a detailed understanding of the atmospheric neutrino flux in the energy regime currently spanned by NA61 will be needed to establish a proton decay signal.

Though the above comments have been made in the context of the Super-Kamiokande and Hyper-Kamiokande experiments, it should be stressed that continued hadron production measurements at NA61 will be an indispensable part of understanding the accelerator and atmospheric neutrino flux for not only these projects but for all experiments making use of these neutrinos.

In conclusion, the Super-Kamiokande and Hyper-Kamiokande collaborations support the NA61/SHINE proposal very strongly. The NA61/SHINE team have proved to be extremely knowledgeable and helpful when applying their results to Super-Kamiokande and T2K and are proving to be a valuable resource for Hyper-Kamiokande.

Sincerely,

Prof. M. Nakahata Prof. M. Shiozawa Prof. F. Di Lodovico

DEEP UNDERGROUND NEUTRINO EXPERIMENT

21th November 2017

Dear Professor Zimmerman,

We are writing on behalf of the DUNE collaboration to express our support for idea of future operation of NA61 to constrain systematic uncertainties associated with the LBNF neutrino beam. Specifically, the target for the LBNF neutrino beam will be four interaction lengths long. Consequently, a large component of the neutrino beam is generated from pions arising from secondary and tertiary interactions in the target. For this reason, hadron production data using the LBNF target could be important for constraining the LBNF beam systematics.

Yours sincerely,

Professor Edward C. Blucher Professor Mark A. Thomson

Co-Spokespersons of the DUNE Collaboration

B DRC Memorandum on Operation of Fixed Target Experiments immediately after LS2

DG-DI-RCS-2017-093
21st September 2017

MEMORANDUM

To : Spokespersons of Fixed Target Experiments

Cc : *Chair of SPSC, Secretary of SPSC*

From : Eckhard Elsen

Subject : Operation of Fixed Target Experiments immediately after LS2

The Research Board (RB) has discussed the operation of the fixed target experiments following the immediate completion of the Long Shutdown 2 (LS2). The long-term future of the fixed target programme at CERN is in the purview of the discussion on the Update of the European Strategy for Particle Physics (largely now prepared by the Physics Beyond Collider Study) and detailed operation will only be decided after its publication, currently expected for May 2020.

The early start-up phase, however, needs to be now prepared, be it to obtain funding or upgrade the detector capability. The Research Board approved the principle of an early post-LS2 fixed target programme and running. The plans for this programme should be evaluated in the SPSC and approved by the RB following the standard procedure.